THEORETICAL AND EXPERIMENTAL INVESTIGATIONS OF MAGNETIC FIELD-ASSISTED ULTRA-PRECISION MACHINING OF TITANIUM ALLOYS

KHALIL AHMED KAMEL ALI BAYOUMY

PhD

The Hong Kong Polytechnic University

2023

The Hong Kong Polytechnic University
Department of Industrial and Systems Engineering

Theoretical and Experimental Investigations of Magnetic Field-Assisted Ultra-Precision Machining of Titanium Alloys

KHALIL Ahmed Kamel Ali Bayoumy

A thesis submitted in partial fulfillment of the requirements for the degree of Doctor of Philosophy

August 2022

CERTIFICATE OF ORIGINALITY

I hereby declare that this thesis is my own work and that, to the best of my knowledge and belief, it reproduces no material previously published or written, nor material that has been accepted for the award of any other degree or diploma, except where due acknowledgment has been made in the text.

_____(Signed)

KHALIL Ahmed Kamel Ali Bayoumy (Name of student

Abstract

Titanium alloys can be used in advanced engineering and biomedical applications. Their outstanding overall properties and high corrosion resistance make them indispensable structural materials for many industrial parts. They are biological implant materials that have been widely used in medicine. However, titanium alloys are poor in machinability in ultra-precision machining (UPM), their poor thermal conductivity results in high cutting temperature, which causes heat to accumulate in the cutting zone. Excessive heat causes most machining challenges because it accelerates tool wear and degrades the cutting tool edge, causing low surface quality. A magnetic field-assisted ultra-precision machining (MFUPM) system was developed in this study to boost the machinability of Ti6Al4V alloy concerning enhanced surface roughness and diamond tool life.

A magnetic field-assisted ultra-precision machining (MFUPM) system was developed for creating the magnetic field. A setup of a magnetic field system with an adjustable intensity has been used to generate a uniform magnetic field in accordance with Maxwell's magnetic-field law. The selection of magnetic field intensity and the movable length for positioning magnets in the magnetic system is based on preliminary experimental results and a theoretical basis, yielding the optimal magnetic effect in UPM. The magnetic field density as well as the distribution of magnetic flux in the cutting zone are critical factors for MFUPM.

For thermal analysis of MFUPM, finite element modeling (FEM) is built following the Johnson-Cook (JC) constitutive model and geometrical model, taking flow stress, strain, strain rate, and temperature into account, with the Johnson-Cook constitutive model serving as a link between material parameters, mechanical loading, effective stress, and heat at the tool/workpiece interface. The JC damage model was used, and the failure evolution-based fracture criteria were applied where the failure energy was taken into account. The geometric

model includes tool settings, workpiece geometry, and machining conditions. An external magnetic field has been shown to improve Ti-6Al-4 V thermal conductivity during UPM. The experimental results in this study demonstrated that the magnetic field improves the UPM performance of the Ti-6Al-4V alloy, and the simulated and experimental outcomes were consistent. These findings revealed enhanced surface quality and increased diamond tool life.

This thesis contributed to resolving the machining difficulties faced by UPM, which aims to uplift the precise level of products, especially for hard-to-cut materials such as Ti-6Al-4V. This study concluded that the machining of Ti-6Al-4 V alloy has been improved with the aid of the magnetic field. The relevant machining factors of tool wear, chip formation, and surface roughness of the machined work material were investigated, resulting in increased tool life and improved machined surface quality for diamond machining. In addition, MFUPM produced the lowest value for surface roughness. This work contributes significantly to supporting the MFUPM by FEM and producing high-quality machined Ti alloys in UPM for related research activities.

Publications arising from the thesis

Journal papers:

Khalil, A.K., Yip, W.S., To, S., 2022. "Theoretical and experimental investigations of magnetic field-assisted ultra-precision machining of titanium alloys." **Journal of Materials Processing Technology** 300, 117429. https://doi.org/10.1016/J.JMATPROTEC.2021.117429

Khalil, A.K., W.S. Yip, S. To. "A Novel magnetic field assisted diamond turning of Ti-6Al-4V alloy for sustainable ultra-precision machining." Journal of Materials Today Communications 2023,105829, https://doi.org/10.1016/j.mtcomm.2023.105829

Khalil, A.K., W.S. Yip, S. To. "Numerical study on chip formation mechanism of Ti-6Al-4V alloy based on different failure energy and cutting speed in ultra-precision machining (UPM)." (Under review, journal of Processes)

Khalil, A.K., W.S. Yip, S. To. "Investigation and modeling of using worn cutting tools in magnetic field-assisted ultra-precision machining (MFAUPM)." (Under preparation)

Khalil, A.K., W.S. Yip, S. To. "Modelling and simulation of Ti-6Al-4V in ultra-precision machining adopting different constitutive models and physical properties." (Under preparation)

Conference papers:

Khalil, A.K., W.S. Yip, S. To., "Improving machinability of Ti alloys in ultra-precision machining by a novel magnetic field system" in The International Conference on Material Science and Engineering: Recent Advances and Challenges (ICMSE-RAC), Egypt-Japan University of Science and Technology, Alexandria, Egypt.

Acknowledgments

I would like to thank my chief supervisor, Prof. Sandy Suet To, Professor of the Department of Industrial and Systems Engineering of The Hong Kong Polytechnic University, Associate Director of State Key Laboratory of Ultra-precision Machining Technology and Advanced Optics Manufacturing Centre, for the supervision of my Ph.D. study and for giving me the opportunity to be one of her students. I also appreciate her enduring keenness to encourage us to learn, work hard, and plan continuously which had a good impact on my study and finalization of this thesis. The same credit goes to Dr. Yip Wai Sze, my co-supervisor, for her valuable guidance and support.

I would like to thank PolyU and all the staff members in the State Key Laboratory of Ultra-precision Machining technology of The Kong Polytechnic University for providing support during my Ph.D. study.

Special thanks to my beloved family, parents, siblings, and my family-in-law for their encouragement and support. I also extend my sincere thanks and gratitude to my wife Mrs. Amany and my daughters Taimia and Safia for their great credit and patience to complete my postgraduate study while being away from home, who also have been extremely supportive of me throughout this entire period and made countless sacrifices to help me be in this place, and without such a supporting family, I wouldn’t get to this point.

Table of Contents

List of figures

List of figures

List of figures

List of tables

Chapter 1: Introduction

1.1 Background

Titanium alloys, compared to others, have unique features. Their superior mechanical qualities, high strength with low density, and corrosion resistance make them stand out from other alloys and serve as the optimal choice for advanced applications like prosthetics, additive manufacturing, marine works, and the aviation industry (Quinn et al., 2020; Maurotto et al., 2013). Also, their outstanding overall properties and high corrosion resistance make them indispensable structural materials for many industrial parts. Since the 1960s, biological implant materials have been widely used in medicine. It is important to note that Titanium alloys are biocompatible; their density and elasticity make them function like human bone, whilst their corrosion resistance makes them promising bioengineering materials (Niinomi, 2003a). Further, their applications have solved significant engineering and technical problems, boosting the progress of science and technology, and have brought clear economic benefits with excellent performance.

However, Titanium alloys are poor in machinability, thus, are regarded as hard-to-cut materials. Their thermal conductivity is low notably at high cutting temperatures, which negatively impacts their machining. During machining, their poor thermal conductivity reduces the heat transmission outside the machining area. As a result, little heat transfers from the cutting zone and leads to a more confined heat at the cutting zone, which worsens the cutting tool’s condition, causing tool wear and reducing the tool’s life. In addition, the worn tool degrades the workpiece's surface and affects the machining performance (Arrazola et al., 2009). To overcome this low machinability, researchers have presented relevant studies that have primarily addressed some challenges to fulfill satisfactory machining behavior.

Furthermore, researchers also proposed many approaches to address titanium alloys' machinability, which resulted in some improvements in their machining performance. These methods include optimizing cutting factors, dealing with tool vibration during cutting, using advanced or coated cutting tools, using cooling means of various types, and applying physical approaches and treatment processes. However, since metal cutting is a complicated process, there is a need for more investigations to explore the machining behavior of titanium alloys. In this study, the magnetic field's impact on the behavior of the machined material during the operation was studied. The utilization of the magnetic field enabled improvement and enhancement in the performance of Ti-6Al-4V's machining operation.

Adopting dry cutting prevents environmental pollution, decreases health risks, and protects the machine operator and technicians from diseases. It also reduces cost and avoids the occurrence of thermal shocks during interrupted cutting. However, the lack of lubricants and cooling fluids during cutting results in more restrictions on the cutting velocity. This may lead to high induced cutting temperature, generating excessive heat and fast tool wear, thereby causing the integrity of the workpiece's surface to deteriorate (Naumov et al., 2016). Some researchers applied dry electrostatic cooling (an inexpensive and environmentally friendly technology that lengthens the tool's life) by injecting ionized gas with ozone molecules into the machining zone (Da Silva et al., 2013). Other researchers proposed the minimum quantity lubrication (MQL) technique. This technique relies on directing a little amount of water and soluble oil toward the cutting edge, which enables reductions in temperature, protects the cutting edges, and lowers surface roughness, and cost of operation. The weakness of this technique involves health hazards because of the mist generation (Veiga and Davim, 2013).

The electro-pulsing treatment (EPT) technique was also employed to upgrade the cutting behavior of titanium alloys. Primarily, the working principle of EPT is achieved by causing microstructural changes, optimizing grain sizes, and reducing distributions of the

dislocation. The (EPT) technology is a functional adoption process and serves as an efficient substitute for conventional thermal treatment methods. The pulses of electric current produce electromagnet forces dynamically, which can augment the motion of the dislocation and enhance the material's microstructure. As a result of increased plasticity, the surface quality gets improved in machining and metal forming (To et al., 2010). Titanium alloy Ti6Al4V is treated with electro-pulsing to promote its plasticity. Hardness and compression tests have demonstrated that following the EPT process decreases stress and hardness (Lou and Wu, 2017).

In this study, a novel magnetic field system was linked to UPM to enhance machinability and improve the machined parts' surface quality. Various investigations have shown the ability to use the magnetic field in metal cutting, which is successfully applied to machine different hard-cut materials. Also, other studies showed improvements in the machining performance of titanium alloys when treated by pulses of the magnetic field. These studies achieved the phase transition from alpha into beta of Ti alloy by lowering the density of dislocations suffering from high dense magnetic field. Several attempts have been made to solve the challenges of the tool's high wear rate. In an investigation, the degree of tool wear was significantly decreased when the electromotive force existed coaxially, based on the induction of the magnet alignment. The basic concept is that, while being affected by a magnetic field, the magnet particles of a conductive workpiece become aligned and parallel with the same direction of a supplied magnetic field. As a result, there is an improvement in thermal conductivity and a reduction of the confined heat in the machining zone. Turning the work material by applying a magnetic field expedite heat transfer and prevent tool wear. This eases the promotion of cutting temperature dissipation, which aids in achieving a successful machining process.

1.2 Research objectives

This study aims at addressing the machining difficulties relating to machining factors and material properties that occur in the UPM of Ti alloys. Therefore, applying a new machining approach is proposed. Firstly, a magnetic field integrated with UPM tool was presented to resolve the machining difficulties currently faced by UPM. This aims to uplift the precise level of products, especially those which are made of Ti-6Al-4V because of their hard machinability. In this study, UPM technology was used to address the following objectives:

1) To use the finite element modeling FEM method to explore the magnetic flux distribution of the system and study the effect of the obtained results on the machining environment of the workpiece.

   The development of different simulation software has triggered researchers to investigate the working behavior of various materials. The simulation results vary when the data or parameters are altered and when fixed. Simulating the produced magnetic field is important for operating the machining process. Thus, the obtained results can be used to control the system parameters. Also, exploring different magnetic materials helps to assess the most effective machining environment.

2) To utilize the magnetic field in the ultra-precision machining technology to achieve uplifted machining performance of Ti-6Al-4V.

   The magnetic field has been used by researchers as an assisting tool in various manufacturing processes to promote process quality. The magnetic field is typically used for increasing the debris removal rate in cutting processes like electrical discharge machining (EDM). Through this, the outcome of Ti6Al4V alloy machined parts would be improved by combining a magnetic field system with UPM employing single-point diamond turning. The experimental results will be used to demonstrate that Ti-6Al-4V alloy

can be machined more effectively with magnetic field assistance. These findings will provide compelling proof that a magnetic field could lengthen the life span of cutting tools, while MFAM also produces machined surfaces with high integrity.

3) To study and model the magnetic field's influence on the material properties of the Ti-6Al-4V in the UP-turning machine.

The UPM technology utilizes a magnetic field to offer a wide range of advanced applications. So, this hybrid method was incorporated into UPM technology to enhance the cutting process and significantly increase product quality. The physical properties of ferrometals, like thermal conductivity, can be increased when metals are subjected to a magnetic field. Ti-6Al-4V alloy will be subjected to a magnetic field during the turning process to enhance the dissipation of heat produced in the cutting zone. Consequently, the excessive heat in the cutting zone was no longer a dominant factor for tool wear, making it a critical point for surface quality. To illustrate how the generated magnetic field affects the machining processes, the finite element method FEM will be employed. The machining process simulation can be cost-effective when examining the cutting performance, aiming to study the chipping mechanism, or cutting temperature during operations. Any cutting simulation model consists of the geometry model, the mesh model, the constitutive material model, the analysis type, and the interaction properties, which are directly related to the simulation results. Modeling is an economic tool that aids in exploring the cutting mechanism of different work materials.

4) To apply the cleaner production strategy by adopting a sustainable magnetic field-assisted machining

This highlights the benefits that the industrial enterprise could achieve due to the application of magnetic fields as a strategy for cleaner production, which is reflected in the

environment and manufacturing resources. Adopting the magnetic field compensated the function of lubrication to reduce the imposed heat during cutting. This method contributes to the preservation of resources and protects the environment from pollution.

1.3 Organization of the thesis

The thesis content is organized into five chapters as follows:

Chapter 1: This chapter introduces the thesis; it covers the research background, which presents the challenges of hard-to-cut materials like Ti alloys in ultra-precision machining. Also, the objectives are enumerated.

Chapter 2: This chapter reviews the literature relating to the research. Thus, it contains knowledge relating to ultra-precision machining technology. It covers basic information about the single-point diamond turning SPDT, titanium alloy's mechanical and physical properties, and their applications. The chapter also elaborates on hybrid machining technologies and their impact on the manufacturing processes, as well as the generation of the magnetic field and their application in the industry and machining. The importance of adopting a sustainable and cleaner production perspective in machining is also highlighted.

Chapter 3: This chapter describes the development of a system able to be linked with the ultra-precision machine tool to generate the magnetic field in the machining zone. It explains the modeling of the magnetic field system using FEM for evaluation and exploring the magnetic flux, the magnetic field application in ultra-precision machining, the working principle of the magnetic field-assisted machining (MFAM), the experimental work, the results, and the discussion.

Chapter 4: Presents the thermal analysis of magnetic field-assisted ultra-precision machining (MFUPM). This chapter includes the FEM of the cutting process of Ti-6Al-4V that considered the material properties changes when material suffers from a magnetic field. The

benefits that the industrial enterprise could achieve due to the application of magnetic field in the strategy of cleaner production are also mentioned. It further highlights the working principle of thermal conductivity enhancement, as well as the magnetic field's contribution to the preservation of resources and environmental protection.

Chapter 5: Presents the conclusions and future direction relating to the development of linking the magnetic field to the UPM technology, and the significance of generalizing this hybrid method to address the challenges when machining hard-to-cut materials.

Chapter 2: Literature review

2.1 Introduction

Since the current generation is looking forward to getting products that can serve the huge technological development, many advanced industries have to produce components with neat features and high integrity that is achievable effectively using ultra-precision machining UPM technology. As the demand for high-precise products is increasing to be used in many engineering applications and the technological advances in humanity, it was necessary to develop advanced techniques to manufacture these parts with high accuracy to meet the requirements of daily life applications (To et al., 2002; Zareena and Veldhuis, 2012).

Any part to be produced from raw material to its final form must go through a long and complex series of processes with a fixed sequence. This processing changes the shape and properties of the part to suit the application's requirements (Creese, 1999). Generally, the parts produced by manufacturing processes after processing the raw material can be divided into semi- and finished products. The semi- finished products are the parts that had some manufacturing processes conducted and are still awaiting subsequent manufacturing processes to modify their properties and shape. While the finished products are parts that have passed through all stages of formation and operation until they are ready for use separately or combined with other elements to form machines or products that are used daily basis lives such as the machine elements used in the aviation industry, automobiles, and medical fields (Budynas and Nisbett, 1983; Clark, 1995; Reddy, 1986). So, any product that is expected to suffer any operation under the manufacturing processes can be classified schematically in Figure 2.1.

Advanced manufacturing technologies are capable of providing high-precision products. These products have many applications, such as medical sectors, buildings, and

optical and electronics applications. Products with high features and complicated requirements can only be obtained by using advanced manufacturing methods capable of reaching high accuracy conditions that make them fit for advanced applications and high expected service needs (Pramanik and Littlefair, 2015). These advanced methods are limited to manufacturing the parts used in advanced applications. They need a strong economy to bear the costs of the used materials and tools such as machine tools, mechanical and electrical devices, and precise and fast controls. Although these advanced industrial methods cost more than conventional manufacturing, they also provide very specific parts in terms of shape and dimensions (Çolak, 2014). Despite the high cost of these advanced manufacturing methods, it is necessary to be adopted them to meet the needs of applications and provide accurate engineering means to obtain parts to be used in micro-industries (Cheung and Lee, 2000). Currently, researchers are working on improving the use of these advanced methods either by reducing costs by maintaining the life expectancy of the machine tools or by saving the operating time of the parts (Nandy et al., 2009).

Ultra-precision machining UPM technology is classified into four categories: ultra-precision grinding, ultra-precision polishing, ultra-precision fly cutting, and single-point diamond turning (SPDT). They are selected based on the machining requirements and application. SPDT is one of the advanced methods used to manufacture complicated parts that require many engineering considerations; this enables getting parts of the highest accuracy without resorting to implementing postprocessing steps (Lee et al., 2000). The SPDT is selected to achieve this purpose when needed to manufacture precision parts, which are often in cylindrical shapes. More details of this method will be addressed in the upcoming topics.

Figure 2.1 Classification of manufacturing processes (Groover, 210AD).

2.2 Ultra-precision machining technology

Following the classification and evolution of the UP-machining technology, the grinding process is carried out to give surfaces high quality and is used for machining high-hardness materials. It has been observed in different cutting operations, such as the turning process, to obtain a high machined surface quality, the feeding value needs to be small, i.e., the distance that the cutting tool advances for each revolution decreases, and also known that the more cutting edges exist in the milling process, the higher the surface quality is attained. From this observation, the idea of grinding could be developed by having a cutting tool with many cutting edges. The process of grinding is necessary to get high-grade machined surfaces and

high accuracy of nano-dimensions, reducing the operating time involved in other different processes; thus, its expenses are reduced (Yang et al., 2021).

The need for precise parts to serve in many engineering applications is increasing, and to reach this degree of accuracy, it is necessary to provide advanced manufacturing capabilities. So, ultra-precision grinding can manufacture high-precision parts in advanced applications such as medical and optical industries (Hadad and Sadeghi, 2012). The UP- grinding operation mainly produces components of higher quality and greater functionality that are hard to machine by other methods. The goal of ultra- precision grinding is to create high-surface finished parts, high precise shapes, and accurate dimensions for the electronics field and optical and astronomical applications (Doman et al., 2009).

The two basic components of grinding tools are abrasive and binder; they are the main substances of the device; the abrasive substance often takes the form of granules whose accuracy is based on the degree of finishing and expected quality of the machined surface (Chen et al., 2002). Abrasive materials are complex materials that can scratch or cut the most known metals and engineering materials. The compositions of the abrasive material are numerous and can be divided into natural substances such as silica, sand, or diamonds; these include abrasive powder consisting of AL2O or diamond granules (Tawakoli et al., 2009).

The abrasive material can also be made from industrial materials like boron and nitride carbide, aluminium oxide AL2O3, and silicon carbide Sic. All these substances, whether natural or industrial, contain mainly oxides or carbides because of their high mechanical properties, ability to withstand high temperatures, and control the size of their granules, especially those manufactured artificially (Ichida, 2008). At the same time, the bonding material's function is to bind the abrasive granules to each other and so-called a bonding material (Yang et al., 2021).

The selection of a suitable grinding tool is challenging to decide, specifically because of the diversity of factors affecting the properties of the tool and the wide range allowed to use each tool, except the usual ones, which are called tools for general purposes. Therefore, the selection of the grinding tool is subject to the cutting conditions and the machining material (Eren Sarici and Ozdemir, 2018).

The ultra-precision grinding technology has not been fully discovered. Still, many engineering applications rely mainly on authentic products that can be obtained if machined using ultra-precision grinding technologies (Brinksmeier et al., 2010). These applications include optics, electronics, and semiconductors, and the inclusion of ultra-precision grinding technology in advanced applications such as lenses and optical components that need high surface quality is required. And as manufacturing progresses elevate, the need to develop this technology increases to accommodate various cutting features and mass production methods (Setti et al., 2015).

Another category is the UP- polishing process which is a primary processing method for machining parts that require high surface quality and high cut dimensions accuracies, such as optical moulds and medical components (Xia et al., 2020). Optical mould materials include hard work materials like silicon and tungsten carbide because they resist corrosion and oxidation, they have a low coefficient of thermal expansion and have high rigidity. Ultra-precise polishing has been developed to serve in the manufacturing of optics and moulds that require high-accuracy parts.

Ultra-precision polishing aims to produce nano-scale machined surfaces, or even sub-nanometer levels, by removing excessive materials with a low depth of cut (Ren et al., 2019). The tool marks are visible on the machined surface when employing the turning process for machining. The ultra-precision polishing process is recommended to get rid of these marks and

has a clear surface topography. Polishing is required to improve the machined surface and remove any surface defects. The increasing demand for the high mirror surface motivated the need to utilize ultra-precision polishing technologies. Since high-surface integrity parts are needed in the optical and medical industries, ultra-precision polishing is under continuous development and exploration (Cheung et al., 2010).

Ultra-precision polishing employs special abrasives that are directed into the sample and pressed against its surface. Abrasives support the polishing process to achieve sufficient friction to remove the remaining machining defects. In this way, very low surface roughness is obtained. Mainly ultra-precision polishing is employed as the last step to ensure getting parts are free from surface defects. Ultra-precision polishing is suitable for making products of high accuracy, such as optical lens moulds used in injection moulding.

The polishing process for highly surface-machined components can be achieved mechanically and non-mechanically. Mechanical methods are widely used to finish the mould surfaces with the aid of abrasives against the inner sides for generating an elevated polished surface. The automated polishing processes are divided into different types according to the integrated tool used in the polishing process, as shown in Figure 2.2. Ultrasonic can accomplish mechanical polishing-assisted polishing, Fluid jet polishing, Bonnet polishing, and magnetorheological polishing. Bonnet polishing is the most used method in automated polishing processes, which can produce optical moulds of highly mirrored surfaces (Guo et al., 2019).

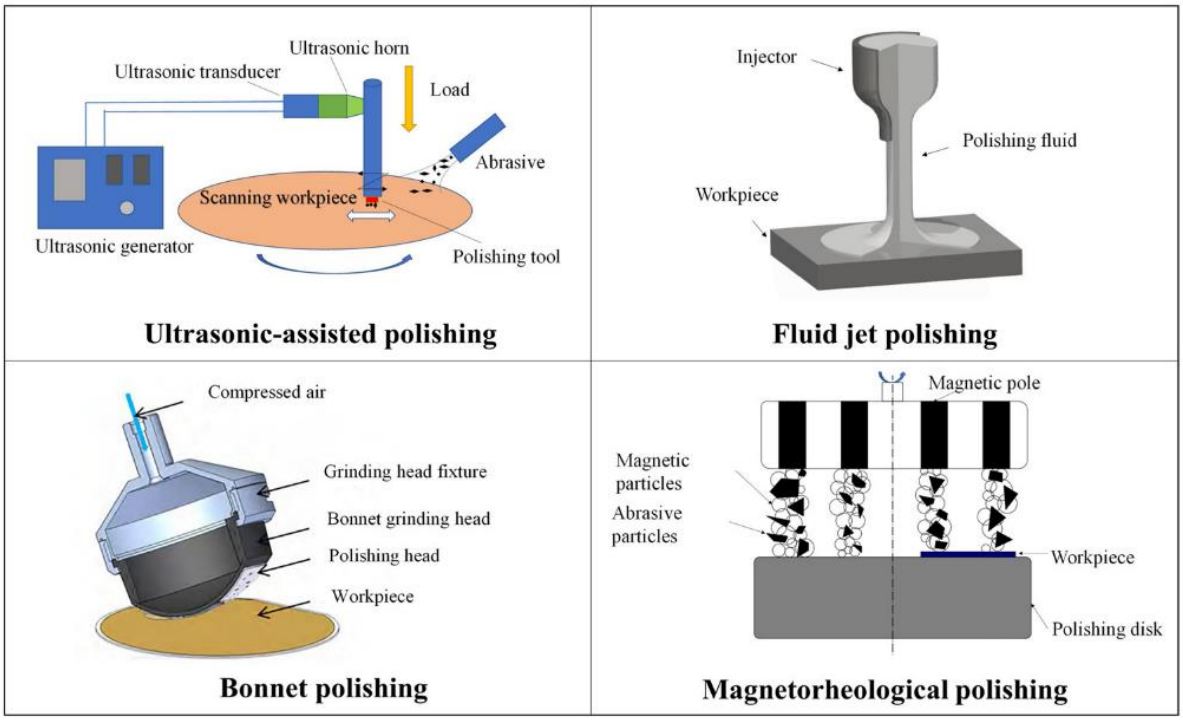

Figure 2.2 Mechanical polishing processes (Suzuki et al., 2006; Wang et al., 2015)

Metal cutting changes the shape of an initial mass material by removing the excess metal in the form of chips, such as in the milling process. With the development of mechanical operations, UPM operations are developed. UP-milling technology addresses many machining process challenges and is frequently used to produce high-quality parts (Zhang and To, 2013a). Milling is an important basic method of the mechanical machining operations and one of the common machine tools for metal removal operations. Milling uses cutting processes with high productivity of multiple cutting edges compared to turning, which uses a single-point cutting tool (Cheng et al., 2008).

The current advanced applications require parts with high accuracy, so manufacturers need to develop milling machines to carry out advanced processes and implement the industry's requirements. Milling is an operation that removes the material with a cutting tool with several edges distributed over its surroundings called the milling tool. The milling operation can

operate with high accuracy and make any complicated shapes and cavities as well as mirrored flat surfaces (Zhang and To, 2013b).

The milling machine has two main types according to the position of the cutting tool holder axis, as shown in Figure 2.3. If the axis is horizontally oriented, called a horizontal milling machine, and if the axis is vertical, called a vertical milling machine. There is a universal type where the cutting tool can rotate according to the horizontal and vertical axes. For cutting in horizontal or vertical millings, the workpiece is mounted on the table and moves in a linear feeding movement, and the cutting tool rotates during cutting. Horizontal milling is usually used in Peripheral down-milling processes, where the rotation axis column is in a horizontal direction parallel to the workpiece surface, and the cutting edges rotate during the movements of the workpiece (Tlusty, 2000). Such machines are used to operate flat, formed surfaces and form gear teeth. The vertical type is commonly used for face milling. It is named vertical for the vertical position of the head axis that is normal to the machine table. The cutting process is carried out by the cutting edges distributed at the perimeter of the cutting tool. These machines are used to produce surfaces with different groove shapes.

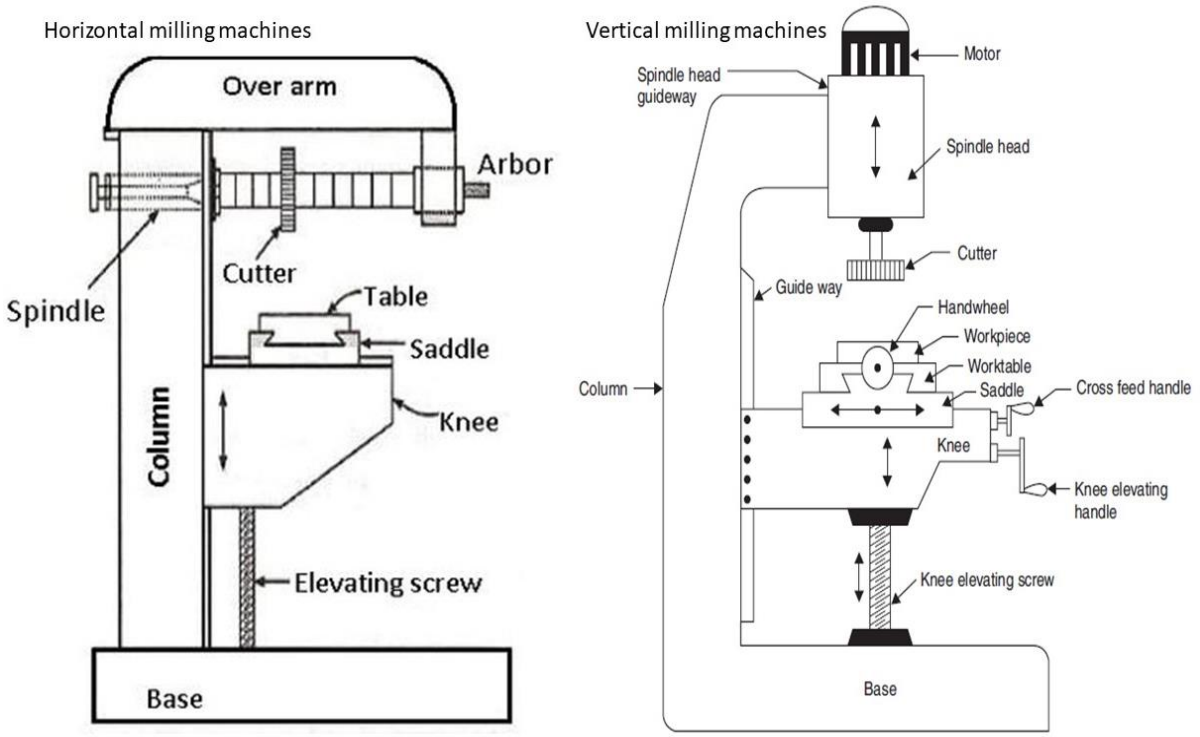

Figure 2.3 The Horizontal and Vertical traditional milling machines (Gupta and (Firm), 2009).

However, with the current increased development of industry and technology, conventional milling is not enough to meet the requirements of the advanced industries and applications. The ultra-precision raster milling process is employed to satisfy the growing demand for high-quality surfaces (Cheng et al., 2008). The manufacturing trend demands parts of freeform surfaces, which are difficult to obtain because of the involved complexity (Zhu et al., 2010).

The ultra-precision raster milling process is categorized into two main types based on the milling direction, horizontal and vertical, as shown in Figure 2.4. The decision to use either strategy is based on the process nature and cutting requirements. The raster and feed motions are the major feature of the raster-cutting operation. The main spindle always holds the cutting tool, which usually is made from diamonds, and they have the same rotation motion, and the materials are removed subsequently (Zhang et al., 2014a).

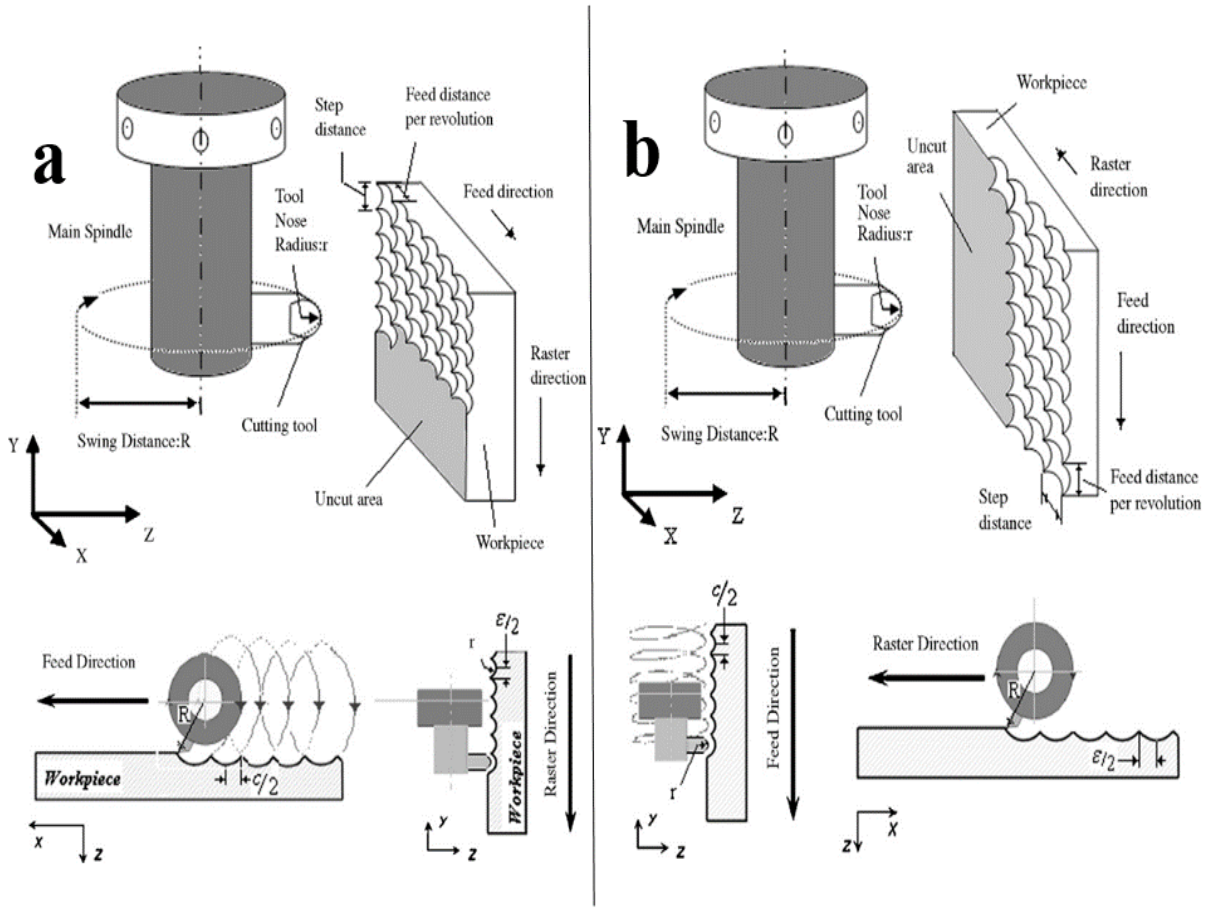

Figure 2.4 Cutting geometry for ultra-precision raster milling using a) Vertical cutting strategy and b) Horizontal cutting strategy (Kong et al., 2009).

So, employing UP-raster milling (UPRM) is a reasonable choice for producing high-quality freeform surfaces as UPRM is considered an advanced manufacturing process capable of reaching nanometric machined surfaces with high accuracy without subsequent finishing steps. Ultra-precision raster milling will be a convenient tool to accommodate a manufacturing process that leads to the manufacture of optics and electronics applications that require high-quality components (Zhang and To, 2015).

2.3 Ultra-precision diamond turning (UPDT)

The process of chip formation is a complicated physical and mechanical process because the work material suffers from elastic and plastic deformation to be removed by the

cutting machine tools. Normally chip formation is accompanied by intense friction between the cutting edge and the workpiece surface, resulting in a rising in heat production, winding of the chips, shrinking, hardening of the work material surface, and subsequently wear of the cutting tool (Zhong, 2002). To show the elastic and plastic behavior of the material, Figure 2.5 presents the stress and strain curve, which consists of the following points: Point A represents the limit of the proportionality, where strain is proportional to the stress under Hook's law relation, Point B represents the elastic limit, which is the limit at which the material can return to its first state after the disappearance of the force, Point C is the point at which the deformation begins and is called the yield point, Point D represents the maximum plastic deformation, where the stress reaches its maximum value and is called the ultimate stress point, Point E represents the stress at which the metal breaks and is called the fracture point, at which the strain increases with a clear decrease of stress, and this point is important for the metal cutting operation. In the plastic strain, some layers of metal move in the direction of slip plans that exist mainly with maximum shear stress. These slipping layers occur between the particles of the crystal. As a result, crystal shape and size change, and the plastic strain occurs accompanied by an extreme increase in temperature as well as metal's properties alterations (Meyers and Chawla, 1998; Kaufman and Rooy, 2021).

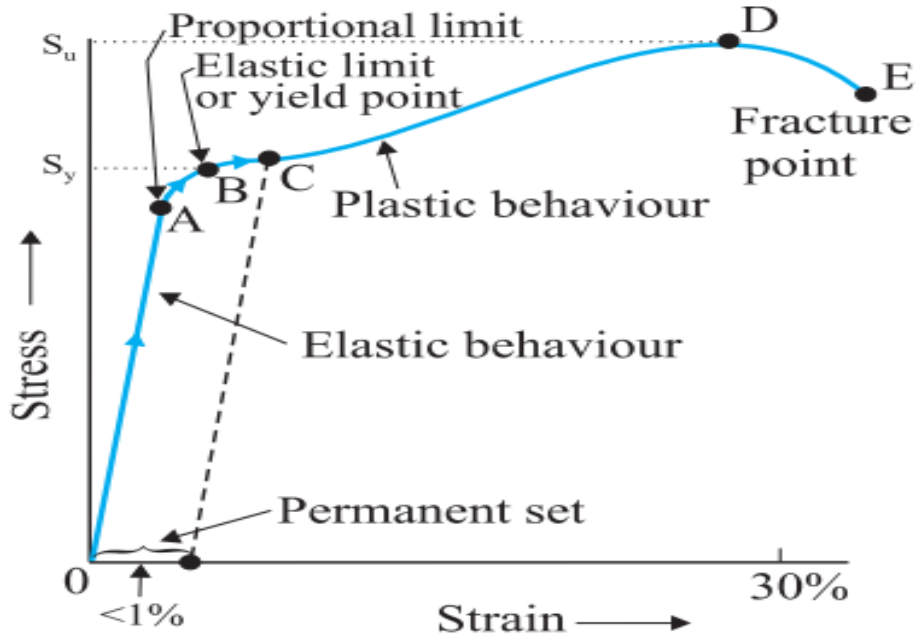

Figure 2.5 A typical stress-strain curve for a metal (Dowling, 1993).

SPDT is regarded as a main method employed in UPM technologies and manufacturing processes. SPDT can produce parts with proper forms, dimensions, and high surface integrity (Huang et al., 2018). The turning operation is a metal cutting process adopted to generate surfaces for cylindrical parts by a machine tool called the lathe. Mainly, the workpiece rotates with the rotational chuck, and the cutting tool feeds inside the workpiece either longitudinally, diagonally, or in both directions simultaneously to give the desired surface. In the general sense, the turning process is indicated to generate any surface with a single-point tool. It is often applied to generate external cylinder surfaces oriented parallel to the workpiece's axis. The longitudinal direction of feeding movement is prevalent in the turning process, and diagonal feeding is used to reduce the workpiece length or perform a facing operation. Both feeding types are needed simultaneously to perform a contour that often refers to a profiling operation.

When looking at how the Single point diamond turning machine works, it operates the same way the traditional lathe does. The ultra-precision turning machine contains a chuck to

hold the workpiece for cutting, and when the machine is turned on, the motor spins, and then the chuck and the workpiece become in a rotational motion. At the same time, the diamond cutting tool moves in a linear movement in the direction of the Z-axis or X-axis when required to complete the cutting and reach the desired shape of the product (Wu et al., 2005). SPDT is considered an advanced method to produce complicated elements that require many engineering considerations. This way provides parts of high surface integrity with final form quality without resorting to a post-machining process (Goel et al., 2012).

The demand for advanced materials that meet the requirements of difficult service conditions has increased the need and desire to develop new and innovative ways of manufacturing and machining. It's noticeable that there is significant progress in the accuracy of the machine tools over time, as shown in Figure 2.6. This progress is due to the growing demand for products with extreme accuracy and competition among machine tool manufacturers.

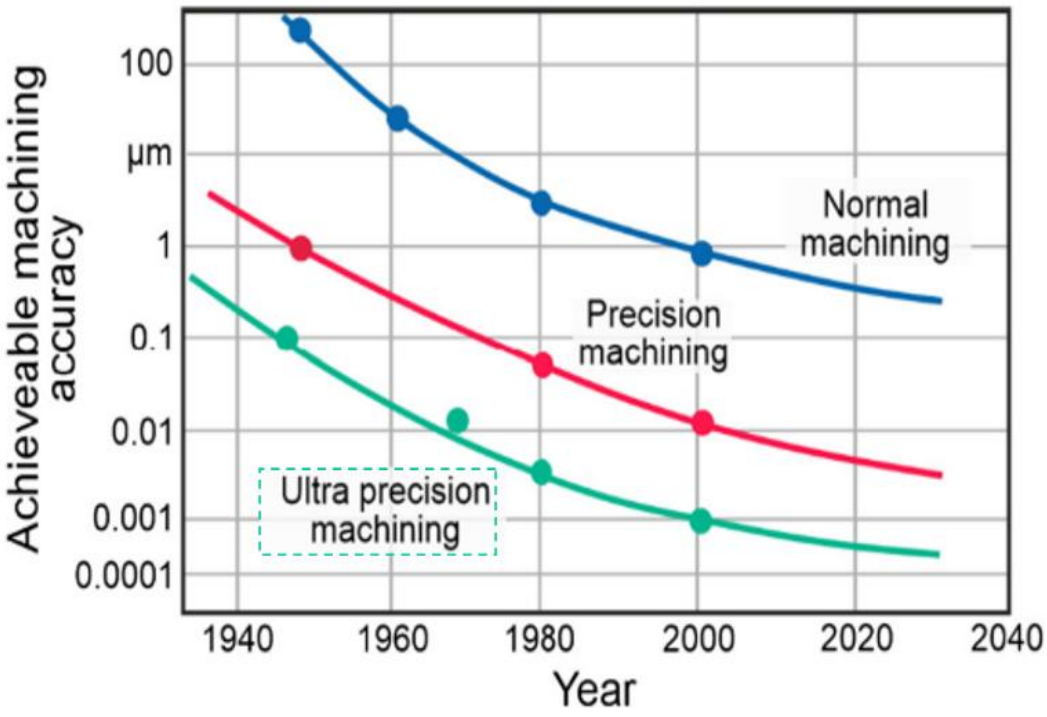

Figure 2.6 The machine tool accuracy advancement over the last decades (Taniguchi, 1983).

The cutting tool's operational time is defined as the time elapsed from the cutting tool starting the cutting process until they stop cutting due to the low-performance quality. The cutting tool has to be changed when the cutting edge reaches a stage where it's incapable of performing proper cutting, the geometry of the cutting angles changes, and the edges are not sharp.

The cutting tools are generally manufactured with standard specifications. They have the basic properties to cut different metals and remove as many chip layers as possible during their operation without changing their shape or losing their rigidity and properties. Therefore, mechanical properties such as hardness must be available in cutting tools and be sufficient to enable the cutting tool to penetrate the material to be cut and resist scratching and wear by the external mechanical effects. The cutting tools should have high strength able to withstand the high pressures, shocks, and stresses they are exposed to without being severely broken and to withstand high cutting speeds without diminishing their rigidity and ability to cut, mainly when

high temperatures exist in the cutting zone. The cutting tools should be hard enough to withstand high temperatures and have wear resistance, which is the cutting tool's ability not to decrease its size due to the friction during the penetration in the metal during the cutting processes.

Diamond tools are among the most solid materials to date compared to other cutting tool materials in terms of their mechanical properties and relatively cutting velocities. Diamonds are characterized by the fact that they consist of one chemical element: carbon. They are made up of pure carbon crystals. Although diamond cutting tools' hardness is higher than any other material, their use in machining cast iron and steel is limited due to the involved dynamic high cutting forces and thermal stresses. Diamond-cutting tools are used in the finish cut of metals such as aluminium and magnesium and in machining hard-cut alloys like titanium. The optimal use of diamond tools is to operate finishing processes for high-quality surfaces and to reach mirror surface quality if used in low values of cutting depth and feeding, as well as proper cooling.

However, one of the problems facing the SPDT in the UPM during cutting is the tool wear. Due to the continuous contact between the cutting tool and the workpiece for cutting, the cutting tool loses its sharpness, and the edges suffer wear, and this certainly affects the cutting operation negatively, and the cutting tool needs to be replaced with a new one (Zhang et al., 2014b). This wearing occurs mostly through the machining of hard-cut materials like Ti-6Al-4V, leading to low machined surface quality and affecting the cutting operation's performance and the high cost of maintaining a new cutting tool. Therefore, researchers must pay more attention, increase research on the tool wear issue, and develop cutting tools with an increased life span.

Cooling liquids protect the cutting tool and workpiece by sucking the heat from the cutting processes. The most common coolant used for this purpose is the mixture of water and sodium solution, soap, and mineral oils, which lead to rapid cooling because they have water as the main element. Many studies had to consider the cooling issue in their experiments. They applied many cooling and lubricant strategies, such as minimum quantity lubricant (MQL) (QIN et al., 2012), and others adopted cryogenic coolant (Bermingham et al., 2011). Also, other techniques, such as water vapour and flood cooling, as well as high-pressure cooling, were adopted, which all contributed to lessening the raised cutting temperature and, accordingly, the tool wear rate.

The chips are formed when the cutting edge presses against the workpiece in the turning processes, resulting in a groove on the workpiece surface that separates a metal part and continues to penetrate the material in this slit until the cutting edge removes materials from the metal surface as chips. The shape and state of the removed chips vary relating to the type of the work metal and the cutting conditions.

The process of chip formation is the essence of the cutting operations. The chipping occurs when the cutting-edge advances toward the workpiece to penetrate inside the material. This step leads to the separation of the metal in the form of chips, while the chips break up occurs due to the compression of a layer of the metal surface under the influence of the cutting tool force. As the plastic strain increases, the stress increases in the removed material. When the shear stresses reach and exceed the ultimate shear stress of the metal, the shearing occurs, and a massive separation of the metal or chipping appears. Such separation occurs towards the shear plane that forms a certain angle with the front face of the cutting tool. After the first chip part is removed, the second part begins to compress and distort the same way as the first part so that the stress exceeds the amount of the metal’s strength at the shear plane.

2.4 Mechanical and physical properties of titanium alloys

Mechanical properties are the reaction or behavior of any material under the influence of external forces. When any material is stripped to an external force, internal forces are created, trying to equalize the effect of these external forces. This behavior can be presented when considering the material as a spring when it is withdrawn or compressed by an external force, in which an internal force is created contrary and is noticed when the external forces are removed, the spring returns to its original state (Dowling, 1993).

When a sample of metal is subjected to a longitudinal pull force, it will suffer a noticeable change in its shape, so-called deformation. If the sample regains its original form after the disappearance of the effect of force, the sample has undergone elastic deformation. But if the sample does not recover its original condition, it suffers a plastic deformation. The amount of change of dimensions in the elastic deformation is very small since atoms were moved from their original positions, not by the amount that makes them move to new locations, so when the forces disappear, the atoms return to their original positions, and the sample regains its original form. Suppose the force's effect is enough to transfer atoms to new locations. In that case, the sample will not recover its original state after the disappearance of the force, and its deformation becomes permanent (Bowman, 2003).

The modulus of elasticity, tensile strength, and other mechanical properties are listed in Table 2.1. Most of the mechanical properties can be collected from the corresponding sample tensile test, which is considered the most important mechanical test for ease of conduct and the possibility of obtaining a variety of data that gives a clear picture of the most significant mechanical characteristics of the material (Rothbart and Wahl, 1964).

Table 2.1 Mechanical properties of commercially pure titanium and its alloys (Williams, 1981; González and Mirza-Rosca, 1999)

Material	Modulus (GPa)	Ultimate Tensile Strength (MPa)	Yield Strength (MPa)	Elongation (%)	Density (g/cc)	Type of Alloy
Cp Ti grade I	102	240	170	24	4.5	α
Cp Ti grade II	102	345	275	20	4.5	α
Cp Ti grade III	102	450	380	18	4.5	α
Cp Ti grade IV	104	550	483	15	4.5	α
Ti-6Al-4V- ELI	113	860	795	10	4.4	α + β
Ti-6Al-4V	113	930	860	10	4.4	α + β
Ti-6Al-7Nb	114	900–1050	880–950	8–15	4.4	α + β
Ti-5Al-2.5Fe	112	1020	895	15	4.4	α + β
Ti-15Zr-4Nb-2Ta-0.2Pd	94–99	715–919	693–806	18–28	4.4	α + β
Ti-29Nb-13Ta-4.6Zr	80	911	864	13.2	4.4	β

The tensile test of metals is carried out on samples with circular or rectangular sections with standard specifications. The sample is mounted between the jaws of the tensile test machine and is dominated by a pull force until the break. Advanced testing machines record the forces data in real-time with elongation. The mechanical properties derived from the tensile test are the modulus of elasticity, which can be extracted from the stress-strain curve in Figure 2.5, showing the proportionality limit at point A, and part OA is elastic deformation of the metal, which is a straight line that can be calculated from equation (2-1). The term "E" is known as the modulus of elasticity, which is also named young's modulus (Shigley, 1972).

$$E = \frac{\sigma\ (stress)}{\epsilon\ (strain)} \qquad (2\text{-}1)$$

While the ultimate strength is the highest value of stress in the stress-strain curve, this value is computed by drawing a horizontal line that is tangent to the stress-strain curve, and the amount of stress at the junction of the stress axis and this line is the greatest value of the stress

that is the ultimate. The figure also shows the yielding stress, which is significant in engineering applications, as it shows the amount of force that the metal bears before the plastic strain occurs. The yielding stress value can be obtained by drawing a straight line of strain equal to 0.002 parallel to the straight part of the stress-strain curve, and from the intersection of this line with the curve, a horizontal line is drawn to cut the stress axis at the yielding stress value. The percentage of elongation can also be obtained as it indicates the change in the length of the metal and is expressed in a ratio by equation (2-2) where L_f and L_0 are the final, and initial lengths of the sample, respectively and the percent of elongation at the breakpoint can be an indicator for the quality of the metal (Reddy, 1985).

$$\% \, Elongation = \frac{L_f - L_0}{L_0} \qquad (2\text{-}2)$$

Titanium alloys are distinctive materials for their high wear resistance and lack of reactivity with the human body. Based on these characteristics, using these materials could significantly benefit the biomedical industry. They also have excellent mechanical qualities, including a high strength, heat resistance, and exceptional corrosion resistance, making them appropriate for application in the offshore, maritime, aerospace, and power-generating industries allowing weight saving in space and marine environments. Titanium is a low-density element, about 60% of the steel density in which the alloy industry can be enhanced. Titanium is non-toxic and generally biologically compatible with human tissue and bones.

2.4.1 Applications of titanium alloys

Titanium alloys are utilized in many systems and fields. Their preference may be based on corrosion resistance or strength properties, with the additional biocompatibility features for applications involving biomedical implants (Koizumi et al., 2019). They are employed in

power-generating systems, tanks, heat exchangers, reactor vessels, and other corrosion applications. High-strength titanium alloys, including Ti-6Al-4V, are used in applications for high-strength performance, especially the Ti-6Al 4V alloy because it combines a group of remarkable properties, good workability, manufacturing availability, and high commercial supply (González and Mirza-Rosca, 1999).

Titanium alloys are employed extensively in advanced industries, particularly in engine and aircraft systems. Weight reduction and high strength are the main justification for adopting titanium alloys in the aircraft sector. Also, Al alloys can be replaced when working at high temperatures by Ti alloys. These characteristics illustrate why titanium alloys are desirable for use in spacecraft and aircraft applications (Peters et al., 2003). They have other benefits in armoured vehicles, helmets, jackets, jewellery, glasses, bicycles, sports gear, and particular dental implants (Williams, 1981), including power plants, other factory fields, roofs, columns, and different building parts. Moreover, titanium alloys are commonly used in the transplant industry; being light and biocompatible, they are utilized in making knees and artificial hips, vital compatibility that prevents biotic reactions inside the body (Smith et al., 2012). Due to their high corrosion resistance, titanium containers can be used as a long-term nuclear waste storage application.

Titanium alloys are involved in the manufacture of high-speed aircraft, marines, components of turbine engines and ships, and also used in missiles and internal combustion engines, scientific research laboratories, and chemical manufacturing being resistant to corrosion (González and Mirza-Rosca, 1999). Due to their high strength, titanium alloys have been used heavily in manufacturing multiple types of strong alloys. Many titanium compounds, particularly titanium dioxide compounds, are involved in the manufacture of white pigments, as well as in the manufacture of fireworks. Large quantities of titanium alloys are used to manufacture military tools and equipment such as aircraft and jet engines. Titanium is mixed

with steel to reduce carbon content. Titanium compounds are used in coatings as well as in the manufacture of plastics and toothpaste. Titanium is heavily used to manufacture multiple gemstones and the cement and graphite industries. Titanium can be adapted to manufacture medical tools and equipment (Kaur and Singh, 2019). They serve in the naval and spaceships industry (Ezugwu, 2005), as well as in the manufacture of missiles and tanks. They are also commonly utilized in automotive and engine parts owing to their lightweight and density.

Figure 2.7 Common applications of Titanium alloys (Mouritz, 2012; Niinomi, 2018).

2.4.2 Ultra-precision machining of Ti alloys

Titanium alloys' poor thermal conductivity during machining reduces heat transfer outside the machining area. Therefore, the elevated heat produced in the cutting zone has little dissipation. The localized heat causes tool wear at the cutting tool/workpiece contact, reducing tool life and degrading the workpiece's surface integrity (Arrazola et al., 2009). It is necessary to find strategies that preserve high surface integrity while cutting hard materials since machining difficult-to-cut materials frequently lead to low machined surface integrity, which also reduces the effectiveness of the cutting process (Maurotto et al., 2013). Finding methods to keep cutting hard materials with excellent surface integrity is crucial since machining difficult-to-cut work materials is considered the main source of low surface integrity, which also influences the efficiency of the cutting operation (Mir et al., 2016).

To achieve surface roughness (Ra) down to 1-100nm for machined parts serving in applications, including aerospace, aircraft, and biomedical field components, the industry relies on ultra-precision machining UPM. UPM involves a sufficient depth of cut, often ranging from tens of nanometers to a few micrometers (Komanduri et al., 2000), and does not require any further post-machining operations (Park et al., 1999). Surface finish assurance is essential to guarantee several functional features of the machined components. Diamond cutting tools are an effective tool in UPM of Ti alloys because they have excellent properties like high hardness, cutting edges of nano scales, high thermal conductivity, low friction, and high wear resistance.

Due to their unique qualities, titanium alloys offer a high potential in optical systems. However, Ti6Al4V's ultra-precision cutting mechanisms are challenging. Research into the titanium alloy's ultra-precision cutting mechanism hasn't been fully explored. Researchers use numerous techniques to address the machinability challenges of titanium alloys that comparatively have improved their machining performance. These techniques include optimizing cutting factors, addressing tool vibration while cutting, using advanced or coated cutting tools, using cooling methods of various kinds of lubricants, and utilizing physical approaches and treatment processes. Several researchers specializing in titanium alloy machining have enriched the research area associated with improving the machinability of titanium alloys. However, since metal cutting is a complicated process, additional studies and investigations are still needed to explore the cutting behaviour of Ti alloys.

The mechanisms of tool wear in titanium ultra-precision machining were investigated by (Zareena and Veldhuis, 2012b). In their investigation, titanium alloys were machined using single-crystal diamond cutting tools. According to their findings, the high pressure and cutting temperature at the tool-chip contact start a chemical reaction between titanium and diamond that causes the diamond tool to deteriorate. The titanium attachment to the tool's cutting-edge results from further chemical and mechanical interaction. The proposed experimental study has

postponed the development of conditions that would have caused quick titanium adhesion to the tool, extending the tool's life span and enabling the production of a larger final item using a single tool. Although using dry cutting reduces environmental pollution and health risks, limits and protects machine operators and technicians from illnesses, lowers costs, and prevents the occurrence of thermal shocks during interrupted cutting. Still, the absence of cutting cooling fluids and lubricants restricts the cutting velocity. This results in high induced cutting temperature, excessive heat, and rapid tool wear, causing integral machining problems (Naumov et al., 2016).

Some researchers employed dry electrostatic cooling, which includes pumping ionized gas containing ozone molecules into the cutting zone. Dry electrostatic cooling is an affordable, environmentally friendly method that has been found to increase tool life (Da Silva et al., 2013). To reduce temperature, the roughness of the machined surface, and the cost of operating the work material. Other researchers proposed the minimum quantity lubrication (MQL) technique. This technique relies on directing a small amount of water and soluble oil toward the cutting edge. The method's drawbacks include potential health risks from mist creation (Veiga et al., 2013). The electro-pulsing treatment (EPT) technique was employed by other researchers for uplifting the cutting quality of Ti alloys. The (EPT) technology is a functional adoption procedure and an efficient substitute for conventional thermal treatment methods, as a result of increased plasticity, the surface quality could be improved in machining and metal forming (To et al., 2010). Many studies examined the cutting process and the main factors affecting the generation of high-integrity machined surfaces of titanium alloys in UPM. These studies, however, had limitations in reaching the high expected quality. These studies worked to direct attention to the problems facing precision cutting without offering decent solutions to overcome these challenges and problems; therefore, it is necessary to develop and mobilize the UPM to reach products operated in high quality.

2.5 The magnetic field in the machining technologies

Some limitations, such as a lack of response to the current advanced manufacturing techniques and the high demand for accurately processed components, restrict non-conventional machining. So, developing new methods like hybrid machining processes is urgent. The concept of hybrid machining is to associate different machining processes with an existing physical theory to elevate the efficiency of the whole manufacturing process and obtain components with an improved machining performance. The primary purpose of the hybrid machining method is to benefit from a group of processes instead of applying a single method, which signifies the impact of the hybrid process to have high capability and enhance the overall processes (Dandekar et al., 2010). There is a trend to implement and initiate novel methods that adopt hybrid approaches due to the high demand of the current advanced industry and the requirements of the super machining technology. Based on the growing demand to provide high-quality parts with complexities in shape and geometry, existing operating methods could not meet the requirements. So, it is necessary to find combined methods capable of achieving these high requirements. The hybrid processes came to combine a group of manufacturing processes or take advantage of the existing physical theories (Saxena et al., 2018).

Magnet is an important material, and one of physics's most significant discoveries emerged. Since discovering the idea of magnetism, researchers have tried to find uses for and utilize the effects emanating from the magnets. With the beginning of development, industrial magnets were manufactured and modified as observed today, and have been used widely, especially in the field of transportation, electric trains, motors, electric devices, computers, sound and image recorders such as hard drives, cassettes and other devices used by physicists. Also, the use of the magnetic field has spread in manufacturing processes that require magnetic phenomena to develop some operations, such as metal cutting processes, which is the main topic of this study.

2.5.1 Generation of the magnetic field

The magnetic field can exist in two forms, either in a permanent magnetic field or an electromagnetic field. Today, no one argues about permanent magnets' wide use in our daily life, like phones, wireless transmitters, and other electrical products. Permanent magnets are sustainable; if a magnetic rod is broken, two pieces of magnets will exist, each with a north and south pole, and with successive breaking, the presence of magnet poles continues to exist until the smallest part of the rod, as shown in Figure 2.8 (Richtmyer, 1964).

In 1820, Dane Hans Christian Oersted discovered that electrical currents generate magnetic fields (Oersted, n.d.). This was followed by a series of discoveries by many scientists related to magnetism and its relationship to currents and electric fields, such as the American Joseph Henry and the Danish Michael Faraday, whose works showed that electricity could be generated by moving magnets (Ionescu-Pallas, 1972).

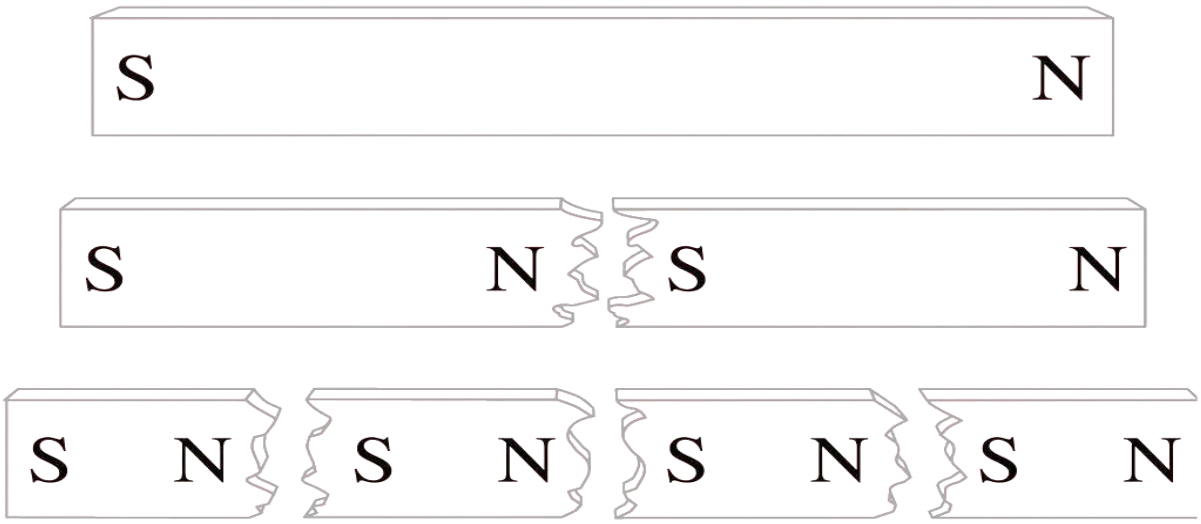

Figure 2.8 The magnetic poles of a broken rod (Pearson Education, 2012).

It's known that electrical charges affect any close charge with electrical force, which means the electrical charge has an electric field (Kraus et al., 1984). By comparison, magnets also affect the magnetic materials nearby, and the strength of magnetic attraction is

concentrated in its poles and decreases in other areas, as shown in Figure 2.9. From this, it turns out that there is an area surrounding the magnets from all sides and at all levels where the effect of magnetic force is shown called the magnetic field, and since the magnetic field is not visible, its effect can be shown by iron pieces or using a compass.

Figure 2.9 The strength of the magnetic field and concentration areas.

Magnetic materials are influenced by the magnetic field's strength when positioned in a magnetized environment. The indication of the magnetic force lines can define the intensity of the magnetic field at some point; the value of intensity at that point is the number of magnetic force lines in the unit of area that traverse a vertical surface on a magnetic field close to point (Planck, 1932). The total number of magnetic force lines that cross the surface is called the magnetic flux (ϕ). The magnetic flux penetrating the surface of area A can be expressed in equation (2-3).

$$\phi = BA\cos\theta \qquad (2\text{-}3)$$

When the area vector is perpendicular to the field vector B, i.e., when the angle θ is 90°, then the magnetic flux value is zero because there are no magnetic force lines that penetrate the surface area, and the magnetic flux becomes a maximum value when the angle θ is zero or 180° as shown in Figure 2.10, and the flux is then positive or negative. The state in which the magnetic flux is positive indicates that magnetic force lines are in the direction of exiting the

surface. If the magnetic flux signal is negative, it indicates that the force lines are inside the surface. In both cases, the equation can be simplified as $\phi = \pm BA$.

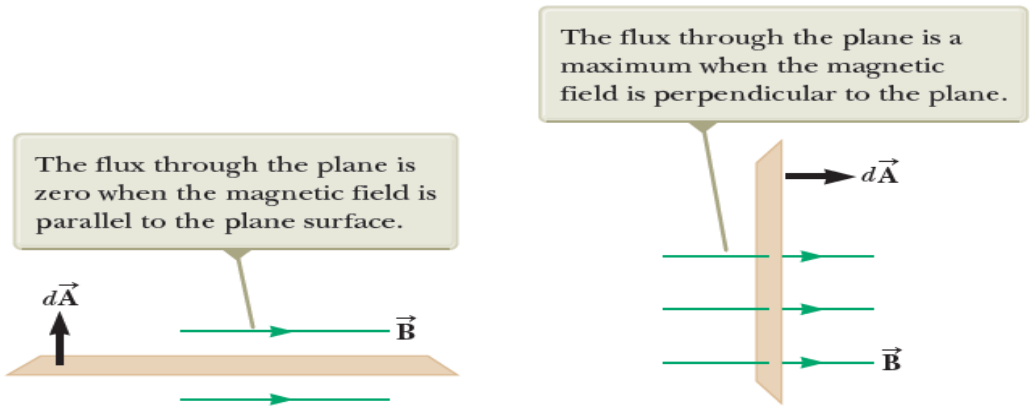

Figure 2.10 Magnetic flux through a surface (Chart, 1997).

In 1819, the Danish physicist Oersted indicated that the magnetic field of a wire carrying an electric current affects a magnetic needle placed nearby. Faraday showed the opposite effect of this phenomenon. He reported that the magnetic field could affect the conductive wire with equal magnetic forces (Stauffer, 1957; Raychaudhuri, 2022).

After Oersted discovered the magnetic effect of a wire-carrying current in 1819, Biot-Savart conducted several experiments with which the outcome was to build a mathematical relationship, as shown in Figure 2.11, to calculate the magnetic field intensity of at any point in the space around a conductive wire carrying an electric current (Mikerov, 2014; Dibner, 1961b). This mathematical model is known as Biot-Savart's law, as shown in equation (2-4), where the u_0 is the magnetic permeability (Wb/amp.m).

$$dB = \frac{u_0 Idsxr}{4\pi r^2} \qquad (2\text{-}4)$$

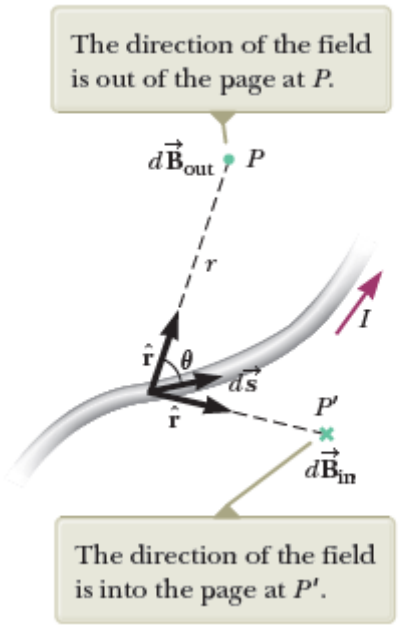

Figure 2.11 Magnetic field of a conductor carrying current (Chart, 1997).

2.5.2 The applications of the magnetic field in manufacturing

El Mansori et al. (2003) explored the application of the electromotive force (EMF) influence by implementing an external magnetic field when machining a work material of mild steel with considering the effect of cutting speeds. The exploration concluded with lowered values of flank wear of the HSS cutting tool that contributed to the extension of tool life. Wu et al. (2015) proposed a novel ultra-precision magnetic abrasive finishing (MAF) method that, when using an alternating magnetic field with a low-frequency, effectively reduced the surface roughness of stainless-steel samples. A tool for creating a magnetic field called magnetic field-assisted finishing (MFAF) was created by Fan et al. (2019) and utilized on Ti-6Al-4 V alloy to improve the surface quality significantly. De Bruijn et al. (CIRP and 1978, n.d.) utilized a magnetic field to clear the EDM process discharge gap and offered a magnetic field for accelerating the gap cleaning process to upgrade the EDM process machining environment. Other researchers have assisted the electric discharge machining (EDM) with magnetic force to eliminate the debris particles from the machining space to improve the machining efficiency (Yamaguchi and Shinmura, 2004; Lin et al., 2009). This research and others demonstrate the

viability of bringing the magnetic field to the different machining processes, as well as the efficiency of this method and its capability to enhance overall cutting performance. In ultra-precision machining, Yip and To (2019) reduced the minimum cutting thickness of Ti-6Al-4V alloy using single-point diamond turning and improved the machined surface quality when the magnetic field was present.

2.5.3 Principle of magnetic field-assisted machining effect

The magnetic field has been widely used in many manufacturing sectors as a complementary system to benefit production; it can be coupled with various processes to enhance process efficiency. The magnetic field is commonly utilized in EDM to increase the debris removal rate in cutting processes, where the created force by the magnetic field is combined with a conventional EDM machine to achieve a successful magnetic field-assisted EDM process to improve the overall machining performance (Lin and Lee, 2008). Also, ultra-precision machining UPM technology utilizes the magnetic field, where the expected grade of the machined parts is high, and the products offer a wide range of advanced applications. As a result, importing such hybrid machining into UPM technology has the potential to enhance the cutting process and increase product quality significantly.

Referring to previous research, the physical characteristics of ferrometals, such as thermal conductivity, can be increased when exposed to a magnetic field, and this has been explained by the movement of molecules and their arrangement from their irregular position by the Law of Van der Waals to a regular and straight state when subjected to an applied magnetic field. Accordingly, the rate of heat transfer increases as these molecules line up and act as extended paths for conveying heat. To demonstrate this concept, in literature, experiments have been performed with the magnetic field as a factor to measure the thermal conduction of the ferrofluid and proved the enhancement of the thermal conductivity when

magnetic fields are applied. Also, it was reported that the magnetic field elevated the thermal conduction of the ferrofluid containing Fe_3O_4 particles for the same reason when the magnetic field changes the random state of the particles to be regular and aligned to facilitate conveying of the heat.

The effect of the Van der Waals forces helps the particles attach randomly, as well as the impact of the dipole-dipole interaction; when a magnetic field is present, the alignment occurs, and a chain of magnet particles acts as a conduit for heat transmission. It is known that during titanium alloy machining, heat is retained within the cutting zone due to the disability of these alloys to convey the thermal energy, which reveals the lack of titanium to deliver the generated heat. And as reported, the thermophysical properties of materials can be adjusted by establishing a hybrid approaches system. Ti-6Al-4V alloy was subjected to a magnetic field in this study during the turning operation to facilitate the translocation of the chips and increase the produced heat dissipation from the cutting zone. Consequently, the excessive temperature in the machining area is no longer a dominant factor for tool wear for both surface quality and hazardous lubricant.

In this study, modeling of the magnetic field distribution in the cutting environment was presented using the finite element analysis method (FEA), and the magnetic field was directed to the cutting zone. The results of the finite element analysis modeling, magnetic flux simulation, and distribution density were presented. With the help of the FEM, the effect of the magnetic field system and the magnetic system simulation in the cutting environment were demonstrated. Also, the impact of the thermal characteristics of the work material was explored using the ABAQUS platform. The cutting experiments validated the simulation results and revealed the effectiveness of the MFAM in achieving improved machining efficiency and lengthened tool life while enhancing the thermal properties of the machined components.

2.5.4 Magnetic field in electro machining process

Since electro-machining technology is capable of machining super hard materials and significantly impacts cutting performance, it is classified as non-conventional machining technology in machining methods. Electro machining technology applies two separate processes to accomplish the discharge corrosion effect. Namely, electrical discharge machining (EDM) and electrochemical machining (ECM) (Lin et al., 2009). The EDM relies on the promotion of the material's ionization process. The dielectric at the cutting space between this electrode and the material's surface is achieved by activating a high voltage (Lin and Lee, 2008). The density of the free electron keeps increasing until a certain value at which the high-temperature plasma forms and delivers heat to the material to evaporate and melt, achieving the cutting. While in electrochemical machining (ECM), as a result of an external electric field, the anode material works to ionize the free electrons, and electrochemical reactions occur between the electrolyte and charged particles, then the anode substance dissolves (Ayyappan et al., 2017).

The cutting is achieved by the effect of the discharge corrosion occurring from the electrode to the workpiece resulting in the creation of surfaces of reasonable quality. However, the application of electro machining method is not optimal for all cutting conditions due to the traditional machining issues and instability but engaging the magnetism with electricity assisted in raising the expectation of the cutting performance and was combined to upgrade the cutting performance of electro-machining and enhance the precision and surface grades of the parts.

2.5.5 Magnetic field in electric discharge machining (EDM) process

Electrical discharge machining (EDM) is a thermal cutting process that removes the excess material without contacting the workpiece. EDM is classified as a method that benefits

from the thermal physical concept to remove excess metal. EDM has a high ability to operate hard and brittle materials and obtain exceptional forms. It is one of the most widespread methods in the industry and has made progress in manufacturing moulds and Products with complicated shapes. The principle work of the EDM process in cutting depends on the generation of an electrical spark resulting from a loaded wide discharge in the cutting area that is sufficient to remove part of the metal due to the highly generated heat that is capable of melting or evaporating a tiny space, i.e., it removes a small part of the cutting area. This method is used for electrically conductive materials and is used heavily in manufacturing molds and hard materials' workpieces (M et al., 2022; Zhang et al., 2021a).

There are challenges in the mechanism of operating metals using electrical discharge, and the development of new ways to manage these challenges became necessary. The removed materials in the EDM process are formed as small particles that crowd near the cutting area, preventing smooth cutting performance as these particles prevent the deionization process and generate unwanted pulse discharge. When debris enters the processing gap, causing sparks to be discharged after the basic cutting process again, this causes the discharge rate to rise incompatibly. The accumulated debris reduces productivity and lowers the MRR; this leads to the necessity of removing this debris from the cutting area and cleaning up the gaps that are responsible for the success of the cutting.

The magnetic field was engaged in increasing the rate of metal removal, getting higher surface quality, and providing environmental conservation. Researchers reported that by employing the magnetic field, the obtained results were improved significantly, showing that the products can outperform the traditional methods in terms of the performance of the operation process and maintain the cutting tool (Zhang et al., 2016; Naveen Anthuvan et al., 2021). The setup of the magnetic field-assisted EDM process is shown in Figure 2.12. Much research has explored the process of electrical discharging machining helped by the magnetic

field. In the EDM process, removing the debris is a critical step that allows for a smooth continuous cutting operation. So, Bruijn et al. (CIRP and 1978, n.d.) utilized the magnetic force to get rid of the remaining crowded chips and accomplished the debris removal by surrounding the cutting zone with an external magnetic field that achieved high cutting quality. Some studies explored the operational principles and theoretical underpinnings of the magnetic field-based electrical discharge mechanism (MF-EDM). Then they examined the effects of magnetic fields on the operating behaviour, involving discharge state, MRR, and other factors, surface quality, and complexity of the produced forms. Since a magnetic field enhances the debris removal rate from the cutting zone and prevents its accumulation, the overall cutting performance improves effectively (Zhang et al., 2021a; Ming et al., 2021).

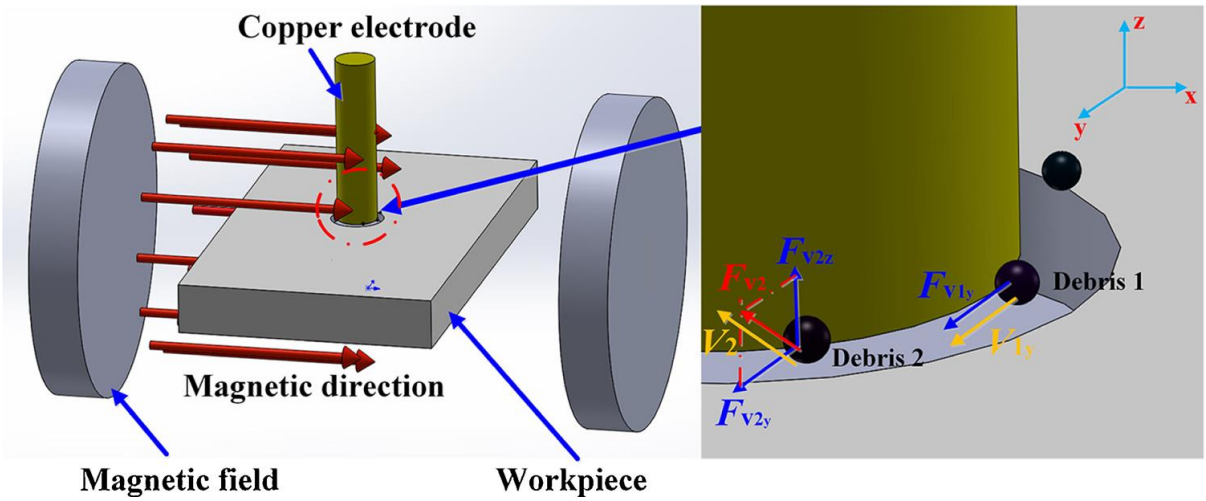

Figure 2.12 The Motion and force of charged debris in the magnetic field-assisted EDM process (Zhang et al., 2020, 2021).

2.5.6 Magnetic field in electrochemical discharge milling (ECDM) process

Electrochemical machining (ECM) is a cutting process that removes the excess materials through anode film dissolution with low performance and low surface integrity. The produced parts have poor surface quality unless machined under the magnetic field's installation which can alter the anode film's response and control the electrolyte flow state. Fan et al. (2008) examined the impact of the magnetic field on the anode film impedance of CrWMn

during an electrochemical machining process. The experiments were carried out using a setup of permanent magnet material that was mounted on the cathode, and the magnetic field affected the anode and generated a more concentrated anode film that made the dissolution of the workpiece more advanced and improved the cutting behaviour regarding the accuracy and quality and reduced the machining errors as well.

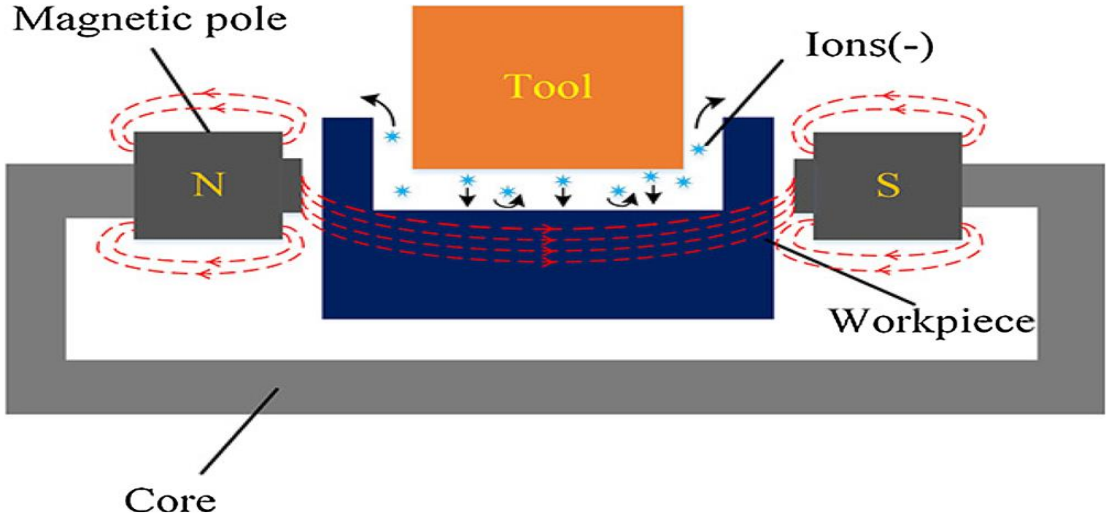

Figure 2.13 Interaction of magnetic flux lines with tool and workpiece (Ayyappan et al., 2017).

Controlling the flow field properly aids to benefit the material removal process and electrolyte circulation so that the machining efficiency can be uplifted, and the surface features can be enhanced. Ayappan et al. (2017) utilized the magnetic field and installed a unit of the magnetic system out of the cutting region, as presented in Figure 2.13. The lines of the magnetic induction affected the process, and the Lorentz forces altered the ion trajectories. The electrochemical machining process has many parameters that influence the cutting performance. The voltage setting is one of them that is related directly to the magnetic field. The voltage value should be set in accordance with the magnetic field; the high voltage leads to poor machining performance due to the excessively generated heat. In the case of low

voltage, insufficient dissolution will occur (Zhang et al., 2021b). In general, the magnetic field helped improve the material removal rate and the electrochemical cutting process.

2.5.7 Magnetic field for ultra-precision machining

In the literature review, many recent studies directed to bring physical approaches into the manufacturing processes and operations to raise the efficiency of production performance and meet the requirements of advanced material applications. Most studies have brought hybrid methods incorporating different techniques to benefit the manufacturing process. Zhu et al. (2009) engaged the pre-treatment processes of the samples in the machining process to get highly machined components. And other studies utilized the magnetic field in conventional and non-conventional machining to enhance the cutting process quality (Yip and To, 2017a; Khalil et al., 2022; Kim et al., 1997). In this study, the results have shown an outstanding combination of the magnetic field with ultra-precision machining. The machined surface integrity was significantly upgraded, and the cutting tool wear rate was reduced. The obtained experimental results have shown the efficacy of the magnetic field in boosting the machinability of titanium alloys in UPM.

Several works analyzed the EDM process aided by the effect of the magnetic field to evaluate the effects of the magnetic force-assisted EDM on the cutting processes for improving the cutting performance and accomplishing a satisfying cutting efficiency (Lin and Lee, 2008). Kim et al. (1997) Combined Lorentz's force effect with the electrolytic finishing process and designed a new finishing process under the magnetic electrolytic abrasive polishing process to achieve higher efficiency and better surface grades. They presented the concept of modifying the process with magnetic field assistance, and its influence on the cutting process was explained and analyzed. Wu et al. (2015) Have used a low-frequency alternating magnetic field in the ultra-precision magnetic abrasive finishing (MAF) process. Their proposed study

targeted to be efficiently applied in ultra-precision finishing of flat and complicated surfaces. They investigated the machining performance for finishing SUS304 stainless steel plate, the cutting parameters were investigated with the magnetic field, and the experimental findings have shown that the process with the assistance of the magnetic field has achieved ultra-precision finishing of the super machined mirror surface category.

Yamaguchi and Shinmura (2004) Have examined the combination of the magnetic field with the finishing operation of the inner surface of alumina ceramic. Their experimental investigation was implemented on alumina ceramic tubes with the assistance of the magnetic field, considering the effects of the different cutting parameters. The process has achieved a relatively low surface roughness and produced surfaces of minimum residual stresses, and their presented study has improved the form accuracy and surface integrity.

To finish Ti-6Al-4V workpieces, Fan et al. (2019) have created a novel magnetic field-assisted finishing (MFAF) tool. A magnetic field generator that is built and combined with permanent magnets was used to generate alternating magnetic areas. Based on an established platform, experiments were carried out to confirm the efficiency of the suggested tool for polishing Ti-6Al-4 V workpieces. The findings demonstrate that with the help of the finishing parameters control and adjusting the finishing factors, improvements were achieved on the surface's roughness, and the surface scratches were much diminished.

2.6 Magnetic field diamond turning of Ti-6Al-4V alloy in ultra-precision machining

2.6.1 Overview

It became essential to carefully consider the various effects of industrial activities on the environment, especially after the late deterioration reached the global and humans. The irrational exploitation of resources and the exposure of some of them to depletion need to be considered in addition to the various forms of pollution that have threatened the safety of

human beings and other creatures and made an unstable future for the next generations. And in return, the manufacturing processes cannot continue their activities are unattended and affected by the environment since it is a source of economic and living inputs and an effective tool for the continuation of life. Although the industrial sector is the main driver of countries' economies, it is one of the most environmentally threatening elements due to the production patterns used. So, it is necessary to think about how to reduce these threats without harming the economic aspect of the industry because it is one of the most important factors for the continuity of nations (Cheung et al., 2015).

Traditional production manner is one of the main causes of environmental elements' degradation, particularly after the recent rapid technological developments in the world that have accelerated the accumulation of negative impacts on the environment. This deterioration has resulted in the emergence of new development concepts, the most important of which is sustainable development, which includes developing strategies to reduce environmental damage and preserve the environment, including a cleaner production strategy. Cleaner production points to the need to integrate new sustainable development methods into the production process, covering all stages of product life through adopting practices that consider these considerations. And this can be achieved by having environmentally friendly methods that create the right environment for its application. To support the application of this concept, many studies have addressed new manufacturing methods to achieve the goal of cleaner production (Mikulčić et al., 2022).

Manufacturing operations are currently active in a dynamic and rapidly changing environment. With increased interest in environmental problems, and the environmental aspect is being considered among the newest areas of production, most research studies have moved towards adopting strategies that take the environmental aspect within manufacturing to maintain and develop the strategy of cleaner production; this helps them to continue with a

clean industry (Cheung et al., 2015). Some studies reported that compliance with environmental requirements is an additional burden that increases production costs and harms the competitiveness of organizations and the industrial sector. And others demand that environmental standards are a useful mechanism for improving production efficiency and reducing negative environmental impacts. Hence, the need to know how adopting cleaner production technologies could increase the capacity of research tools and generate new manufacturing methods for preserving the environment (Khalili et al., 2015).

2.6.2 Cooling and lubrication

One of the main reasons preventing the realization of the clean production strategy is the use of lubricants in the industry, particularly in metal cutting. This use has resulted in many environmental problems that affect the environment and human beings. Liquid and solid waste, fumes rising in the air, and the irrational use of environmental resources are the most harmful reasons that come from the manufacturing processes. And these issues are sufficient reasons that contribute to making efforts move towards the search for a new operating pattern that takes into account the environmental dimension along with the manufacturing and economical to achieve sustainable development (Severo et al., 2015).

The oils as a material for lubrication were used thousands of years ago, and various natural and industrial oils are still used as a material for lubrication to this day. Lubrication was known in the modern era with the invention of steam machines, followed by the emergence of other driving powers such as electricity and petroleum, which significantly impacted the development of machinery and the advanced industries of this contemporary world. Different machines, whether small or large such as the small wristwatch and the largest such as turbines, cannot function to the fullest capacity without a lubricating material, as it is a necessary material for each mechanical element whose function is to generate or transport power.

When one part of a machine moves to contact with another part, resistance is generated between them is called friction. The higher this movement speed, the higher the friction and heat generated. The greater the force for the movement of machine parts is required to resist friction, resulting in a rise in emerging temperatures and the subsequent wear of these parts. Therefore, surfaces that encounter each other need to be hardened as high as possible to reduce friction forces; thus, lubrication and greasing can significantly reduce friction energy. Lubrication is a substance used to reduce friction and wear resulting from the movement between surfaces and to help the parts not to contact each other directly. This means that the lubrication process of the moving parts of different machine elements is an important basic step on which the validity and function of the machine depend. The presence of lubrication reflects the ease of movement of machine parts, the speed of operation, and the production quality, in addition to the lengthy process duration that could be achieved (Denkena et al., 2020).

Heat typically generates when surfaces are in contact with each other, especially if the two surfaces are of two incompatible metals. And these surfaces may weld with each other and then separate repeatedly, which leads to a severe deviation of the surface accuracy and wear due to friction, which is not desirable in metal cutting processes. So, adequate lubrication must be ensured on an ongoing basis. Oily materials are highly effective for lubrication and cooling because they are liquid and pure. The lubrication oil performs many functions in all operations, production, and cutting machines to reduce the lost power due to friction between moving surfaces, minimize elements' wear, and eliminate the heat caused by friction, especially in the long cutting processes. Hence, it works as a cooler; it can clean and maintain the sliding surfaces from wear and rust. The lubricant absorbs shocks and reduces noise, increases mechanical quality, prolongs the life span of the machine elements, and maintains the moving parts from consumption and replacement (Hong and Ding, 2001).

In metal cutting, cooling liquids are used to reduce the cutting tool's temperature resulting from friction due to the cutting edge's penetration into the workpiece surface, which contributes to increasing operation period and productivity. The most important function of the coolant is conveying the heat induced by the cutting process because a large amount of generated heat needs to be transported by a continuous cooling fluid flow to keep the cutting zone at a low temperature. During cutting, the tool edges are subjected to significant stress due to their penetration into the metal to be cut. This step leads to a sharp rise in temperature at the cutting area to achieve the chipping process. Ti-6Al-4V alloy is recognized as a difficult-to-cut material due to its low thermal conduction. Traditional ultra-precision machining of Ti-6Al-4V alloy requires a large amount of cooling fluids to lower the raised cutting temperature and prevent tool wear (Tan et al., 2020). The status of the formed chip and workpiece can be changed because of the strength, increasing friction, and the speed of cutting, and continuing to operate without proper cooling leads to poor surface and damaged cutting tool edges. In this case, the cutting tool must be removed for resharpening and then installed in the correct position or replaced by a new one, which causes more effort and a waste of time (Zhang et al., 2012).

This part concludes that the machining operations involve a normal growth in temperature that significantly influences the cutting tool's properties and the workpiece. So, a cooling mean should be adopted during operation or when needed to keep the cutting edges from rapidly consuming and to get a highly machined surface. From the literature, it’s found that there are certain temperatures to which the turning cutting tool rises for every cutting speed level for each material. The sharply high temperatures are directly related to the speed of cutting. Thus, it was proven that the temperature levels of the machining area and tool edges result from cutting speed which is considered the most significant factor, feed rate, the chips’ cross-section area, and the cutting tool material and geometry.

2.6.3 Cleaner production and environmental aspects in ultra-precision machining

Technicians use turning cutting tools to form and cut metals according to the required specifications. Turning cutting tools have different shapes and sizes based on the process of cutting needed plan (Stephenson and Agapiou, 1996). They consist of either one or two pieces with a holder and insert from a harder material than the holder; the insert is interchangeable (Kalpakjian, 1984). If the cutting tool edge is worn and cannot resume the cutting processes, it is, therefore, necessary to be replaced; otherwise, it will lead to poor machining performance (Hamdan et al., 2012; Stephenson and Agapiou, 2016).

Clean technologies balance industrial production with protection (Shokrani et al., 2012), and their adoption efficiently brings economic benefits to its users. To protect the environment in the context of sustainable development, economic institutions must include the environmental perspective in their policy to promote ecological orientation and make it more considered (Ming et al., 2019). As shown in Figure 2.14, When actual consumption equals sustainable consumption, sustainability can be attained. Life cycle assessment can help close the gap between current and consumption rates required to achieve sustainability. Environmental pollution, irrational use of resources, and inequities against the environment have made it imperative to direct human beings toward the environmental aspect of development, as the environment is the only medium in which human beings and organisms live and are inevitably be affected if it was affected (Shokoohi et al., 2015). The industry was used as a tool to exploit nature and its resources in irrational ways. The industrial revolution pushed productivity and consumption, continuing without concern for the environment and its resources (Lawal et al., 2013). Alternative methods must be implemented in line with the requirements of manufacturing and the environment through a change in the production methods' characteristics, the extension of the product's life is needed, and the reduction of

waste produced during manufacture and consumption should be considered to lessen its effects on the environment (Mia et al., 2018; Munsamy et al., 2014).

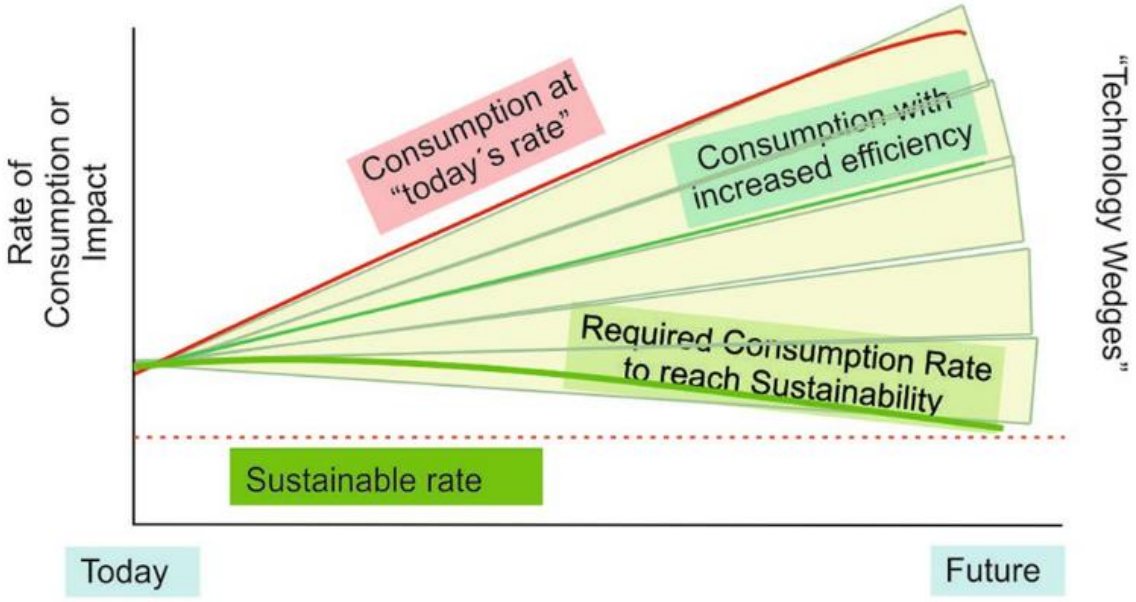

Figure 2.14 Consumption rate for sustainability (Dornfeld, 2011).

Applying cleaner production strategies, represented by changing the technology method or materials used, adopting preventive measures, and using modern techniques, leads to increased costs. It may alienate some production processes applying this strategy. However, in this study, costs have also been reduced with limited resources that do not affect the economic aspect (Jozić et al., 2022; Sacchelli et al., 2014).

Diamond cutting tools are used mainly in computer numerical controlled (CNC) machines in the final finishing step of accurately machined metals such as aluminium and magnesium and hard-to-cut materials like titanium (Stephenson and Agapiou, 1996). The diamond inserts are made from diamond powder and are usually fastened with the tool body by welding the insert or by casting a gap at the cutting tool tip (Stephenson and Agapiou, 2016; Wang et al., 2013). The rake angle normally used on external surfaces is zero. In contrast, on the interior surface, it ranges between 5-15 degrees, and when used for cutting at high speeds,

cooling liquids with high thermal conduction factors, such as oil, are used (Chetan et al., 2015). The appropriate use of diamond cutting tools is to operate in finishing processes for obtaining high-quality surfaces such as mirror surfaces if used at a low feed rate and reasonable cutting depth, as well as using appropriate cooling fluids. Supporting clean production, in this study, magnetic field diamond turning (MFDT) was utilized for improving thermal conductivity. Thus, Ti-6Al-4V alloy machined parts were improved with enhancing the diamond cutting tool lifetime.

2.7 Summary

In this chapter, the UPM technology was discussed, the SPDT and the mechanics of cutting were deeply analyzed, and the classification of the UPM technology was presented. SPDT can machine parts with proper forms, dimensions, and high surface integrity. The challenges of machining Titanium alloys were highlighted. Though titanium alloys have unique properties combining high strength with low density, high corrosion resistance, and non-toxic property that make them biologically compatible with the human body, they have low machining performance. The applications of Ti alloys were presented. Titanium alloys are used in manufacturing high-speed aircraft, marines, and ships, in missiles and internal combustion engines, and inside scientific research laboratories. The concept of hybrid machining was presented in the literature and shown how it was validated to associate different machining processes with an existing physical theory to elevate the efficiency of a whole manufacturing process and obtain components with improved quality. The magnetism property is important and useful for hybrid machining. The literature reviewed the recent studies that directed to bring the physical approaches into the manufacturing processes and operations to raise the efficiency of the process performance. The applications and generation of the magnetic field were discussed deeply, and magnetic field-assisted machining was also presented. Its assistance in electro, electric discharge, and electrochemical machining, including the processes' principle

work, was discussed. The equations identifying the magnetic field were also presented, the sources, calculations, and showing its effect on objects.

Chapter 3: Investigation of magnetic field system for Ultra-precision machining (MFUPM) of titanium alloys

3.1 Introduction

Because they have high wear resistance and lack reactivity with the human body, titanium alloys (Ti-6Al-4V) have unique advantages. Based on these characteristics, using titanium alloys could have a significant impact on the biomedical sector. They are ideal to be used in offshore, aerospace, marine, and power generation systems due to their excellent mechanical qualities, which include a high strength-to-weight ratio, heat resistance, and extraordinary corrosion resistance (Maurotto et al., 2013). However, titanium alloys are categorized as hard materials due to their poor thermal conductivity at high temperatures, which adversely affects their machinability. The titanium alloys' lack of thermal conduction minimizes heat transmission from the cutting region to the surrounding area during machining. Therefore, the heat produced in the cutting zone doesn’t dissipate properly. Localized heat causes tool wear and reduces the tool life and resulting in degrading the machined surface quality and integrity (Arrazola et al., 2009). The effectiveness of the cutting operation has an impact on the surface quality, which is mostly caused when machining difficult-to-cut materials. As a result, techniques for preserving high surface integrity when cutting difficult materials must be developed (Mir et al., 2016).

The cutting parameters and how they impact the cutting process have been the subject of numerous studies. In order to better understand how the cutting parameters affect surface quality, Hou et al. (2018) applied a multi-step cutting process to Ti6Al4V alloy. They identified the ideal cutting conditions for producing excellent surface quality in rough and semi-finishing operations. The optimal fit of cutting parameters was investigated by Ruibin and Wu (2016). They concluded that the best cutting performance of titanium alloys in single-point diamond

turning SPDT could be obtained by using a low feed rate, a short cutting depth, and a reasonably high cutting speed.

Liang and Liu (2017) studied the impact of tool flank wear on the surface quality of Ti6Al4V during orthogonal cutting and provided experimental results. However, analyzing the cutting parameters and how they affect surface quality is challenging and dependent on several variables, including the state of the cutting tool, cutting forces, and chip formation mechanisms. Researching the impact of a single element is challenging since the factors involved in cuttingi6Al4V are complicated, linked, and not independent (Yip et al., 2020). One of the factors causing poor surface integrity is the localized heat produced at the point where the workpiece and the cutting tool interact, which causes excessive heat in the cutting zone. Researchers used a variety of lubricant approaches, such as minimum quantity lubricant, to address this issue (QIN et al., 2012). Others used cryogenic fluid (Bermingham et al., 2011). In addition to high-pressure cooling, water vapour or flood cooling was also used to lessen the cutting temperature and surface roughness.

However, there are risks associated with these techniques for both the environment and the individuals. New cutting tools constructed of advanced cutting-edge materials were introduced based on several studies, which enhanced the machining operation (Yoshiaki et al., 2015). Although Da Silva et al. (2016) have shown the applicability of using a variety of cutting tools, including different materials like carbides, ceramic boron nitride (CBN), and polycrystalline diamond (PCD) tools, and showed the superiority of PCD over carbide and CBN tools, machining titanium alloys remains challenging, mainly when operating at high cutting speeds, due to the presence of tool wear that resulted in poor surface integrity. According to the literature, numerous techniques have been revealed to enhance the cutting capability of titanium alloys. Some have demonstrated improved machining by the optimized set of cutting parameters, the application of lubricants and cooling techniques to lower the

raised temperature and friction at the cutting region during the cutting operation, the prevention of heat confinement in the cutting zone, or the use of new cutting tool materials to achieve better surface quality and reduced tool wear.

Recent research has concentrated on applying physical principles, including pre-treatment procedures (Zhu et al., 2009) and magnetic fields (W. S. Yip and To, 2017b; Zhu et al., 2009), to manufacturing processes to enhance the cutting performance of difficult-to-cut materials. The electro-pulsing treatment (EPT) was engaged in a technique that incorporates physical theories and intends to modify the mechanical properties of the work material by reducing the value of the yielding stress after applying the EPT step to reach a smooth plastic deformation. Ultra-precision machining has been utilized after EPT. Lou and Wu (2017) performed ultra-precise machining tests on Ti6Al4V before and after EPT, demonstrating the efficiency of the procedure via comparison of the surface roughness and cutting force results.

The use of the machined work material is restricted to light-duty applications since the EPT decreased the work material's mechanical strength. To increase cutting performance, several researchers investigated how magnetic fields affected cutting operations (Lin and Lee, 2008). In order to improve the debris removal mechanism, which is a key step in electrical discharge machining (EDM), Bruijn et al. (CIRP and 1978, n.d.) applied an external magnetic field all around the cutting area. This technique utilized the magnetic force to produce high cutting quality. The utilization of the magnetic field was optimized by (Teimouri and Baseri 2014) to enhance the debris removal from the cutting gap in EDM. By introducing a magnetic field to the electrolytic finishing process, Kim et al. (1997) modified the electrolyte's path through ion migration, producing an enhanced surface finish and an efficient finishing process.

Several studies concentrated on finishing the parts’ surfaces by utilizing the magnetic field abrasive finishing process by applying an external magnetic field, which removes material

relying on the relative motion of the abrasive particles on the work material surface (Wu et al. 2016; Jayswal et al., 2005). This technique enhances cutting performance in finishing procedures, whether interior or external surfaces are being targeted (Guo et al., 2017). Other research connected the use of magnetic field to the finishing procedures like polishing, which utilized the magnetic field to create components with excellent surface integrity (Wang et al., 2020). D. Wang et al. (2004) used the magnetic field in the finishing process. They investigated the effects of the operational gaps and the magnetic field intensity on the workpiece's surface roughness, which were identified as dependent factors. D. Wang et al. (2004) adopted a finished process for a diffractive optical element (DOE) lens with magnetic field-assisted polishing, resulting in low surface roughness. Wu et al. (2015) presented a novel magnetic abrasive finishing (MAF) operation in ultra-precision machining to considerably reduce the surface roughness of samples manufactured of SUS304 stainless steel using a low-frequency alternating magnetic field. El Mansori et al. (2003) investigated the effects of an external electromotive force (EMF) when machining mild steel using a magnetic field. The results revealed decreased flank wear of the HSS tool, which resulted in a prolonged tool life. Fan et al. (2019) created a magnetic field-assisted finishing (MFAF) tool that was utilized in the cutting of Ti-6Al-4V alloy to upgrade the surface integrity greatly.

The experiments mentioned in the literature demonstrated the validity of introducing a magnetic field into the manufacturing process, the potency of this approach, and its capacity to enhance overall cutting performance. For achieving an efficient cutting performance of Ti6Al4V alloy during ultra-precision machining UPM, W. S. Yip and To (2017c) installed a magnetic field system with a SPDT machine. By utilizing a magnetic field, Wai Sze Yip and To (2019) increased the surface quality and decreased the minimum cutting thickness of Ti6Al4V alloy during ultra-precision diamond cutting (UPDC). In addition to utilizing the magnetic damping effect of the eddy current, W. S. Yip and To (2017a) suppressed the

variations of the values of cutting force in single-point diamond turning SPDT and reduced tool wear.

A review of relevant literature reveals a need to improve the machinability of difficult-to-cut materials such as Ti6Al4V alloy. Recent research has affirmed the viability of employing a magnetic field to enhance the single-point diamond-turning SPDT and cutting operations. This part's major objective and contribution are to use a magnetic field to perform hybrid ultra-precision cutting. The methods indicated in earlier studies did not achieve the highest expected machining quality because of the poor machinability of Ti alloys; additionally, the majority of the studies depended on conventional techniques to accomplish a smooth cutting process without attaining cutting tool preservation. Because titanium alloy machining is still in its early stages of research and development, developed methods to address titanium machining difficulties are needed. This study linked the UPM with the applied physical approaches to achieve proper SPDT performance of difficult-to-cut materials. Given the rising need for titanium alloy in the industry, it is necessary to research the machining of titanium alloy and its difficulties, including limited thermal conductivity, heat generated during cutting, high rate of tool wear, and low machined surfaces. This study fills a research gap by investigating the effects of magnetic fields on ultra-precision machining, demonstrating the feasibility of this method, and allowing for improved cutting performance and the production of parts with high surface quality made of titanium alloys. This study, therefore, integrated magnetic field-assisted machining with ultra-precision turning technology employing a single-point diamond cutting tool.

As the cutting process is based on a permanent magnet source, it is inexpensive, safe for the technician, and ecologically benign, which are all advantages of utilizing this technology. The findings demonstrated that machining with the magnetic field effect significantly improved the samples' surface roughness reaching 13.33 nm. The experimental

results show that the magnetic field affected the machining behavior of Ti-6Al-4V alloy in UPM, allowing for the production of parts with high-quality surfaces.

3.2 Working principle of magnetic field-assisted machining (MFAM)

The force acting on an object surrounded by a magnetic field is determined by the properties of both fields and the target object (Phys. Rev. E 73, 061919 (2006). Applying the "effective" dipole moment method (O'Handley, 1999), where an "equivalent" point dipole replaces a magnetic object has a moment m, the acting magnetic force on a magnetic microstructure can be modeled, and the force exerting on the dipole is defined by Eq. (3-1).

$$F_m = \mu_f(m_{p_{eff}}.\nabla)\ B \qquad (3\text{-}1)$$

Given that μ_f is the medium magnetic permeability, $m_{p_{eff}}$ is the object's "effective" dipole moment, and B is the magnetic field produced by an external source at the target object's center, where the corresponding point's dipole is situated. The dipole moment m can be defined as in Eq. (3-2), depending on the object's volume and magnetic properties:

$$m = MV \qquad (3\text{-}2)$$

M and V are the dipole's magnetization and volume, respectively. As mentioned, the magnetic field sources' characteristics are changed by applying force to such a dipole. Additionally, it is affected by the separation distance between the source and the object. Since the magnetic field source is in a permanent state in this study, Eq.(3-3) provides a calculation for the magnetic field density at the cutting zone, where r is the vector representing the distance between the field source and the object.

$$B = \frac{\mu_0}{4\Pi}\left(\frac{3\,(m.r)\,r}{|r|^5} - \frac{m}{|r|^3}\right) \quad (3\text{-}3)$$

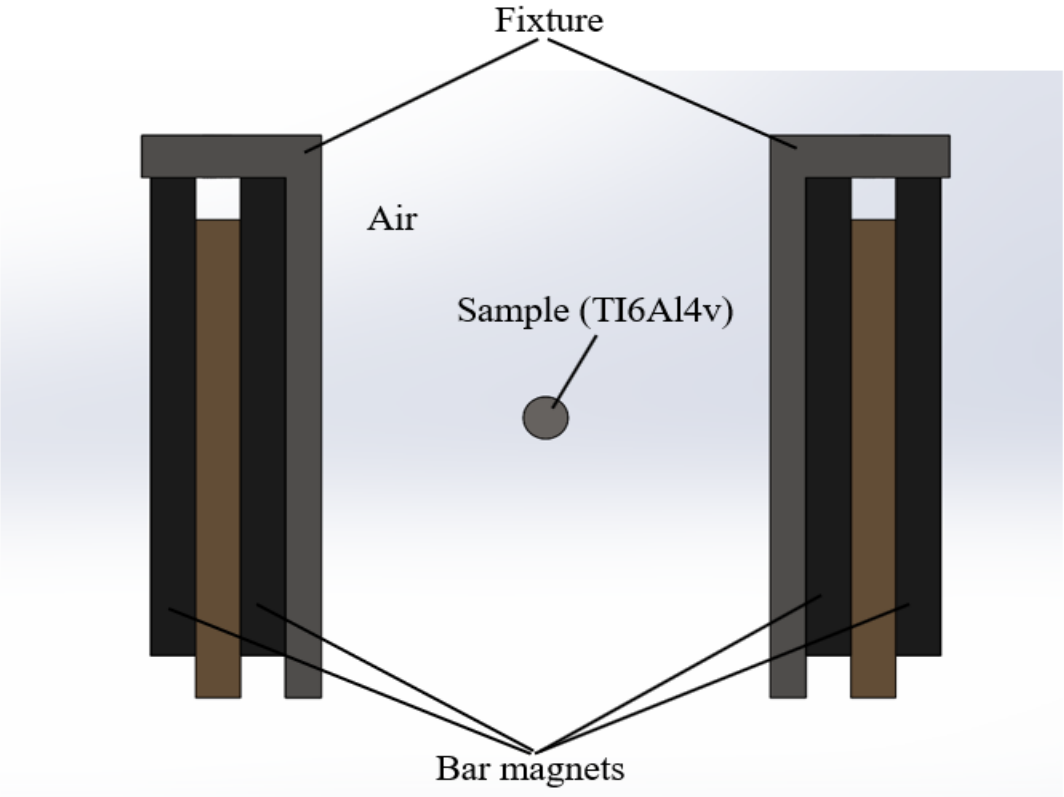

Figure 3.1 Magnetic field-assisted machining (MFAM) system.

Figure 3.1 displays the MFAM system's configuration. The existence of a magnetic field while operating the turning process aids in chip transit, avoiding the cutting tool from developing a built-up edge and preventing chips from sticking to the tool edge. Furthermore, the produced chips could exit the cutting area quickly, and reduces heat accumulation in the cutting zone, which is critical for the machining process's achievement.

3.3 Finite element analysis (FEA) of the magnetic field distribution

For the explanation of the applied magnetic field in the cutting experiments from the magnetic system, Figure 3.2(a-d) depicts the FEA modeling and magnetic field simulation results represented in magnetic flux density distribution by utilizing the magnet and

electromagnetic software (EMS). The finite element method FEM technique has been adopted to simulate the magnetic field system and provide the effect of the permanent magnet device. EMS is a simulation tool that uses accurate finite element modelling and meshing techniques to compute magnetic flux and the corresponding magnetic field. The model comprises four N42 neodymium magnets, a steel fixture to hold the magnets, and an aluminium fixture that serves as a chuck to hold the workpiece. Because the air surrounding the magnets is important, the air geometry was considered and modelled. The meshing was accomplished and controlled by choosing the element sizes of 5mm and 50 mesh elements per diagonal of each solid body. Maxwell's magnetic field law describes the magnetic flux in Eq. (3-4).

$$\emptyset = BAcos\Theta \qquad (3\text{-}4)$$

Where:

Ø=magnetic flux, B=magnetic field, A=area, and Θ=the angle between a perpendicular vector to the area(A) and the magnetic field(B).

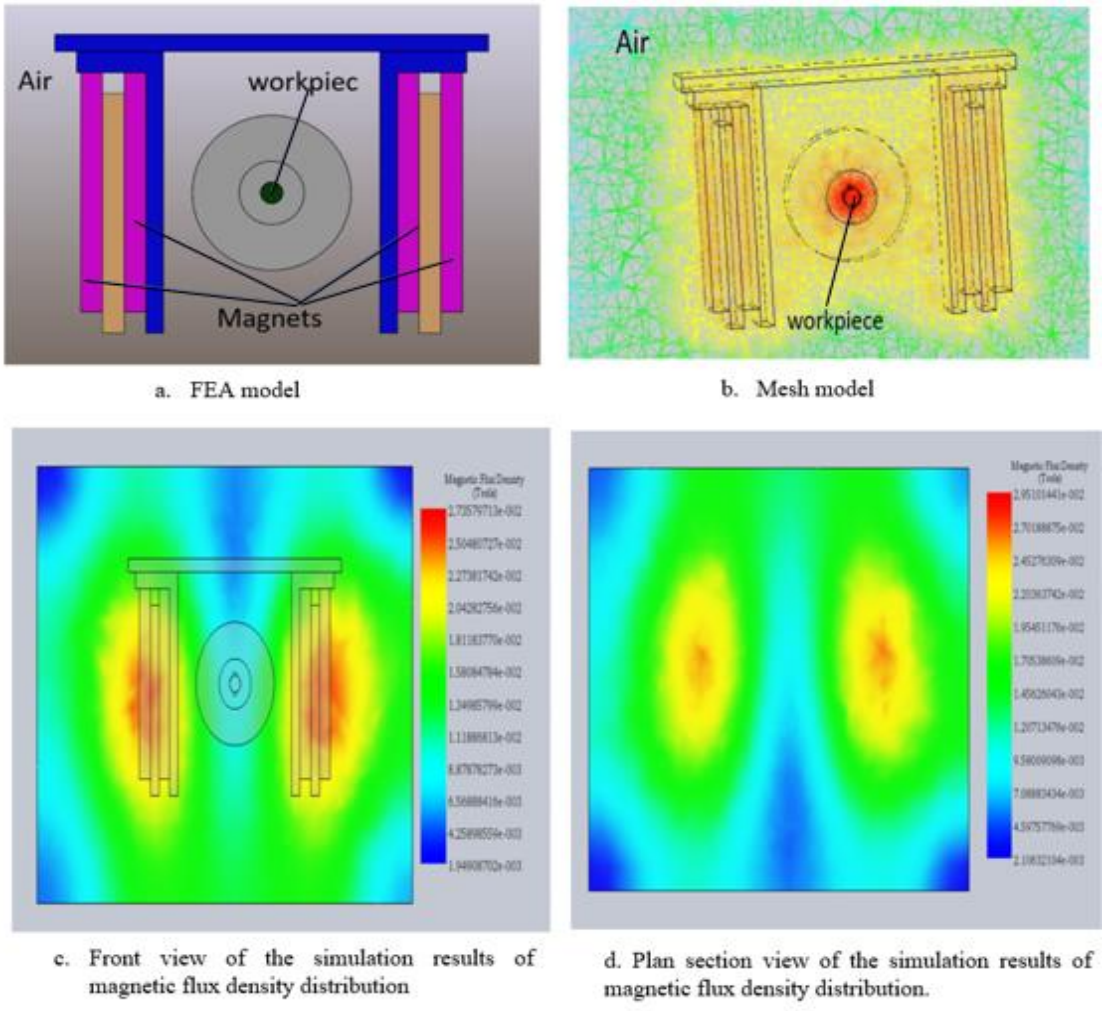

a. FEA model

b. Mesh model

c. Front view of the simulation results of magnetic flux density distribution

d. Plan section view of the simulation results of magnetic flux density distribution.

Figure 3.2 Finite element analysis (FEA) of the magnetic field distribution.

3.4 Experiments

The cutting was conducted on the UP-machine tool, as Figure 3.3 shows the experimental setup for the process. A single-point diamond tool of radius and length of: 0.773mm and 10.476mm, respectively was used as the cutting tool to cut the workpiece made from Ti6Al4V alloy of a chemical composition shown in Table 3.1. The workpiece is cylindrical with a diameter and length of 15mm and 25mm, respectively. The magnetic field was generated by the installed four permanent magnets, all made of neodymium with dimensions of 100*45*8 mm, supported by a custom-made steel frame whose primary function was to fix the magnets and regulate the location of the magnetic bars. An aluminium fixture

was used to hold the workpiece to the main spindle. The cutting experiments were carried out on a Moore Nano-tech 350FG (4-axis ultra-precision turning machine). The machining experiments were divided into two groups: conventional diamond machining and magnetic field assisted machining (MFAM), with the magnetic field applied at two intensities of 0.01T and 0.02T. The cutting parameters were set to cutting depth: 4μm, feed rate: 8mm/min, and rotational speed: 1200rpm and held unchanged for all experiments. The chips formed during the cutting were collected and examined with a scanning electron microscope (SEM). Following the experiments, the samples were examined by a high-precision optical component, Zygo, to examine and measure surface roughness and explore the surface quality. SEM was used to examine the diamond tool edges after cleaning them with hydrofluoric acid.

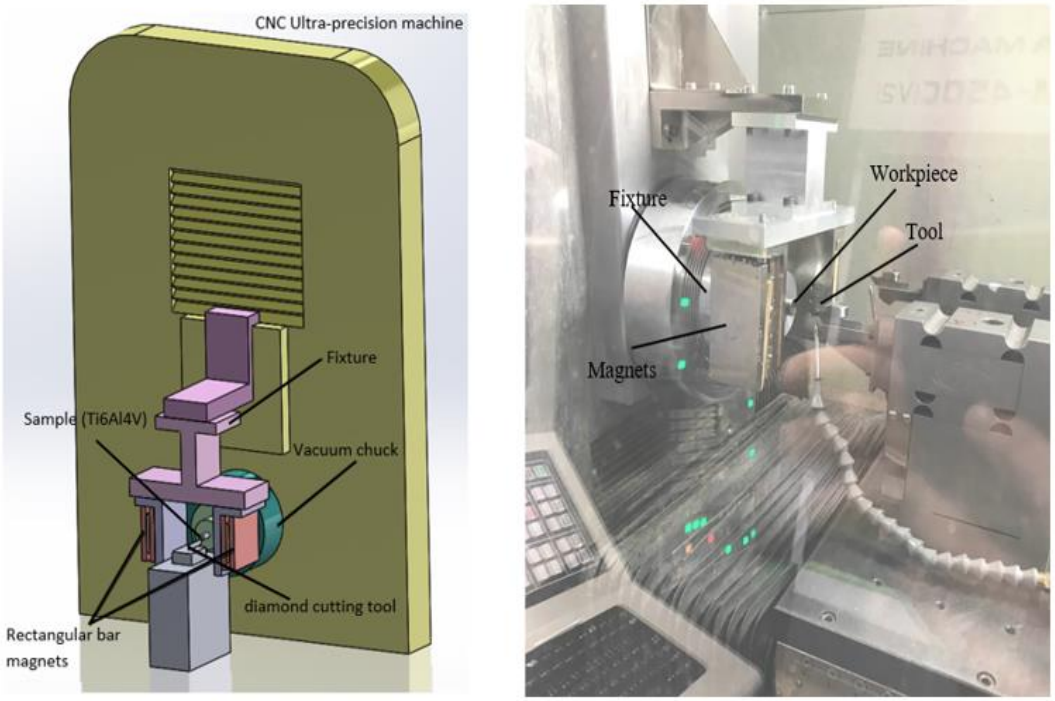

Figure 3.3 Experimental setup of the magnetic field-assisted machining (MFAM).

Table 3.1 The composition of Ti-6Al-4V Samples used in the experiments.

Element composition (%)						
Al (Aluminum)	V (Vanadium)	Fe (Iron)	N (Nitrogen)	O (Oxygen)	H (Hydrogen)	C (Carbon)
6	4	0.3	0.05	0.2	0.012	0.1

3.5 Results and discussion

3.5.1 Influence of magnetic field-assisted machining (MFAM) on-chip formation

In UPM, chip formation is an important indicator of the machining effectiveness. The formed chips condition can reveal important details about the cutting, and chip formation can also influence other cutting factors, such as cutting force and surface roughness. Chipping occurs when the material interface deforms and is subjected to shear load; the deformation mode is determined by cutting factors such as tool geometry, workpiece material, and cutting parameters.

Figure 3.4(a-c) shows that the chips were collected during machining and examined using a scanning electron microscope. Figure 3.4(a) depicts SEM images of SPDT chips formed without a magnetic field and shot at various magnifications. When machining hard-to-cut materials like titanium alloys, the generated chips flow in a serrated manner with a saw-tooth shape, implying a low cutting performance. The chips segments adhere to the machined surface, resulting in poor surface integrity compared to the chip formation morphology in MFAM. The SEM results in Figure 3.4(b) and Figure 3.4(c) have shown longer and continuous chips with flat edges, indicating relatively better machining conduct with applying magnetic fields at 0.01T and 0.02T, respectively.

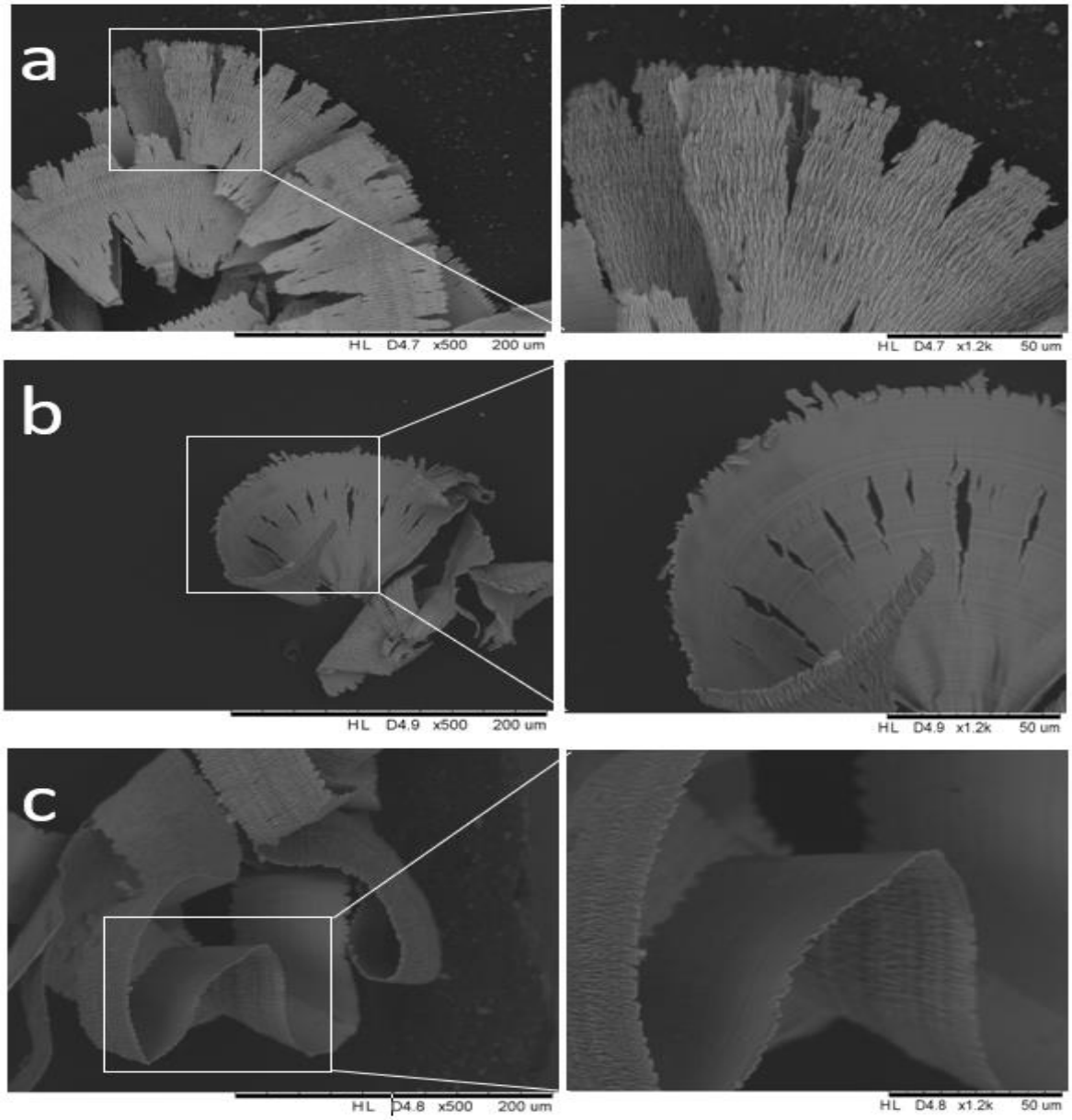

Figure 3.4 SEM images chip formation in (a) the absence of magnetic field, (b) MFAM of the intensity of 0.01 T, and (c) MFAM of the intensity of 0.02 T.

3.5.2 Influence of the magnetic field-assisted machining (MFAM) on the surface roughness

Machining parameters like feed rate, cutting speed, and depth of cutting can impact the machined surfaces' quality. The surface integrity level of products is also impacted by cutting tool characteristics, such as tool material, shape, and wear rate. Observations on the samples' machined surfaces were made and analyzed. Figure 3.5(a-c) displays the SEM images of surface samples machined by SPDT. The sample in Figure 3.5(a), machined without a magnetic

field, exhibits relatively poor surface finishing, with obvious tool marks and irregularities on the surface created by the workpiece material fracture during the operation. As seen in Figure 3.5(b) and Figure 3.5(c), the MFAM-generated surface, in contrast, has a reasonably flat surface that indicates a smooth machining operation without any scratching by the uncut material chips and revealed considerably fewer tool marks. Since surface roughness is an assessment factor in determining whether a cutting process will be successful and the machined parts have high surface integrity, the surface roughness values for both samples were measured. Eight distinct areas from each sample were chosen to determine the values of the average surface roughness. The results are displayed in Table 3.2. MFAM produced the lowest surface roughness value, which was a 33 percent reduction in surface roughness value compared to the sample machined without the magnetic field. Additionally, it was demonstrated that a smaller standard deviation for MFAM was attained, demonstrating the impact of magnetic fields on the enhancement of machined surface uniformity.

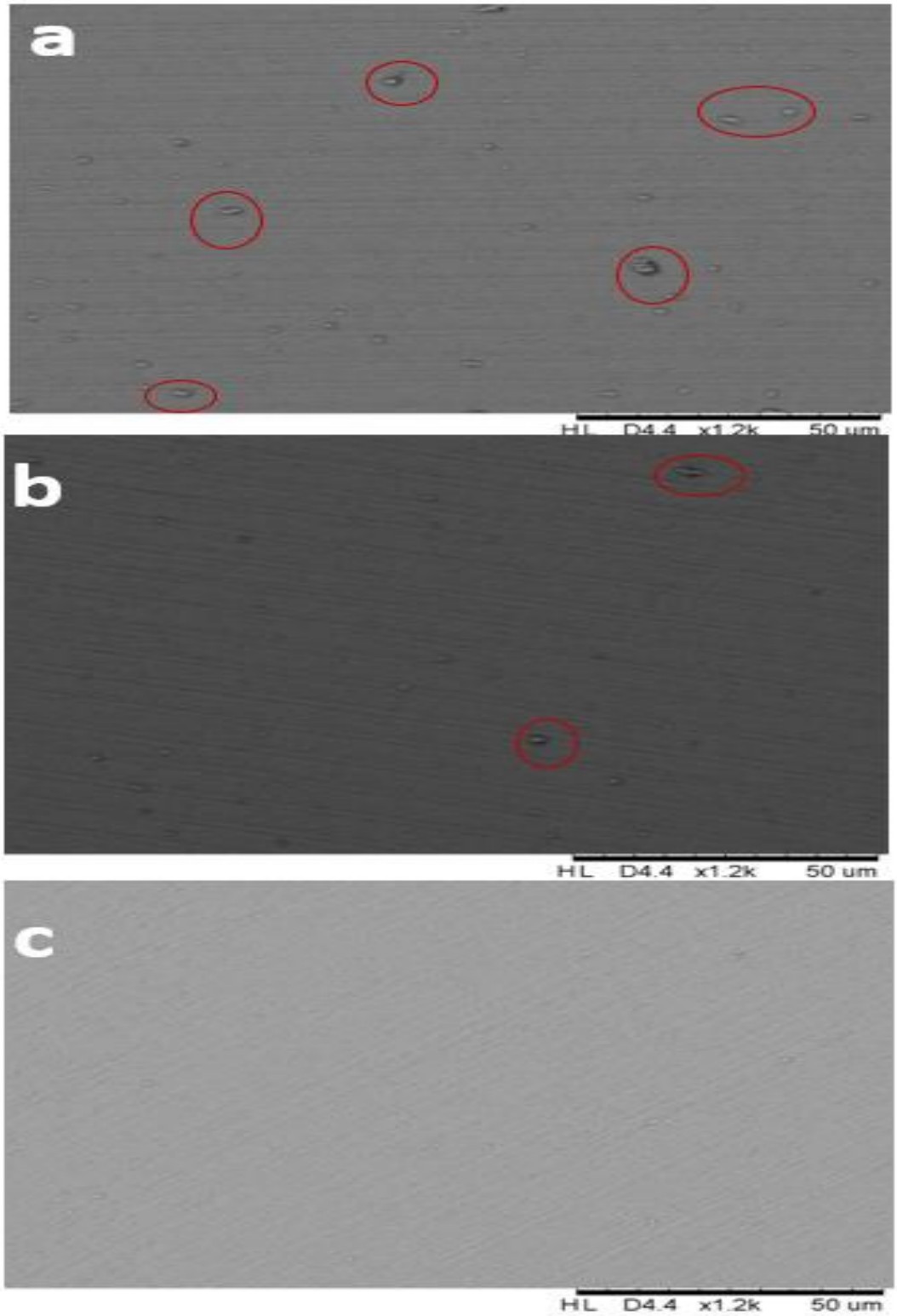

Figure 3.5 SEM images of surface topography of samples machined under the (a) absence of magnetic field, (b) MFAM of 0.01 T, and (c) MFAM of 0.02 T.

Table 3.2 Average surface roughness of the samples.

Magnetic field intensity (T)	0	0.01	0.02
Surface roughness (nm)	19.89	18.50	13.33
Standard deviation	1.88	1.66	1.63

3.5.3 Influence of the magnetic field intensity

The magnetic field's strength could be altered by varying the gap between the two magnets. It was discovered that the gab distance needed to be carefully managed so the cutting zone could receive the optimum magnetic flux, resulting in machined products with excellent surface quality. The effects of the magnet's intensity on the caliber of the work-piece surface were investigated after conducting several simulations and experimental tests with the magnets in various positions to get the ideal magnetic field intensity for the implementation of the cutting process. The correlation between the magnetic field's strength and the samples' surface roughness is depicted in Figure 3.6. It was noted that surface roughness was improved when magnetic field intensity increased; surface roughness reached its lowest value at a magnetic field strength of 0.02 T. The lowered distance between the cutting area and the source of the magnet, and the enhanced field on the cutting area are the causes of the increased magnetic field intensity.

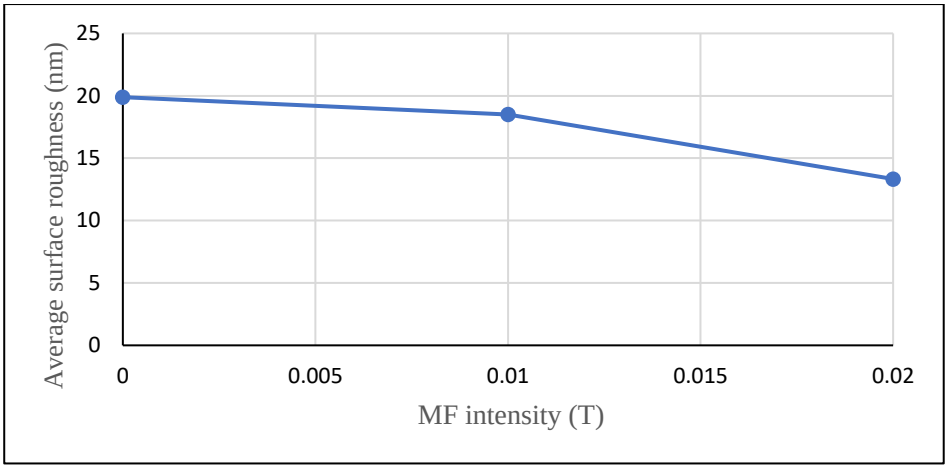

Figure 3.6 Magnetic field intensity Vs. Average surface roughness.

To analyze the magnetic field's intensity and how it relates to the distance, a series of simulation tests were carried out by varying the distance between the magnets, as illustrated in Figure 3.7. To compare the experimental findings with the findings of the parametric study, the magnetic field's strength was measured at various distances. The modelling results confirmed the experimental findings, demonstrating that a smaller gap between the magnets increased the magnetic field's strength. This clarifies the connection between surface roughness and magnetic field strength and supports the simulation's ability to estimate magnetic field strength.

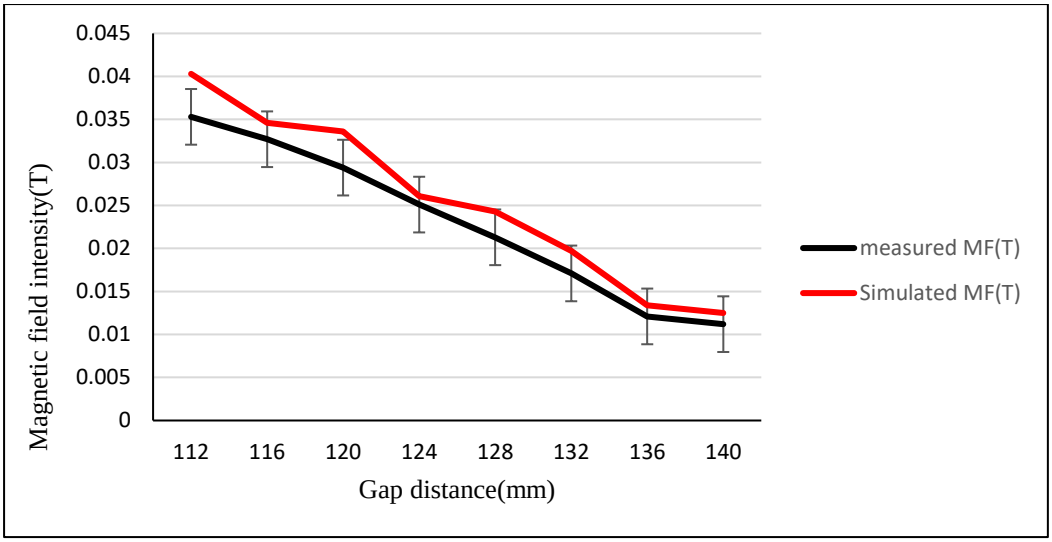

Figure 3.7 The average surface roughness and magnetic field intensity changing with the gap distance.

For the magnetic field-assisted diamond turning to be well designed and allow for better quality and use of the applied system, it is crucial to comprehend the coverage of the parts by the magnets and the interactions between them. Most of the time, tests are utilized to find the ideal magnet characteristics and specifications to reach meaningful values that can be used to carry out the process, which is regarded as time- and resource-intensive. In this study, magnets and the magnetic field of the integrated magnetic system were modelled using equations and simulations utilizing the finite element method FEM. In essence, the finite element approach is used to estimate the field strength values in order to avoid errors and achieve the best magnetic field-assisted diamond turning process. Magnets are employed to create a permanent magnetic field. The findings were verified by contrasting the experimental findings with the simulated findings obtained using finite element analysis.

3.6 Summary

In this chapter, the presented machining method offers a machining strategy that improves the precision components' surface quality and overall machinability. The permanent

magnetic field was created using a unique magnetic field system that included steel mounting components and bar magnets for fixing on the UPM. To achieve the optimal magnetic field intensity in the cutting zone, the magnetic flux distribution was first explored utilizing the FEM, and the experimental findings confirmed the simulated results.

Experimental outcomes from machining suffering the influence of a magnetic field verified the effectiveness of ultra-precision machining UPM paired with the magnetic field in optimizing the machining operation of Ti-6Al-4V alloy. The magnetic field's presence during cutting facilitated chipping and prevented the creation of built-up edges. Additionally, the chips were released smoothly, preventing an unfavorable accumulation of heat in the cutting area.

The fundamental cutting variables of chip generation, and sample surface roughness were investigated. According to the experimental findings, the cutting tool edges of MFAM had a lower rate of wear for both the rake and flank faces while machining under the influence of a magnetic field than those of the edges used without MFAM. The potential of a magnetic field to prolong cutting tool life, which subsequently enhances machining performance and product quality, was strongly supported by achieved results. The minimum surface roughness value was achieved by machining, while the workpiece was influenced by a magnetic field, which also produced continuous chips. All of the experimental findings supported the successful coupling of the MFAM with UPM to manufacture high-precision components. Additionally, the suggested FEM reveals the MFAM system's machining environment, particularly the magnetic field's density and the magnetic flux distribution covering the cutting area, which aided in obtaining the ideal magnetic field intensity for the UPM process.

Chapter 4: Development of finite element modelling FEM of magnetic field ultra-precision machining (MFUPM)

4.1 Introduction

Titanium alloys are capable of serving as remarkable materials in a range of advanced and biomedical fields because of their high strength, rigidity with low density, and biocompatibility, whereby these material characteristics enable saving in space structures and other high-performance applications (Maurotto et al., 2013; Niinomi, 2003). On the other hand, being have low machinability performance and low thermal conductivity, titanium alloys are classified as tough-to-cut materials. Lack of heat transfer causes heat to accumulate in the machining zone (Che-Haron and Jawaid, 2005). The majority of machining issues lie in the excessive heat that promotes tool wear and degrades the cutting edge of the cutting tool, which results in a built-up edge on the workpiece (Komondor and Von Turkovich, 1981). Vibrations result from cutting tool degradation, resulting in parts with low precision and poor surface features, in addition to an increase in the cutting tool cost. Zhang et al. (2017) observed that using diamond-cutting tools to cut hard materials like titanium alloys reduces their tool life because they experience high wear rates. In order to address this issue, various studies have concentrated on employing coated cutting tools to protect the tool or developing coolant-based methods to remove the excess heat from the cutting zone. Several researchers applied various cooling approaches and different strategies for lubricants, such as (MQL) (QIN et al., 2012), and others used cryogenic coolant (Bermingham et al., 2011). Water vapour, flood, and high-pressure cooling all contributed to reducing the cutting temperature and tool wear rate.

Since cutting fluids help to reduce friction, increase the heat transmission rate from the machining zone, and reduce the cutting tool wear rate, which could improve machining performance, several studies have been carried out to examine the influences of cutting fluids. Flood cooling is a technique used to preserve tool edges from wear and reduce heat generated

during cutting. It involves circulating a large volume of coolants on the cutting surface at a low speed and lower pressure. Even so, it restricts cutting speed to modest levels. However, even though applying a little lubrication enables it to go over the cutting speed restriction, it pollutes the environment and endangers the machine tool technician(Pervaiz et al., 2018). Hong and Ding (2001) applied the cryogenic cooling approach and found that it effectively lowered the cutting temperature. Cryogenic cooling is a cooling technique that typically uses nitrogen in the liquid state as the cutting fluid, which is aimed at the cutting area to lower the raised cutting temperature and prevent rapid tool wear. Even with all of these unsustainable cooling methods, the presence of induced heat at the cutting tool/workpiece interface still poses a challenging issue because it accelerates cutting edge wear and reduces tool lifespan.

Additionally, as a consequence of the tool damage during machining, the surface quality of the machined parts degrades (Arrazola et al., 2009). According to Mir et al. (2016), the surface quality degrades when operating difficult-to-cut materials, due to the lack of their thermal conductivity and cutting tool wear, both of which have an impact on machining performance, as a result, new techniques are needed to maintain a smooth cutting process when cutting difficult materials. Many studies have investigated the effects of cutting parameters on cutting performances. Hou et al. (2018) optimized the cutting parameters to achieve a high surface quality by carrying out a multi-step cutting technique on Ti-6Al-4V alloy. Ruibin and Wu (2016) demonstrated that titanium alloys can be machined to a high degree of precision in SPDT by adjusting the cutting parameters to a low feed rate and a shallow cutting depth combined with a relatively high spindle speed. To investigate the relationship between the cutting tool condition and surface roughness, Liang and Liu (2017) carried out orthogonal cutting experiments on Ti6Al4V alloy. They studied the influence of the cutting parameters on the surface quality, discovering that the machining performance was complicated and linked to multiple factors like tool wear status, resulting cutting forces, and the chip formation process.

Yip et al. (2020) revealed that it is challenging to estimate the cutting performance from a single factor because the parameters impacting the cutting performance of Ti-6Al-4V are complicated and not independent. However, these methods, which implement cooling approaches or optimize the cutting parameters, are insufficient to upgrade the machining of difficult-to-cut materials for economic or environmental concerns, as they consume cutting tools and expose the machine tool technician to potentially hazardous situations. Several experiments have been carried out to determine the outcomes of utilizing advanced material cutting tools manufactured from hard materials (V. P. Astakhov, 2014). To overcome the difficulties with the operating of hard-to-cut materials, some studies demonstrated acceptable cutting performance by utilizing coated cutting tools with appropriate cutting parameters to avoid environmental pollution caused by the cutting lubricants (Devillez et al., 2011). It was reported that those cutting tools facilitated the machining operation (Yoshiaki et al., 2015). Da Silva et al. (2016) demonstrated the use of polycrystalline diamond (PCD) tools, carbides tools, and ceramics boron nitride (CBN), concluding that PCD tools are more efficient among all these different cutting tool materials; however, PCD cutting tools still face difficulties to machine hard to cut materials like Ti alloys, particularly at high cutting speed, as tool wear rate increases and tool life decreases. While studies focusing on avoiding generated heat and extending tool life have demonstrated machining improvements, additional research is required to overcome the challenges inherent in cutting hard-to-cut materials.

In an attempt to reduce the use of cutting oils or eliminate them during cutting in addition to protecting the environment from oil contaminants and reducing the cost of machining, Zhang et al. (2012) used dry and minimal coolant cutting to cut Inconel 718 and investigated the difference between the state of the cutting edges and the cutting forces in both processes. The results indicated that the machinability was enhanced at a higher level. Hadad and Sadeghi (2013) machined the AISI 4140 in a turning operation using minimum quantity

lubricant and flooded coolant; the outcomes showed that there was no noticeable variation between the surface roughness and the cutting forces in both operations, indicating that applying minimum quantity lubricant can be used in place of the more hazardous flooded cooling. On the other hand, the cost of using lubricants also increases due to their treatment to maintain their lubricity properties against the growth of bacteria, as the presence of such bacteria and fungi reduces the efficiency of oil, which can cause the formation of rust and corrosion in machines and workpieces, impairing the machine tool's performance and worker's health (Pervaiz et al., 2018). Additionally, there is possible that workers will inhale these fumes, affecting their lungs and causing them to suffer from lung diseases, including respiratory problems, asthma, and many types of cancers (Dhar et al., 2006a). The effects of aerosol on worker health can also increase the risk of esophageal cancer (Dhar et al., 2006b). It is challenging to rely on dry cutting because of the accompanying flaws like increased heat produced during the cutting operation and restriction of cutting speed at relatively low levels, even though the use of lubricants cooling is not environmentally preferable due to the numerous problems associated with the working environment and human life quality. In addition, dry cutting speeds up the rate of tool wear, reducing the lifespan of the cutting tool.

Some studies have been driven by the finite element approach to further elucidate the mechanism of metal cutting in response to the demand for exploring this mechanism, including the machining of titanium alloys. Some information, such as cutting temperature, chipping process, and stresses, can be gained aided by FEM. Kara et al. (2016) have predicted the cutting temperatures in the orthogonal cutting process by using FEA and employing Johnson–Cook (J-C) material model, and the simulated and experimental results demonstrated an agreement. According to the features specified in FEA methodologies, Soliman et al. (2020) simulated the motion of the chipping process by using FEA by employing the Eulerian (EUL), Lagrangian (LAG), and Arbitrary Lagrangian Eulerian (ALE) methods. Wan et al. (2016) conducted

cutting simulations and experiments to study the impact of cutting speeds. They discovered that the cutting speed is a key factor in chip segmentation degree and the creation of the serrated chips during the machining process. A two-dimensional finite element modeling of burr generation during the machining of Ti-6Al-4Valloy was presented by (Lu et al., 2016). They adopted the J-C material model and Cockroft-Latham damage criterion to understand better plastic flow and chip formation in the machining process. They investigated the influences of cutting parameters and cutting angles to design optimized cutting parameters. Therefore, it can be stated that the machining process could be optimally simulated and properly predicted depending on the given model utilizing FEM. As a result, using FEM in an orthogonal cutting simulation encourages attaining reliable findings.

The demand to create a method that can replace risky environmental practices while extending tool life is growing as modern manufacturing technology develops and environmental protection awareness among the public rises. The impact of applying physical approaches to operate metal cutting on the development of cutting technology has been the subject of numerous research. Recent studies have focused on combining physical methods with manufacturing techniques to enhance the machining performance of hard-to-cut materials. These techniques alter the materials' physical or mechanical properties through pretreatment procedures or the application of magnetic fields (Yip and To, 2017b; Zhu et al., 2009). Lou and Wu (2017) conducted cutting experiments on a pre-treated Ti6Al4V alloy in ultra-precision machining to determine whether this method improved cutting performance by comparing the outcomes of the cutting forces and surface roughness of treated and untreated samples. Although this method improved the parts machined surface, it is limited to the materials used in non-heavy-duty applications.

Several research has been conducted to apply physical theories to manufacturing and carry out improved operations by incorporating magnetic fields into the manufacturing

processes to obtain products of high quality. Lin and Lee (2008) have explored the magnetic field's effectiveness on cutting processes and the impact of the magnetic force assisted EDM on the metal removal rate and surface integrity to improve the machining performances. To improve cutting quality, Bruijn et al. (CIRP and 1978, n.d.) demonstrated a debris removal process in which a magnetic field surrounds the cutting area in the electrical discharge machining (EDM). Teimouri and Baseri (2014) presented an increase in debris removal rate during cutting by incorporating an external magnetic field into the EDM. Kim et al. (1997) used the magnetic field to induce ion migration and changed the electrolyte bath in the electrolytic finishing process, which resulted in a better finishing process.

On the other hand, numerous researchers have investigated the application of the magnetic field abrasive finishing technique (Wu et al., 2016); V. P. astakhov, (2014), in which removing the material occurs when the work material and the abrasive particles move relative to each other with the magnetic field effect. The use of magnetic fields in finishing processes has increased in recent years to obtain high-quality products. Suzuki et al. (2014) used a magnetic field to polish components for optical applications with high quality. Wu et al. (2015) machined SUS304 stainless steel with significantly improved surface quality in an alternating magnetic field at a low frequency. El Mansori et al. (2003) used an external electromotive force to reduce tool flank wear, resulting in increased tool life. Fan et al. (2019) have employed a permanent magnet-based magnetic field system to perform a finishing process of Ti-6Al-4 V workpieces. The results showed an improved surface quality when other finishing parameters were controlled. Numerous studies have demonstrated the potential use of a magnetic field to assist in cutting operations, proving that this hybrid process can effectively enhance the performance of work materials' cutting. Yip and To (2017b) developed a magnetic field device for an ultra-precision turning machine to overcome the cutting force variation using the damping effect of the eddy current, thereby reducing tool wear rate and lengthening the

operation time of the cutting tool. Yip and To (2017c) improved the cutting behavior of Ti6Al4V by utilizing the magnetic field effect in SPDT. Yip and To (2019) have reached a minimized cutting thickness of Ti6Al4V in ultra-precision diamond turning; the minimum cutting thickness was lowered, and the obtained surface quality improved when the magnetic field was present. In the studies relevant to the machining operation for hard-to-cut materials, it is clear that this area of research requires additional exploration to overcome these materials' machining challenges, and the magnetic field application is a promising method to be implemented in SPDT.

The main goals and objectives of this study are to increase the cutting tool life by protecting it from the increased cutting temperature, to achieve an environmentally friendly cutting method capable of overcoming the induced heat during the machining of difficult-to-cut materials, to simulate the optimal magnetic field value and intensity in the cutting zone, and investigating the impact of the magnetic field on the cutting zone. Considering that the methods utilized in prior research were either conventional or did not match the requirements for an ecologically friendly cutting process and the cost-effectiveness of machining these materials, a novel approach is proposed. In this work, the magnetic flux intensity was tuned and experimentally confirmed in combination with the other machining parameters. Simulations were utilized to show chip formation and temperature distribution, and the results were experimentally confirmed. Zygo measured the roughness levels of the obtained surfaces. By utilizing the atomic force microscope (AFM), the condition of the machined surface was investigated. X-ray diffraction (XRD) for the machined samples helped to identify the phase change of Ti-6Al-4V. An optical profiler was utilized to measure the surface profiles of the machined samples. This study revealed that the machined surface produced by the MFDT was of a higher integrity quality than that generated by conventional diamond turning (CDT), indicating the preservation of the cutting edges from the wear occurrence and enhanced service

tool life, as supported by the findings of chip formation, cutting tool conditions, and surface roughness.

4.2 Methodology

As per the literature review, the magnetic field has been used as an assisting tool in various manufacturing processes to promote productivity and quality. The magnetic field is frequently used to increase the debris removal rate in cutting processes such as EDM, where the generated magnetic force is combined with a conventional EDM machine to assist the process of the EDM to improve the overall machining performance (Lin and Lee, 2008). Also, ultra-precision machining UPM technology utilizes a magnetic field, where the expected quality level of the machined parts is high, and the products offer a wide range of advanced applications. As a result, incorporating such hybrid methods into UPM technology has the potential to enhance the cutting process and increase product quality significantly.

According to previous research, the physical properties of ferrometals, such as thermal conduction property, can be increased when exposed to a magnetic field. The movement of molecules has explained this and their alignments from their random states by the Law of Van der Waals to a regular and straight state when subjected to an applied magnetic field. The heat transfer rate is raised as these molecules line up and act as extended paths for conveying heat. Gavili et al. (2012) carried out experiments when the magnetic field is present to measure the thermal conductivity of the ferrofluid. They proved that utilizing a magnetic field increased the thermal conductivity. Lajvardi et al. (2010) reported the effectiveness of the magnetic field in elevating the thermal conductivity of the ferrofluid containing Fe_3O_4 particles for the same reason when the magnetic field changes the random state of the particles to be regular and aligned to facilitate conveying of the heat. Due to the effect of the Van der Waals forces (Dormann and Fiorani, 1992), the particles attach randomly, as well as the effect of the dipole-dipole interaction; when a magnetic field is present, the alignment occurs and a chain of magnet

particles act as a conductor for transferring the heat and the dipole-dipole interaction energy E_{ij} can be described from Eq (4-1).

$$E_{ij} = -KV\,(\vec{e}\cdot\vec{u})^2 - \Sigma_j K_m^{ij}\overrightarrow{Mi}\cdot\vec{M}_j \qquad (4\text{-}1)$$

Where:

K: the energy constant for magnetic anisotropy,

V: the term of volume,

$\vec{e}$: a unit vector pointing in the direction of magnetization,

$\vec{u}$: a unit vector pointing in the particle's magnetization vector's direction,

$\overrightarrow{Mi}, \vec{M}_j$: the particles i and j 's corresponding magnetization vectors, and

K_m^{ij}: the particle i and particle j interaction's magnetic coupling constant.

As stated previously, the thermophysical properties of materials can change based on the machining approaches used. This study applies a magnetic field to the Ti-6Al-4V alloy during the machining operation to increase the dissipation of the induced heat from the cutting region. Consequently, the excessive heat due to the cutting is no longer a dominant factor for tool wear for both surface quality and the hazardous lubricant.

4.3 Development of FEM of the magnetic field-assisted machining

4.3.1 Geometric model of orthogonal cutting

Many experimental works provide comprehensive reviews on the machining capabilities of titanium alloys to understand the mechanism of chip formation and its implications for titanium machining (Che-Haron and Jawaid, 2005; Dandekar et al., 2010; Hou et al., 2018; Kaur and Singh, 2019; Pramanik and Littlefair, 2015; Veiga et al., 2013; Zhang et

al., 2017b). Other researchers adopted the finite element (FE) method to explore the cutting mechanism of Ti6Al4V alloy further and comprehensively investigate its machinability (Harzallah et al., 2017; Molinari et al., 2013; Yaich et al., 2017). Mehmet suggested a novel FE-based numerical model of orthogonal machining and employed the JC damage model with the displacement-based ductile failure criterion to study the machining performance of Ti-6Al-4V (Aydın, 2021). Xu et al. (2021) presented a model for simulating the serrated chip formation of Ti-6Al-4V by coupling the Eulerian-Lagrangian approach and a constitutive model considering the stress state to investigate the material side flow and the cyclic modification of the surface topography. Jiang et al. (2012) explored the influence of material models on chip formation type in Ti-6Al-4V alloy cutting using simulation. The results revealed that material flow stress significantly impacts chip formation type, cutting forces, and temperatures. Qian and Duan, (2019) used FE modeling to investigate the influence of materials on the serrated chip formation in Ti-6Al-4V alloy machining by applying heat treatment with adopting the Johnson-Cook (J–C) constitutive model, an orthogonal cutting simulation was established under two different numerical calculations, the results revealed that the adiabatic analysis type is more realistic for simulating the cutting of Ti6Al4V alloy since it has low thermal conductivity.

The evolution of machining modeling enhanced operation performance, manufacturing capability, and productivity. Modeling also avoids the manufacturing cost and effort due to the expensive experiments and the involved difficulties. Applying numerical modeling in metal cutting processes can get difficult-to-obtain data such as stress distribution and cutting temperature from experiments. The development of new models has enabled researchers to investigate the cutting behaviuor of many materials. Furthermore, the modeling approach of the machining processes can be utilized to examine the chip formation or the cutting temperature. Mainly, the cutting modeling consists of the geometry model, mesh model,

constitutive material model, and interaction property, which directly influence the simulation results.

Because of its simplicity and informative results, orthogonal cutting is widely used in machining simulation. This study assumed orthogonal cutting, and a FE of a two-dimensional model that was presented for the cutting operation of Ti-6Al-4V using the ABAQUS platform. As Yip and To (2017c) demonstrate the ability of the magnetic field to increase the thermal conduction property of the Ti6Al4V when exposed to an external magnetic field during machining, the change of the corresponding thermophysical property was considered in the finite element analysis. Titanium alloys are known to be hard-to-cut materials due to their lack thermal conductivity, which causes localized heat to exist in the cutting region. While this raised heat exists during machining, the interaction between the tool and workpiece causes tool wear and affects the surface integrity of the machined parts.

As seen in Figure 4.1, the FEM consists of the work material, Ti-6Al-4V, and the cutting tool, which was set as a rigid body because it is harder than the workpiece. Because machining Ti-6Al-4V is a thermal-mechanical process, the orthogonal cutting of Ti-6Al-4V was assumed and performed in a two-dimensional plane strain. The analysis step was set as Dynamic, Temp-disp, Explicit. The cutting area was finely re-meshed, as shown in Figure 4.1 of type CPE4RT, to improve the precision level of the obtained results and shorten the processing time. The simulation cutting parameters have a 50 m/min cutting velocity and a 5um depth of cutting. The initial temperature was set to the ambient temperature of 20 °C, meaning no cooling was required during the cutting operation.

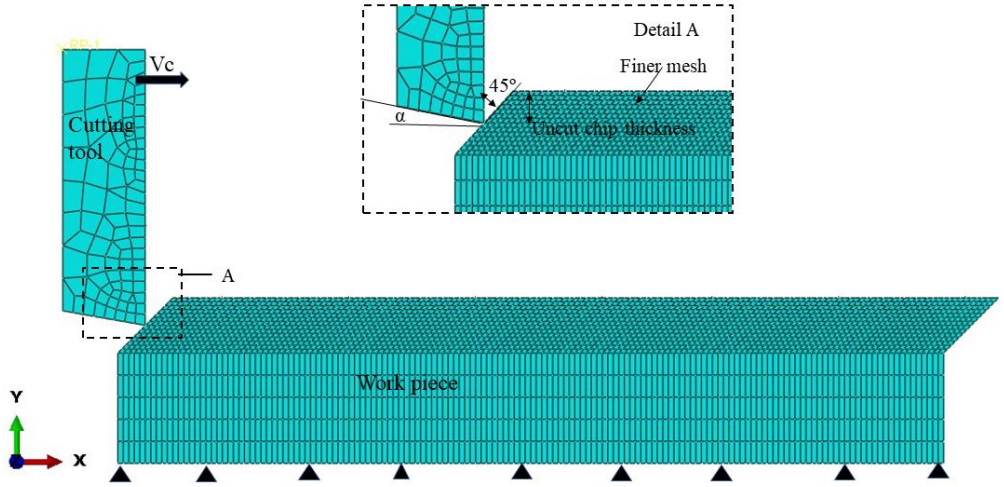

Figure 4.1 The geometry of the 2D orthogonal cutting FE model.

4.3.2 Element failure models of the material

Chip formation of machining is complicated in finite element simulation as it depends on different factors besides the material properties and cutting conditions. To address this issue, the chipping process is normally performed under techniques and criteria such as adaptive meshing, damage, and failure criteria. In adaptive meshing, the meshing process is optimized during the chipping. To investigate chip formation in cutting simulation, plastic, and damage models are commonly used to represent material deformation; these models include the separation of the work material and the chipping process. Figure 4.2 depicts a general schematic of a complete stress-strain response for material deformation; as shown, various deformation zones exist until the cutting occurs; the first stage is the elastic stage, followed by the plastic stage, and finally, the damage evolution stage.

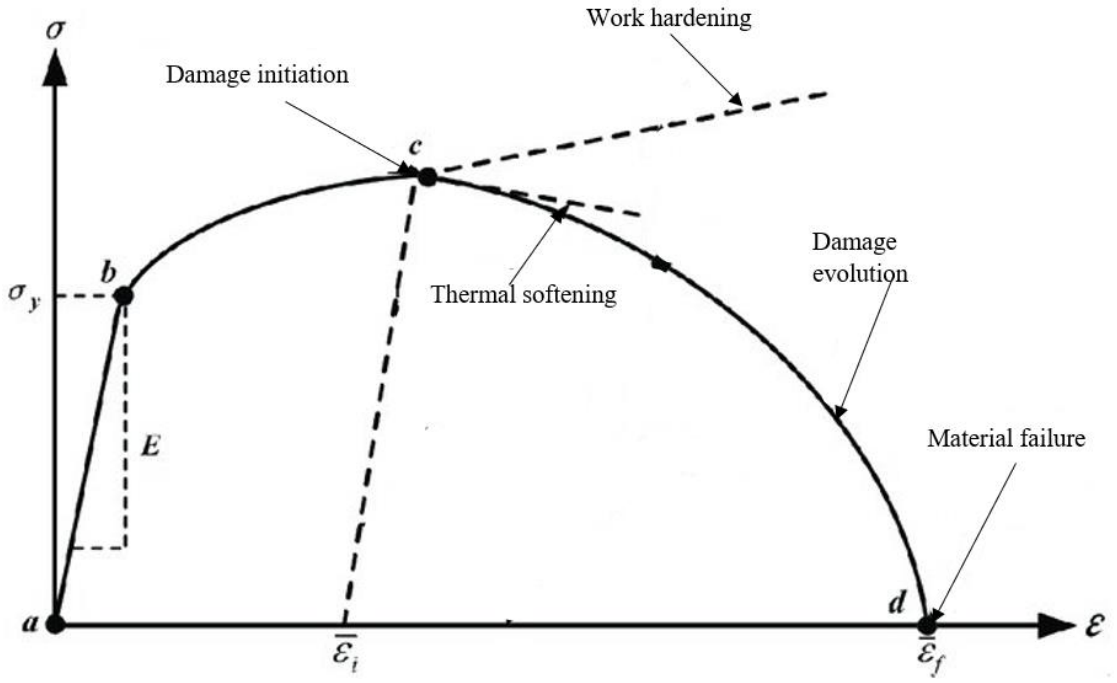

Figure 4.2 Stress-strain response of material failure process

Regarding the material's failure models, several models are normally adopted to represent the failure criteria of the material, the most common of which is the Johnson-cook (JC) model, which has been proposed in this study(Johnson and Cook, 1983). The Johnson-cook flow stress low is related to strain, strain rate, and temperature, as shown in Eq (4-2).

$$\sigma = (A + B\varepsilon^n)\left[1 - \left(\frac{T - T_r}{T_m - T_r}\right)^m\right](1 + C\ln\ \dot{\varepsilon}) \qquad (4\text{-}2)$$

Where A, B, c, m, and n are material model parameters, σ is the flow stress, and T_r, T_m are the room and melting temperatures, respectively. It can be noticed from Eq.3 that the J-C constitutive model consists of three parts describing the isotropic strain hardening behavior, strain rate sensitivity, and thermal softening behavior. The material constants of the J-C model for Ti6Al4V are listed in detail in Table 4.1.

Table 4.1 The material constants of the JC model for Ti-6Al-4V

A	782 MPa
B	498 MPa
c	0.028
m	0.8
n	0.28
T_r	293 K
T_m	1903 K

4.3.3 Chip separation criterion and fracture energy analysis

The chips are created when the cutting edge applies pressure against the outer surface of the workpiece during the cutting operation, resulting in an insertion on the workpiece surface that separates a material part. The cutting tool keeps penetrating the material until the separation of different layers from the metal surface in the form of chips as shown in Figure 4.3. The shape and state of the removed chips vary according to the type of machined metal and the machining conditions. Chips break up during the cutting process due to the compression of a metal surface layer under the exert of cutting-edge force. When the shear stresses reach and exceed the metal's ultimate shear stress, shearing occurs, and a massive separation of the metal or chipping appears. Such separation occurs towards the shear plane that forms a certain angle with the cutting tool's front surface. Chipping is repeated in subsequent layers until the cutting process is completed, removing the specified thickness to achieve the machined surface with the desired form.

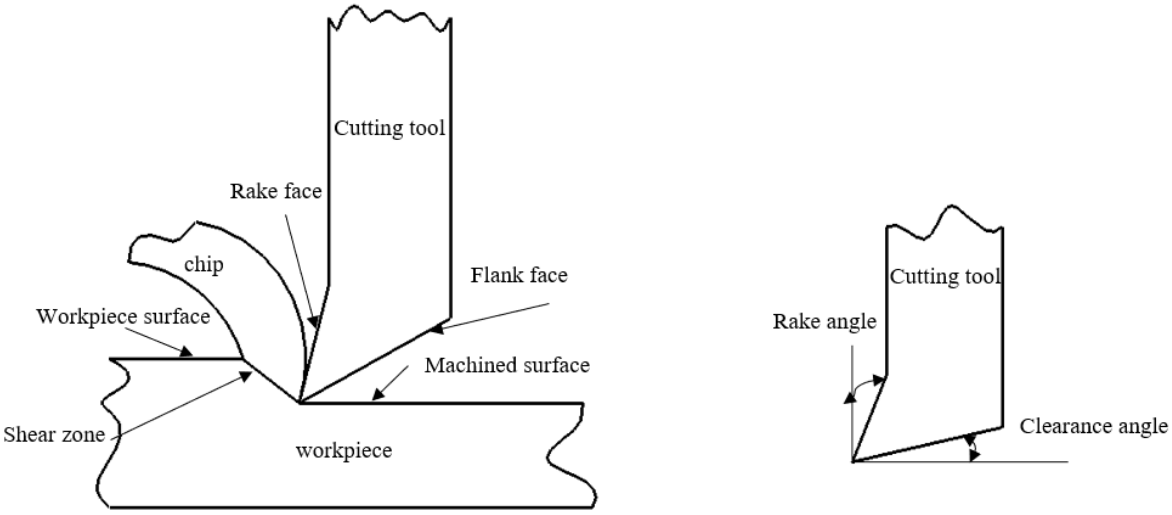

Figure 4.3 Chip formation in the machining process

The type and shape of the chips produced by the cutting operations vary depending on the following factors: the cutting tool angles, particularly the rake angle, different cutting speeds, and workpiece materials. As illustrated in Figure 4.4, chip types are classified as follows: chips generated continuously, discontinuous generated chips, continuous chips suffering built-up edge, and serrated chips.

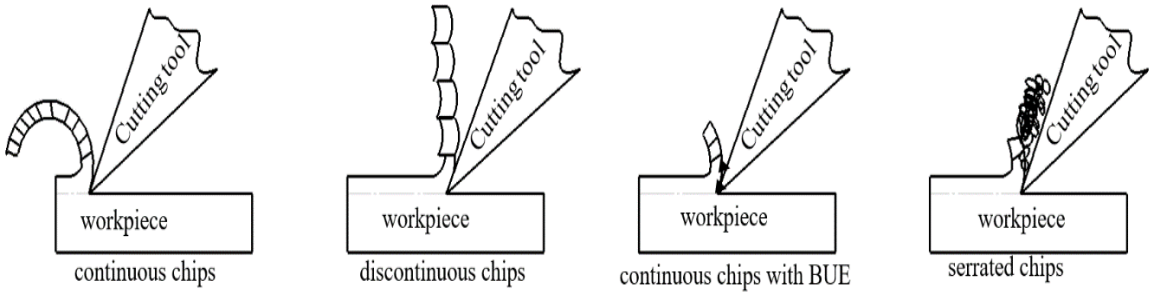

Figure 4.4 Types and shapes of the chips resulting from the cutting operations.

As illustrated in Figure 4.5, the chip formation process passes through three major deformation zones, known as the primary, secondary, and tertiary deformation zones. The

workpiece material is pressed to deform and change under severe shear elastic-plastic straining in the primary deformation zone in the machining processes. The secondary deformation zone is between the cutting tool's rake face and the sliced workpiece layer. The heat source is generated due to plastic deformation and friction between the tool rake face and the work material. Then, heat is produced further in the tertiary deformation zone due to continuous contact between the clearance face of the cutting tool, including the flank face, and the machined surface of the workpiece (Abukhshim et al., 2006; Black, 1961).

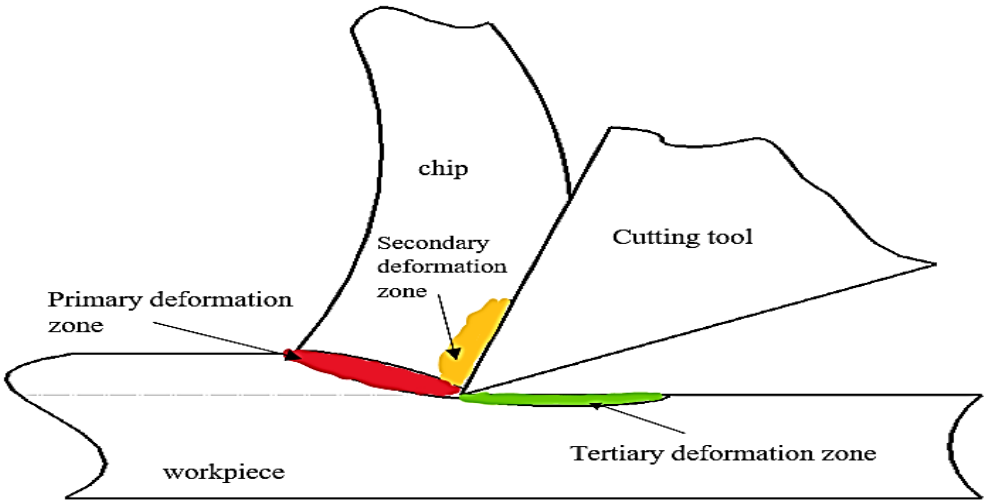

Figure 4.5 Different deformation zones in metal cutting

The chip separation begins in the primary deformations zone, and the material is removed due to the high plastic strain and friction. The machining operation can be assessed on the chip formation analysis. Removing the excess material can be described as a series of steps that begins with concentrated stresses at the cutting contact area between the cutting tool and the workpiece and continue to occur as the workpiece and cutting tool are moved. When the cutting begins, and the material is chipped at the plastic point of the work material, the cutting performance is typically determined by observing the chip shape, considering each material has a unique chip formation behavior.

The chip formation step indicated by the workpiece's damage evolution can be described by utilizing the J-C fracture model, as shown in Eq.(4-3) and Eq.(4-4). where D is the damage initiation that the failure occurs when its value reaches one, $\Delta\bar{\varepsilon}^{pl}$ is the incremental value of equivalent plastic strain, and $\bar{\varepsilon}_f$is the equivalent strain which can be calculated from Eq.6. it can be noticed from Eq.(4-4). that the effect of the stress, strain rate, and temperature are considered, and d 1~5 represent the JC failure parameters and are listed in Table 4.2.

$$D = \sum \frac{\Delta\bar{\varepsilon}^{pl}}{\bar{\varepsilon}_f} \tag{4-3}$$

$$\bar{\varepsilon}_f = [d_1 + d_2 \exp(-d_3\sigma^*)]\left[1 + d_4 \ln\left(\frac{\dot{\bar{\varepsilon}}^{pl}}{\dot{\varepsilon}_0}\right)\right]\left[1 + d_5\left(\frac{T - T_r}{T_m - T_r}\right)\right] \tag{4-4}$$

The energy-based fracture criterion is adopted in the FEM during the failure evolution step, and the failure energy can be expressed as follows from Eq.(4-5).

$$G_f = \int_{\bar{\varepsilon}_{oi}}^{\bar{\varepsilon}_f^{pl}} L\sigma_y d\bar{\varepsilon}^{pl} = \int_0^{\bar{u}_f} \sigma_y d\bar{u}^{pl} \tag{4-5}$$

Where:

G_f: the fracture energy

$\bar{u}^{pl}$: the equivalent plastic displacement

σ_y : the yield stress

L: the characteristic length, which is an element geometry factor

Table 4.2 The failure parameters of the JC model for Ti-6Al-4V (Recht, 1964).

d_1	d_2	d_3	d_4	d_5
-0.09	0.25	-0.5	0.014	3.87

To investigate the influence of fracture energy on the cutting simulation of Ti-6Al-4V and select the most proper value of the failure energy G_f for running the simulation, a series of simulations were run with varying failure energy G_f values. Because each set of cutting parameters has a different value of G_f, this study investigated cutting simulations using a set of different values ranging from 1000 to 2000 mJ/m^2 till the correct range is observed. Figure 4.6 depicts chip formation when G_f varies, and cutting parameters remain constant at 50 m/min cutting velocity and a 5um depth of cutting. In the cutting simulation of Ti-6Al-4V, it is clear that fracture energy influences chip formation. Fracture energy G_f is a parameter that must be known for cutting simulation in the FEM modelling. Since it's difficult to determine the precise value for the fracture energy during the cutting simulation with different cutting parameters, the chip creation is typically simulated with a range of fracture energy values, which results in the generation of various chip shapes. Furthermore, fracture energy is frequently a major determinant of chip morphologies. As a result, one of the crucial elements in determining the chip formation behavior during cutting simulation is fracture energy.

Damage evolution is challenging because it requires an input parameter with a known fracture energy value. This influence changes when different cutting parameters are used, like feed rate and cutting speed. This means that a fracture energy value shall be computed in a particular range of fracture energy to fracture the material at an identified series of feed with cutting speed. According to the literature, fracture energy varies with cutting speed, feed rate, and cutting force (Bermudo Gamboa et al., 2021). Hence, the chip formation in the machining process varies when the fracture energy changes. The simulated chips were displayed with all

of the parameters set fixed except for G_f. Different behaviors can be seen depending on the G_f that is being used. It is also insufficient to have the fracture energy parameter set for the extensive range of simulated cutting parameters. This is mostly because it depends on changes in fracture mechanics during the cutting process simulation. The work material performance is greatly influenced by the cutting parameters used in machining processes. Hence the failure energy should not be kept constant but rather adjusted, specifically in the machining processes, where the material behavior is impacted by the cutting conditions that are present during the entire cutting process.

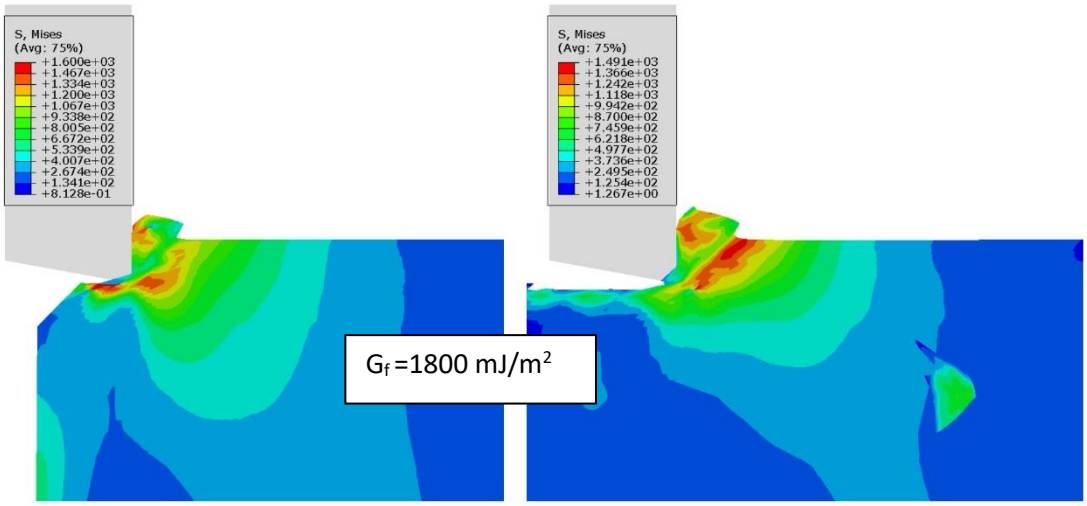
S, Mises
(Avg: 75%)
+1.600e+03
+1.467e+03
+1.334e+03
+1.200e+03
+1.067e+03
+9.338e+02
+8.005e+02
+6.672e+02
+5.339e+02
+4.007e+02
+2.674e+02
+1.341e+02
+8.128e-01
S, Mises
(Avg: 75%)
+1.491e+03
+1.366e+03
+1.242e+03
+1.118e+03
+9.942e+02
+8.700e+02
+7.459e+02
+6.218e+02
+4.977e+02
+3.736e+02
+2.495e+02
+1.254e+02
+1.267e+00
Gf =1800 mJ/m2

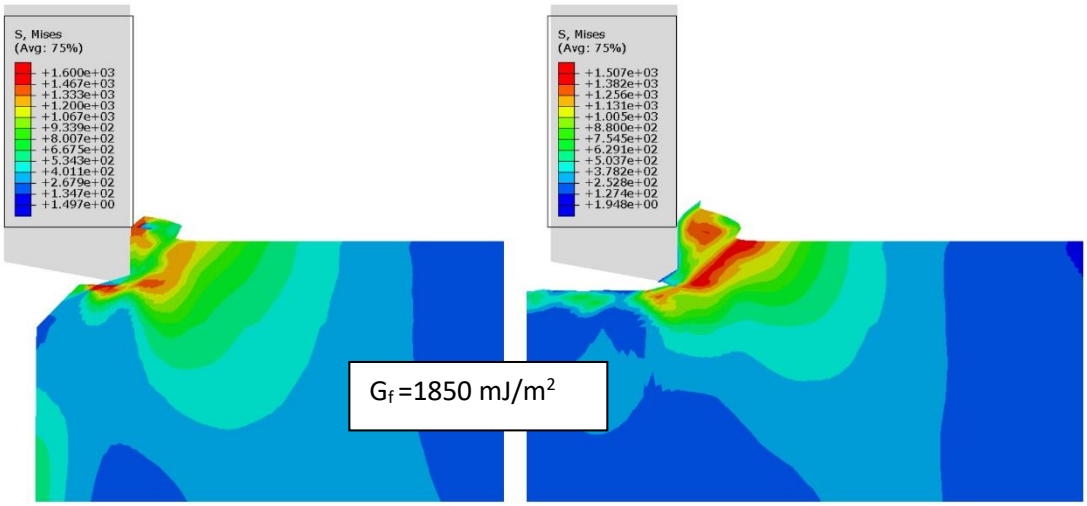
S, Mises
(Avg: 75%)
+1.600e+03
+1.467e+03
+1.333e+03
+1.200e+03
+1.067e+03
+9.339e+02
+8.007e+02
+6.675e+02
+5.343e+02
+4.011e+02
+2.679e+02
+1.347e+02
+1.497e+00
S, Mises
(Avg: 75%)
+1.507e+03
+1.382e+03
+1.256e+03
+1.131e+03
+1.005e+03
+8.800e+02
+7.545e+02
+6.291e+02
+5.037e+02
+3.782e+02
+2.528e+02
+1.274e+02
+1.948e+00
Gf =1850 mJ/m2

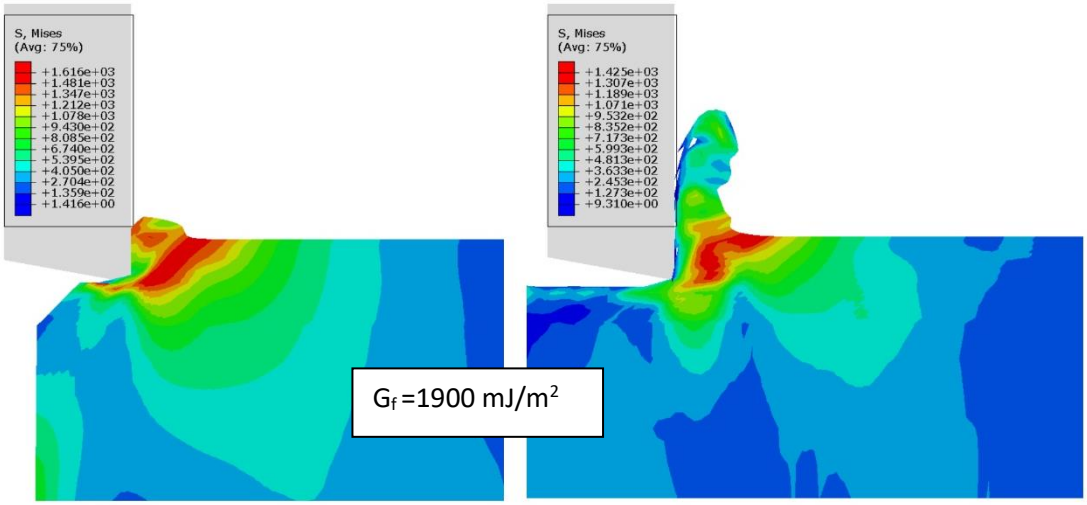
S, Mises
(Avg: 75%)
+1.616e+03
+1.481e+03
+1.347e+03
+1.212e+03
+1.078e+03
+9.430e+02
+8.085e+02
+6.740e+02
+5.395e+02
+4.050e+02
+2.704e+02
+1.359e+02
+1.416e+00
S, Mises
(Avg: 75%)
+1.425e+03
+1.307e+03
+1.189e+03
+1.071e+03
+9.532e+02
+8.352e+02
+7.173e+02
+5.993e+02
+4.813e+02
+3.633e+02
+2.453e+02
+1.273e+02
+9.310e+00
Gf =1900 mJ/m2

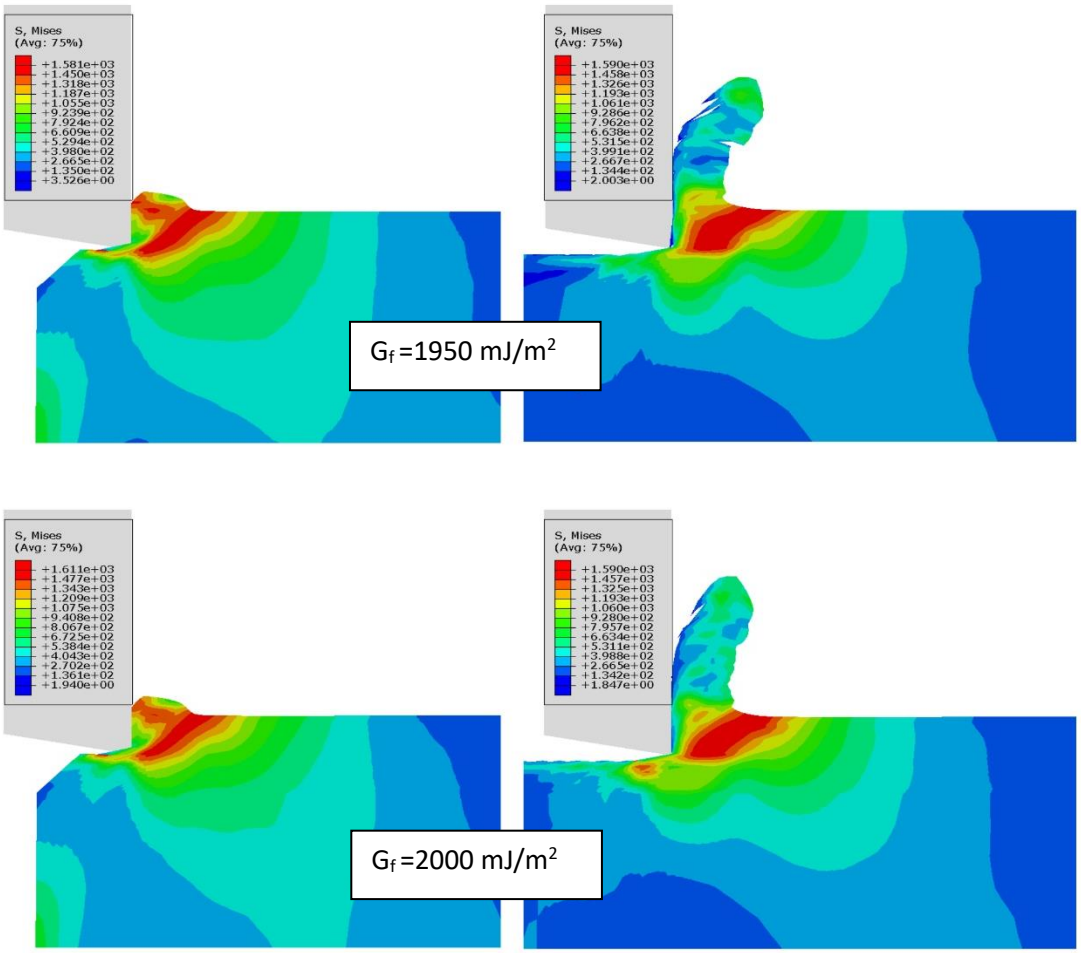

Figure 4.6 The chip formation observed at different fracture energy.

4.3.4 Friction and heat generation

Since the cutting edges normally interact with the workpiece, friction exists. Friction generation is a necessary process for the cutting operation to be completed. Friction is one of the most influential parameters in the simulation results of the cutting, as well as a main source of the induced heat. Since inelastic deformation and friction generate heat and constantly change material characteristics, they are critical for cutting. Tool wear occurs during the operation process and continues until the life end of the tool. The effective cutting tool life is when the cutting edge can operate at appropriate cutting rates to generate technically acceptable workpieces. The main indicators determining cutting tool life are surface roughness, form accuracy, wear resistance, and chip formation state. These indicators change depending on the

cutting type, whether rough or finished cut. In operating a finish cut, the cutting edge is worn out when it cannot form a specific value of surface roughness, at which wear is not allowed for continuous cutting.

In ultra-precision diamond turning, tool wear occurs, and several types of wear could exist due to mechanical stresses applied to the cutting tool. Abrasion wear is the main mechanism for tool wear and is caused by the hard particles in the workpiece materials. This mechanism is similar to the grinding process, where abrasive particles make surface-to-surface intersession between the workpiece surface and the abrasive tool; when hard wear particles from the tool and work material are interposed between the machined surface and the tool at the cutting contact, abrasion wear results (Astakhov, 2004; Yume and Kwon, 2007). Therefore, the abrasion wear process results from the load or mechanical stress on the cutting tool. Another type of wear is diffusion wear, this wear occurs by the effect of the chemical reaction between tool and workpiece materials during machining processes, the chemical properties of the cutting tool metal, and the chemical mutual effect between the metal of the cutting tool and the metal of the work material determines the mechanism of the occurrence and development of the diffusion wear (Zhang et al., 2017a). The primary types of tool failure during the machining of the Ti-6Al-4V alloy include flank wear, crater wear, plastic deformation because of abrasion wear, and dissolution-diffusion mechanisms (Astakhov, 2004).

As a result, the research focused primarily on the generated heat, material stress, and temperature status distribution during the cutting operation process. Friction between the tool-chip contact surface is a relatively complicated aspect of the cutting process, and it significantly impacts machining accuracy and surface integrity. In the metal cutting simulation, correctly identifying the interaction between the cutting edges and the workpiece geometry is critical when expressing the interaction property in metal cutting simulation, which is necessary for a fraction model between the tool and workpiece to exist. In the metal cutting process, the contact

action between chips and tool edge is significant, which involves high stressed regions, high strain rate, and high induced temperature. Zorev, (1963) demonstrated two contact regions at the interface between the cutting tool and the chip. The contact area has two regions: the sliding and the sticking regions. The sliding region adopts Coulomb's law of friction. The frictional stress and shear stress are proportional at the sticking region. The connection can be explained as follows. Using the modified Coulomb friction model:

If $\mu \times \sigma_{\mathrm{n}} < K_{\mathrm{chip}}$ Then $\tau_{\mathrm{f}} = \mu \times \sigma_{\mathrm{n}}$ Sliding region

If $\mu \times \sigma_{\mathrm{n}} \geq K_{\mathrm{chip}}$ Then $\tau_{\mathrm{f}} = K_{\mathrm{chip}}$ Sticking region

Where:

μ : friction coefficient

σ_{n}: normal stress

τ_f: friction stress

m_{Tresca} : Tresca factor

K_{chip}: shear flow stress.

4.3.5 The thermal analysis of the Ti-6Al-4V cutting process

As previously stated, the cutting process involves heat, which originates from the interaction between the cutting tool and the workpiece. It is also obvious that the heat was generated as a result of friction between the surface of the metal and the cutting tool edge, which requires the development of a method to get rid of heat so as not to affect the performance of the cutting and the accuracy of the product as well as the surface integrity. It's aimed that this study investigates the impact of this heat's existence on cutting performance. The removal of the chips from the metal is accompanied by the generation of

heat, which originates from the presence of friction, as described by Eq. (4-6),(4-7), and (4-8), where part of the heat is produced by the plastic work of the hard-to-cut material and refers to this by $\dot{q}_p$ in Eq. (4-6), and the other part is generated by friction arising from the movement of the cutting tool at the metal surface, and is referred to this part of the heat by $\dot{q}_f$ as described in Eq.(4-7).

$$\dot{q}_p = \eta_p \bar{\sigma} : \dot{\varepsilon}_p \quad (4\text{-}6)$$

$$\dot{q}_f = \eta_f \times \tau_f \times V_s \quad (4\text{-}7)$$

$$\dot{q}_{\rightarrow Tool} = f_f \dot{q}_f \quad (4\text{-}8)$$

Where:

η_p : Fraction of energy produced by material plastic work

η_f: fraction of the energy generated by friction work

τ_f: friction stress

V_s : material sliding velocity

f_f : fraction of the heat transferred to the cutting tool.

$\dot{q}_{\rightarrow Tool}$: heat flux due to material friction transferred to the cutting tool.

In this study, the above material models were applied to study the effect of the change of thermal property factor when cutting titanium alloy. A 2-d orthogonal cutting of titanium alloy using ABAQUS Software has been simulated. As mentioned, the adjustment in the thermal physical properties of the work material assisted to improve the cutting performance. A thermal study has been conducted based on changing the values of the thermal properties of the machined workpiece. The thermal study was carried out based on changing the thermal

conductivity coefficient values. As shown in Table 4.3, different values are used for thermal conduction property analysis, and the effect of this change was monitored in the cutting process simulation. The results of the cutting simulation of Ti-6Al-4V under different thermal conductivities are shown in Figure 4.7. It was discovered that there is a difference between the chip morphology in this study when the thermal conductivity changes, and from the perspective of temperature distribution and heat transfer, as shown in Figure 4.8, it can be seen that the diffusivity rate increased, and the localized temperature decreased.

The temperature distribution over the titanium cutting simulation is shown in Figure 4.8, along with the occurrence of adiabatic shear and plastic strain to form a smooth chip that prevents generated heat from diffusing. When heating softens the metal and thus overcomes strain hardening, more strain is concentrated until the metal becomes hotter and softer. As thermal conductivity increases, the adiabatic shear decreases and affects the chip formation slightly, and heat generated from the cutting process decreases near the interface between the cutting tool/workpiece interface. Given that Eq. (4-9) describes the fundamental of transferring heat in two dimensions that occur when dealing with orthogonal 2d cutting, the temperature distribution over the cutting zone can be predicted, as shown numerically in Figure 4.8, where ρ, c, k, T, and q are the density, specific heat, thermal conductivity, temperature, and heat generation rate per unit volume, respectively; x, y are the coordinates, and u_x and $u_y$are the velocity components in the x and y directions.

$$\rho c\left(u_x\frac{\partial T}{\partial x}+u_y\frac{\partial T}{\partial y}\right)-k\left(\frac{\partial^2 T}{\partial x^2}+\frac{\partial^2 T}{\partial y^2}\right)+q(x,y)=0 \qquad (4\text{-}9)$$

The results of the finite element analysis conducted with the ABAQUS software assisted in investigating the cutting mechanism of Ti-6Al4-V when the thermal property of the work material was altered. They demonstrated the effect of thermal conductivity on reducing

the heat generated during machining, thereby enhancing cutting performance in a clean environment without using coolant.

Table 4.3 Values for the thermal conductivity coefficient in the cutting simulation of Ti-6Al-4V.

K	k_a	k_b	k_c	k_d	k_e
(W/m. K)	3.55	7.10	10.56	14.20	17.75

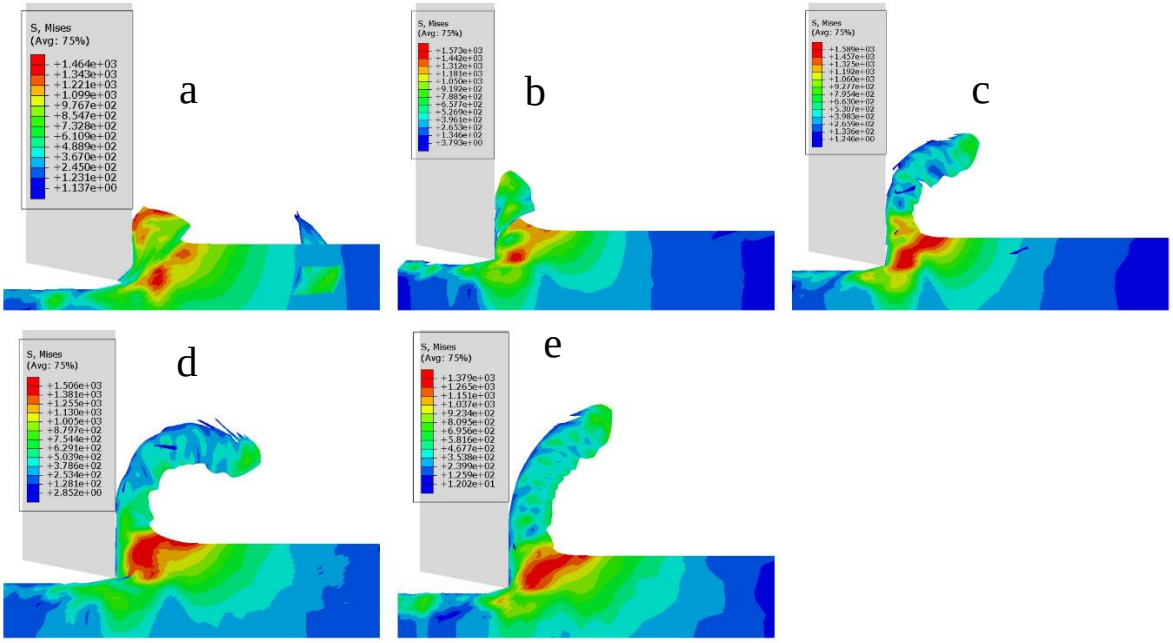

Figure 4.7 The chip formation, and chip morphology of Ti-6Al-4V acquired for orthogonal machining at different thermal conductivities.

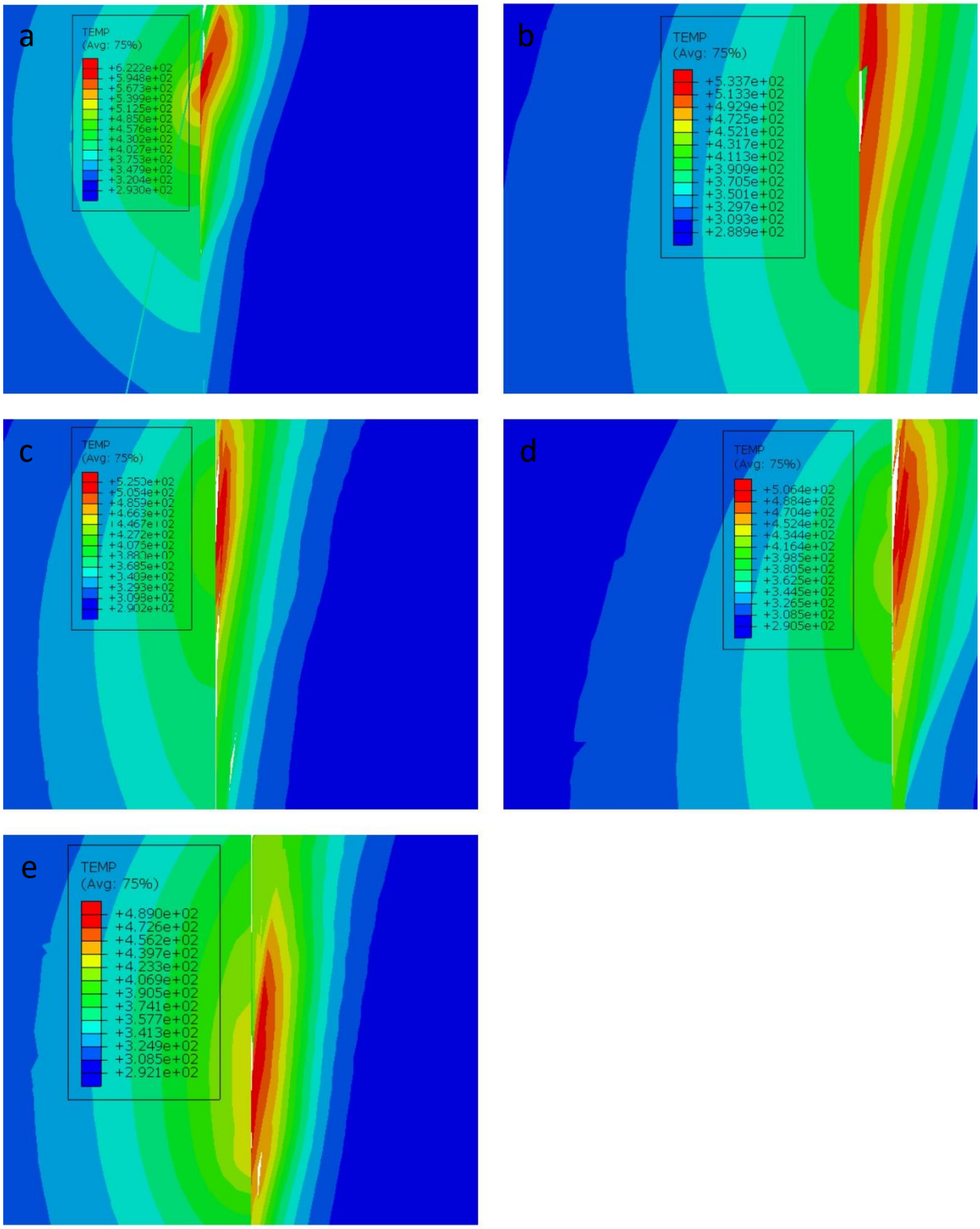

Figure 4.8 The temperature distribution during the cutting simulation of Ti-6Al-4V at different thermal conductivities.

4.4 Experiments

Figure 4.9 illustrates the experimental configuration for magnetic field-assisted machining. The workpiece is made of Ti-6Al-4V alloy, and its chemical composition is listed in Table 4.4. The cylindrical workpieces used in the experiments have a diameter and length of 15mm and 24mm, respectively. The cutting tool employed was a single-point diamond tool, a type of tool that is frequently used in single-point diamond turning. The workpieces were roughly machined to ensure the axis symmetry and remove any irregularities caused by a mounting, and then the finish cut was carried out. As illustrated in Figure 4.9, a custom setup was used as a permanent magnetic field source during the cutting process. This setup consists of rectangular pieces of the same material that serve as the primary source of the magnetic field. These magnets are connected with an aluminium part attached to the ultra-precision machine through a steel fixture. An aluminium fixture was employed to hold the workpiece to the vacuum chuck. The experiments were conducted on a Moore Nano-tech 350FG (4-axis ultra-precision turning machine), typically is employed for diamond turning. The machining experiments were categorized as conventional diamond turning (CDT) and another as magnetic field diamond turning (MFDT), which experienced a 26mT magnetic field intensity. The cutting depth was set to 5µm, the feed rate was set to 10mm/min, and the cutting speed was set to 50 m/min, which all maintained unchanged throughout the cutting operations. The produced chips were examined under the SEM. Following the experiments, the samples were examined for surface roughness using a high-precision optical profiler, Zygo. To study tool wear, the cutting edges were cleaned with hydrofluoric acid and then viewed through a scanning electron microscope to observe the rake and flank faces of the diamond tools.

Table 4.4 The composition of Ti6Al4V samples used in the experiments.

Element composition (%)						
Al (Aluminum)	V (Vanadium)	Fe (Iron)	N (Nitrogen)	O (Oxygen)	H (Hydrogen)	C (Carbon)
6	4	0.3	0.05	0.2	0.012	0.1

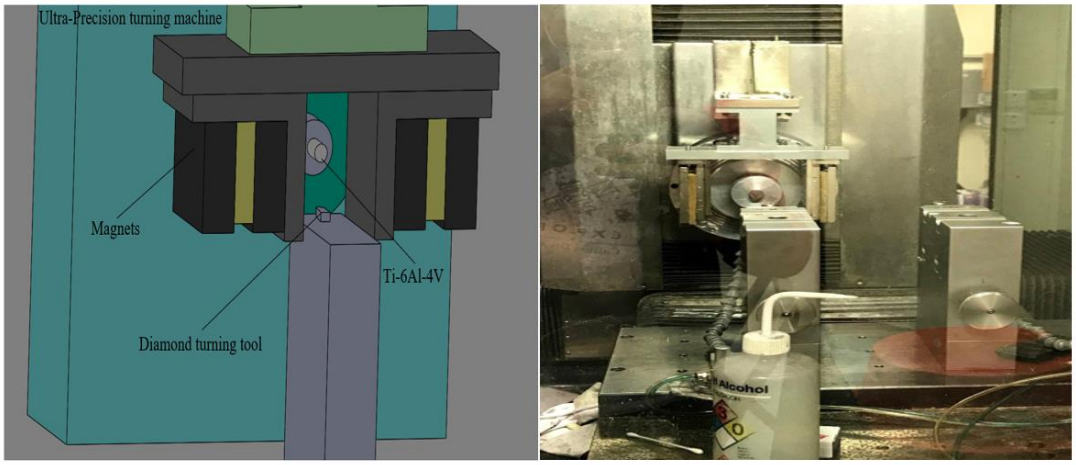

Figure 4.9 The experimental setup.

4.5 Results and discussion

4.5.1 Influence of the magnetic field diamond turning (MFDT) on the surface quality

To get parts with high surface quality that meet the requirements of the advanced application, the hard-to-cut materials received more attention by exploring advanced machining methods leading to a defected-free surface. It is essential to comprehend the significance of the surface quality of the parts correctly and to analyze the related various operating factors that could affect the surface integrity in the cutting process. Hence, improving surface quality leads to enhanced product performance and sustainability.

The surface roughness values of MFDT and CDT samples are shown in Table 4.5, where eight points were chosen on the diagonal of each sample's surface as shown in Figure

4.10 where the machined surface of MFDT presented the lowest surface roughness. Normally the improved surface roughness is observed under smooth machining conditions, which was caused by utilizing the magnetic field in this study as an assistive tool for increasing the heat dissipation from the cutting area. Figure 4.11 shows the captured surface images of the samples at different magnifications; it offers a significant difference between the surfaces obtained regarding smoothness and integrity; the MFDT machined surface, as seen in Figure 4.11 (a) presents fewer marks that can be hardly observed, and the surface is less wavy which indicating high surface integrity. In Figure 4.11 (b), the marks caused by the cutting tool can be seen obviously, and some surface irregularities were observed, revealing a relatively low machining performance for CDT. For further investigation on the machined surface, Figure 4.12 illustrates the difference between the surfaces of the two samples based on visual inspection, demonstrating the superiority of MFDT in obtaining a highly mirrored surface and increasing the potential of titanium alloys' application in optical industries.

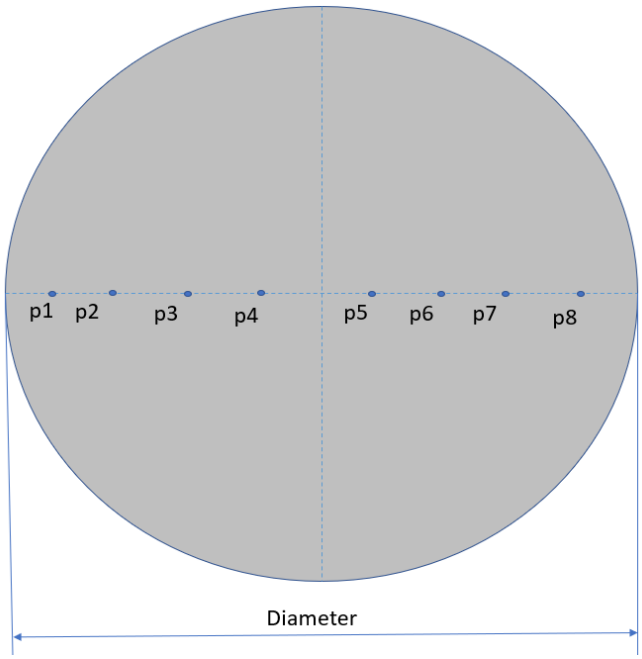

Figure 4.10 The measured points on the sample’s surface.

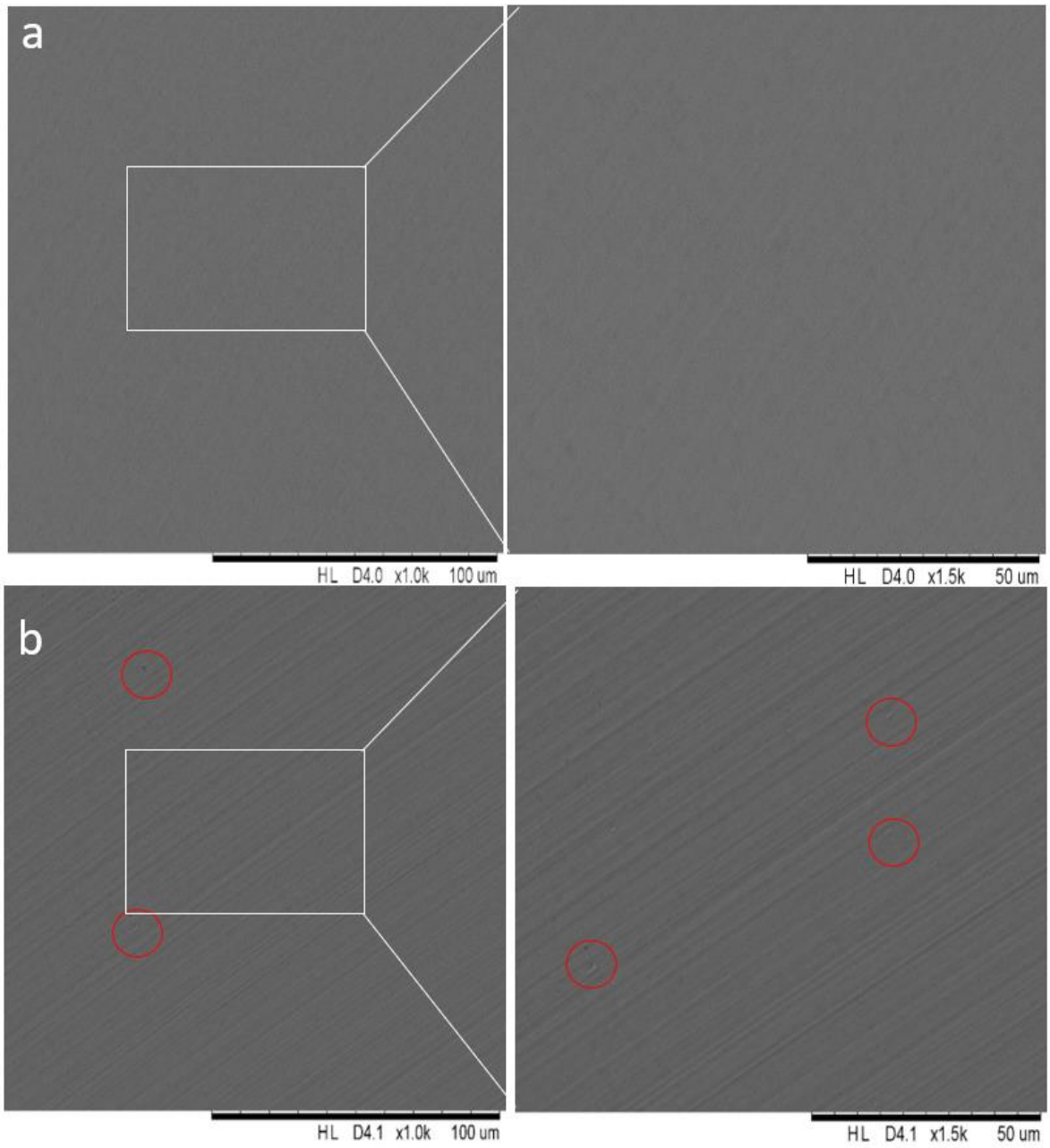

Figure 4.11 Scanning electron microscopes7 of surface topography of samples machined under (a) MFDT (b) CDT at different magnifications.

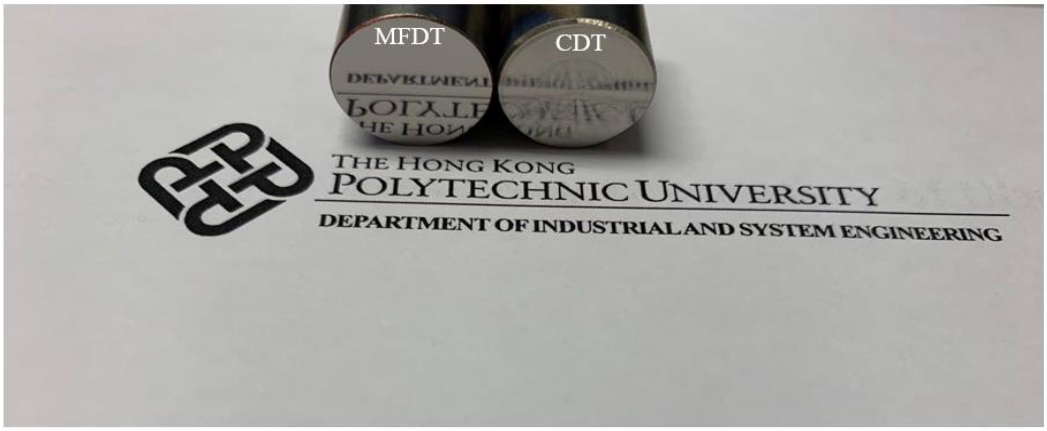

Figure 4.12 The machined surfaces of the two samples.

Table 4.5 The surface roughness of the samples (nm).

Point	1	2	3	4	5	6	7	8	**Average**
CDT	37.14	42.68	71.65	51.09	52.5	68.13	41.15	34.51	49.86
MFDT	16.84	15.94	16.33	15.3	16.9	17.32	16.39	16.74	16.47

For further investigation of the machined surface integrity, the surface profiles of the samples were measured by Zygo, and a random area was chosen and captured, as shown in Figure 4.13. Prominent irregular peaks are noticed on the sample surfaces machined by CDT, the flatness of the sample surface varies largely through the sample's machined area, and large beak heights were observed. Given the results of observation of more serious tool wear for CDT, it can be stated that the worn tool generated in CDT caused irregularity to the machined surface, as shown in the surface topography, since the induced heat results in a worn tool that worsens the machined surface, this is clearly shown by the tool edge marks on the captured machined surface and also from the surface roughness values. When a magnetic field is present, the sharpness of the cutting edge is maintained; the machined surface of MFDT exhibits a fairly uniform topography with only slight height variations, and the tool marks do not exist, indicating a mirrored flat surface which is revealed in the surface roughness values. Overall, the machined surface profiles exhibited superior surface generation when the induced cutting

temperature was regulated under a magnetic field influence, chips were removed smoothly, and surface quality was preserved.

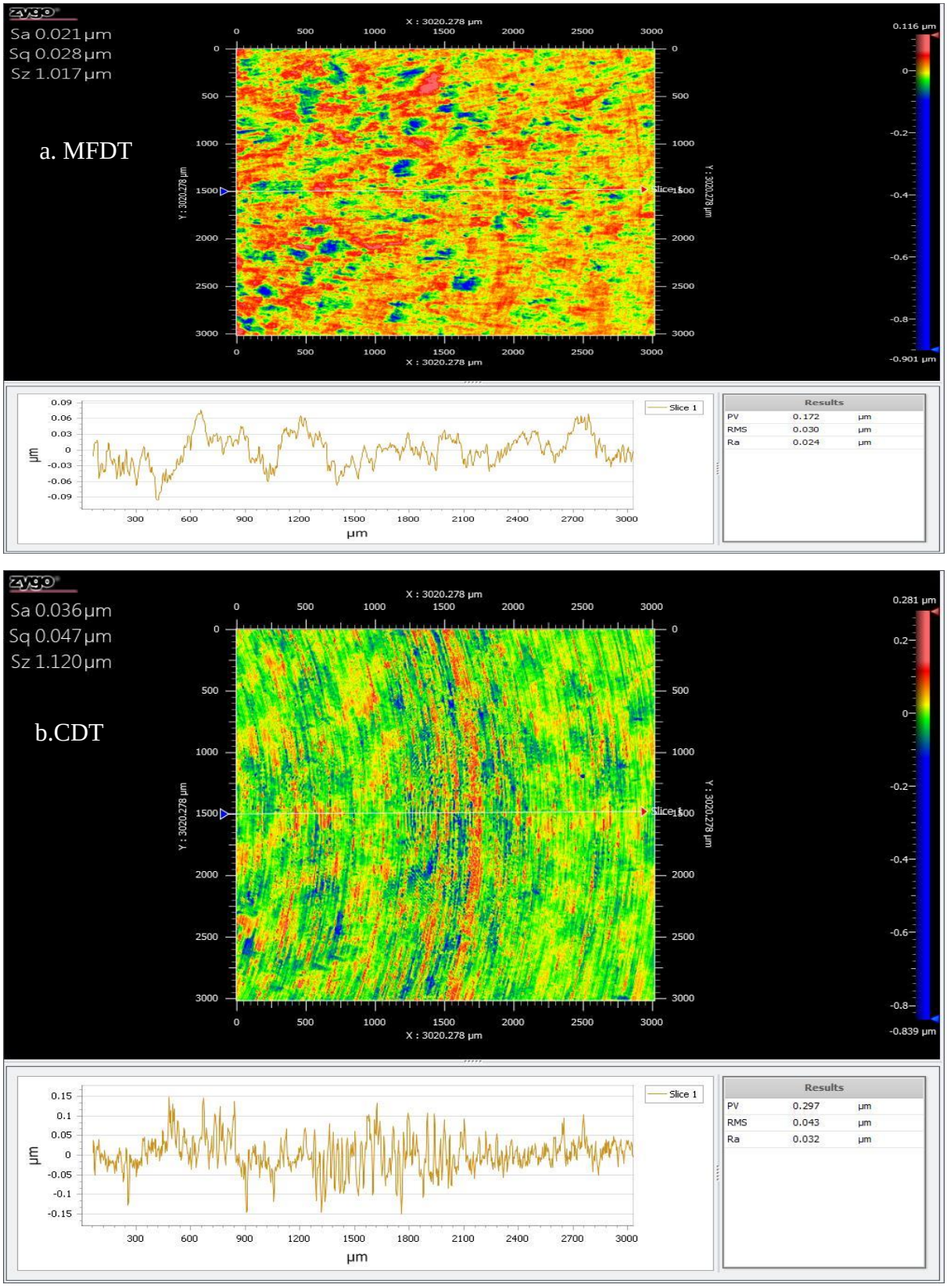

Figure 4.13 Machined surface profiles for a) MFDT and b) CDT.

In addition, the AFM results of the surface of the machined samples were captured. As seen in Figure 4.14, the tool edge marks are clearly visible and larger on the surface of the CDT sample, where the tool trajectory is observable. In contrast, the MFDT sample exhibited relatively shallow tool marks for the same area size analyzed.

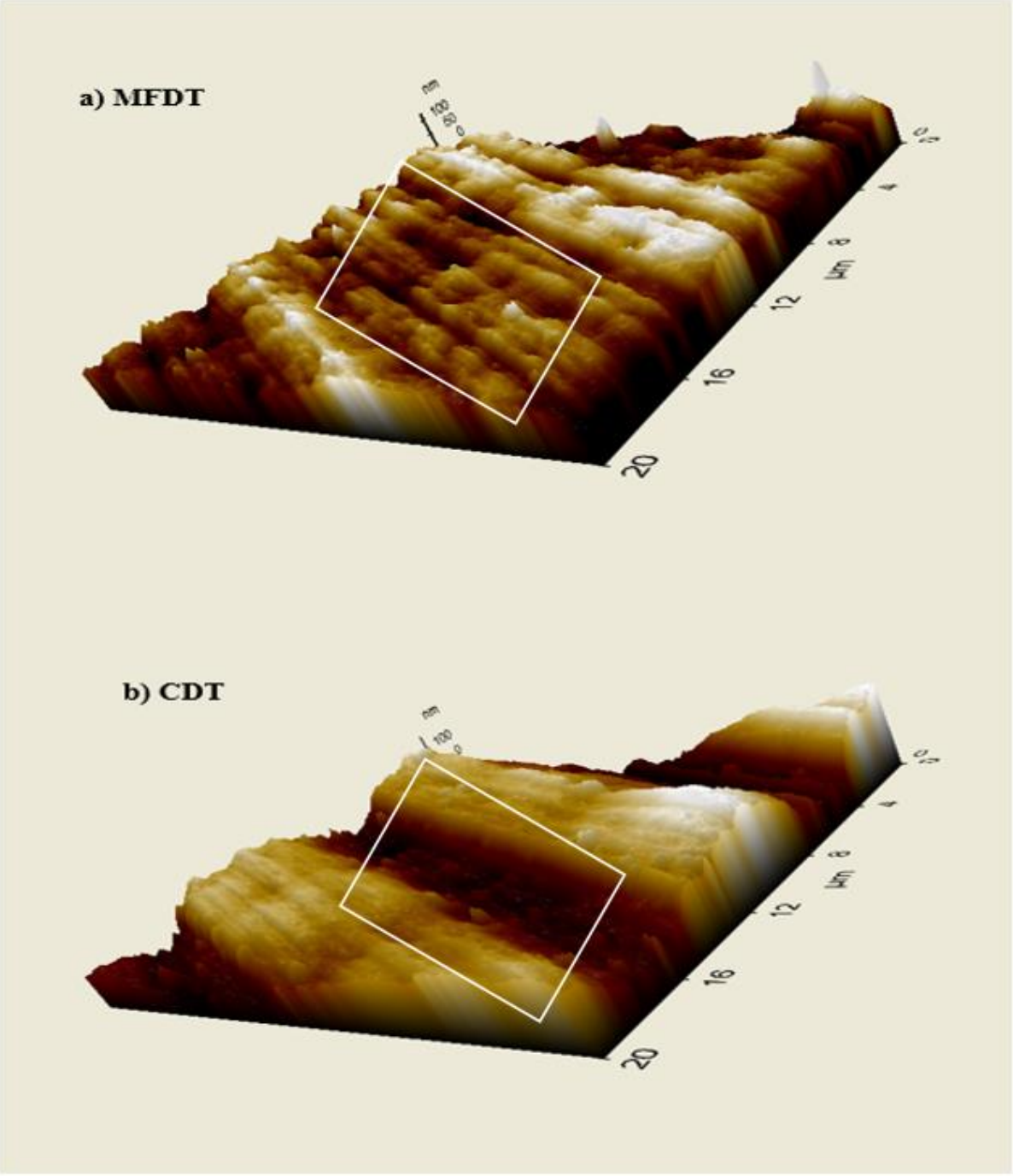

Figure 4.14 AFM images for a) MFDT b) CDT

4.5.2 Effects of Magnetic Field on Ti-6Al-4V phases

Figure 4.15 displays the XRD results for the Ti-6Al-4V alloy. XRD was used to determine the phases of the MFDT and CDT samples following machining. The diffraction peaks of the α and β phases are observed, and it can be seen from the figures that both samples retained the same pattern after machining, indicating that the magnetic field had no detrimental effect on the compositions of the machined surface. Since the XRD results conform to the standard data, this demonstrates the efficiency of magnetic field application without sacrificing phase stability.

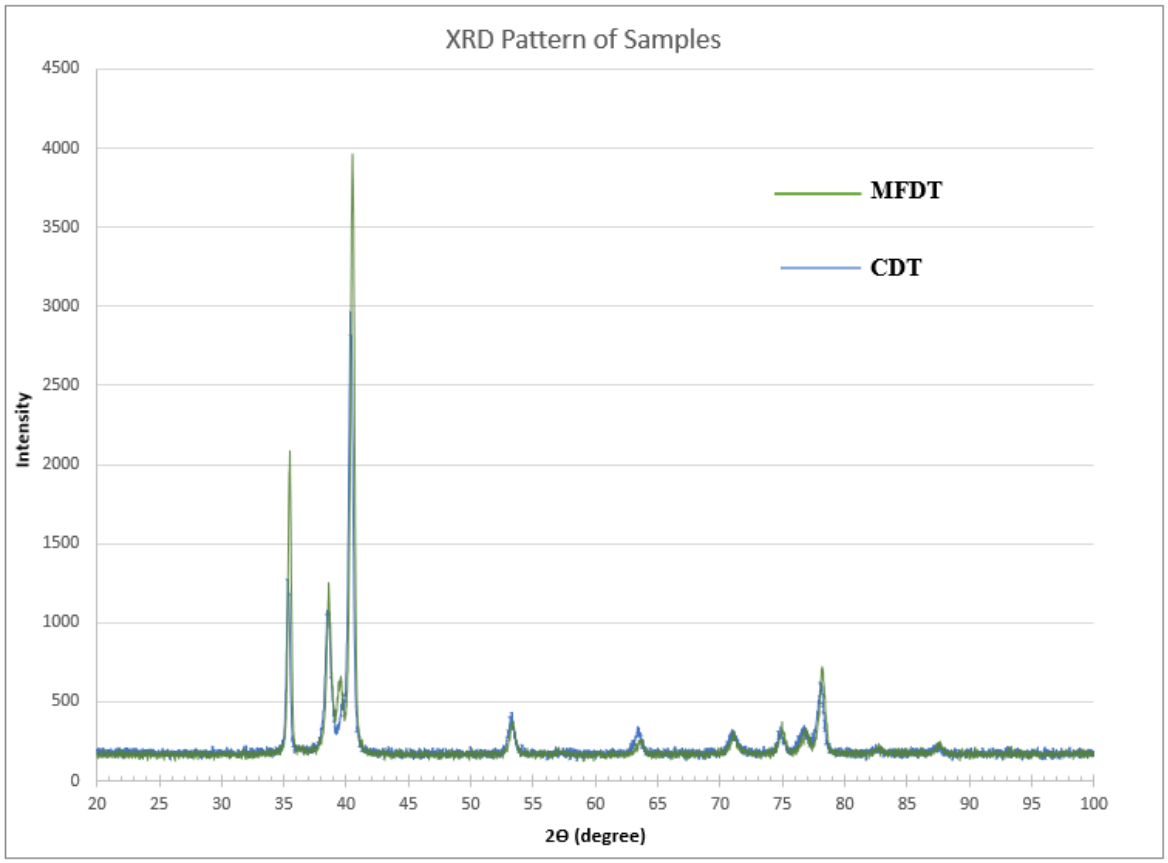

Figure 4.15 XRD results for the machined samples generated by MFDT and CDT.

4.5.3 Influence of the magnetic field diamond turning (MFDT) on the cutting tool

Because the diamond tool's condition plays a significant role in estimating the quality level of machined parts, cutting tool wear should be monitored during and after the cutting

process. Observing the online cutting temperature is one issue that arises in Ti alloys machining. Because of the limited thermal conductivity of titanium alloys, which causes the temperature to rise during high-speed cutting operations and poor heat dissipation outside the cutting zone, the tool is affected (Bordin et al., 2015). The studies of the cutting tool during and after the cutting operation reflect the cutting process's quality and indications of potential problems in the machining processes, which leads to further investigation of the cutting tool's degradation. Several studies have analyzed the cutting tool's performance to predict the cutting operation's overall efficiency. Since elevated cutting temperature is present and unavoidable, generated chips roll and adhere to the cutting tool edges, forming adhesive wear (Rahim and Sasahara, 2011). It is known that when titanium alloys are machined, heat is retained within the cutting zone due to the disability of these alloys to convey the thermal energy, which reveals the lack of titanium to deliver the generated heat. One of the problems that arise when the heat generated exists during machining is the formation of weldments on the cutting edge, and this leads to cutting tool vibrations during the cutting operation. Zlatin and Field (1973) stated that titanium alloys tend to weld with the cutting tool edge in the case of high spindle speeds and start to wear. Compared to other metals, titanium causes the cutting tool to be worn at a faster rate due to the disability of titanium to dissipate the generated heat to the surroundings. From an economic standpoint, production costs also include the cost of cutting tools, and every reduction in the cost of the cutting tool leads to a reduction in overall production costs. Because the condition of the cutting tool can be used to evaluate machining performance, the investigation of cutting tool wear is crucial in evaluating the sustainability of the machining process. As the accuracy of machined parts' profile and surface finish is determined by the cutting-edge condition, many researchers consider the investigation of the tool wear mechanism in UPM to be a crucial evaluation factor for a successful sustainable machining operation.

Figure 4.16 displays SEM images of the cutting tool; Figure 4.16(a) reveals that during CDT, the cutting tool experienced adhesive wear; the adhesive wear was caused by the cutting chips adhering to the cutting edge and the elevated cutting temperature with inadequate heat dissipation. According to (Dearnley and Grearson 1986) research, the welded chips on the cutting tool edges are the primary causes of the adhesive wear that can lead to surface cracks. Nonetheless, when the MFDT was implemented, severe adhesive wear was prevented, as shown in Figure 4.16(b), due to the magnetic field's ability to reduce the high heat. Figure 4.16(c) shows that the flank face exhibited abrasion wear. As a result of the friction that existed at the interface between the workpiece and the tool flank, flank wear accelerates when excess heat becomes trapped in the cutting zone. As shown in Figure 4.16(d), the presence of a magnetic field reduced the flank wear rate compared to conventional diamond turning, resulting in a longer tool life when a magnetic field is present. Applying a magnetic field reduced the trapped heat and friction, thereby protecting the tool, following the results of an investigation into the machined surface, which revealed a high-quality surface.

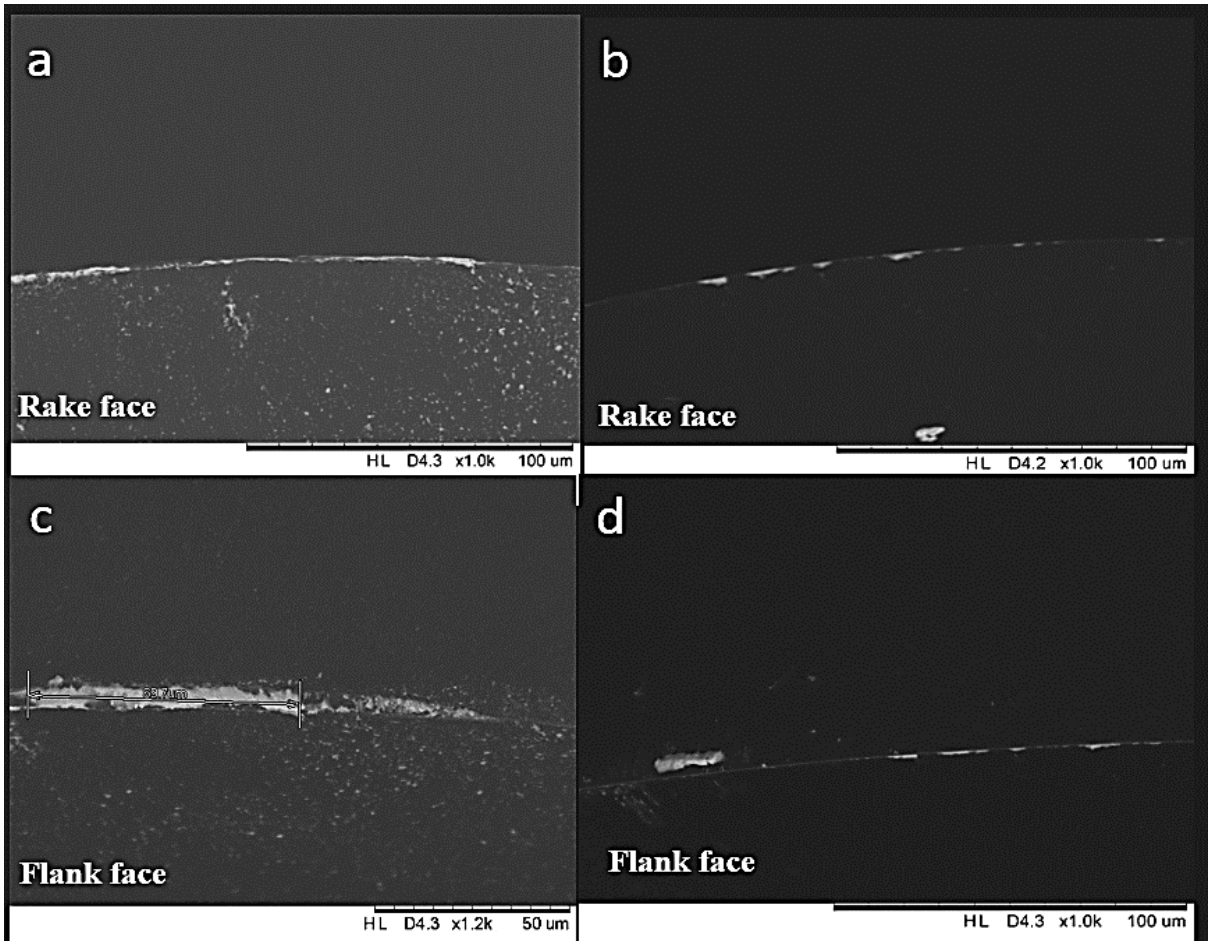

Figure 4.16 SEM images of the tool: (a) tool rake face in CDT, (b) tool rake face in MFDT, (c) tool flank face in CDT, and (d) tool flank face in MFDT.

4.5.4 Influence of the magnetic field diamond turning (MFDT) on the chip formation

The process of chipping occurs as a result of an interaction between the cutting edge and the workpiece with a sufficient shear load that exceeds the limits of deforming the metal, resulting in the removal of the material in the form of chips. The state of the chips can be used to determine the success of the machining process; when these chips are smooth, the cutting process has been completed satisfactorily, whereas if the chips are in an irregular shape, it implies difficulties happened during cutting.

As the chip generation in UPM is an evaluation factor of the machining performance and can affect the cutting tool and surface roughness, the chips created during the machining were collected and analyzed by scanning electron microscope, as seen in Figure 4.17. As shown

in Figure 4.17(a), the edges of the chips generated by MFDT have a finer formation. While the chips generated in CDT) as shown in Figure 4.17(b), are serrated with sharp edges identical to chips formed machining of difficult-to-cut materials, which indicates a relatively lower machining performance and a product with a low integrity surface due to the presence of uncontrolled heat in the machining zone. Clearly, in this eco-friendly procedure - MFDT, the smooth chipping process occurred when machining was performed under the influence of a magnetic field. Also, it's observed that by overcoming the heat produced during the cutting process, the formed chips change from serrated to continuous. This can be shown by combining the results of chip formation obtained from the FEM and the analyzed chips collected from the machining of Ti-6Al-4V under the influence of the magnetic field, which can be demonstrated by the effect of the thermal softening and its relationship to strain and strain rate as a result of rapid heat induced at the cutting area.

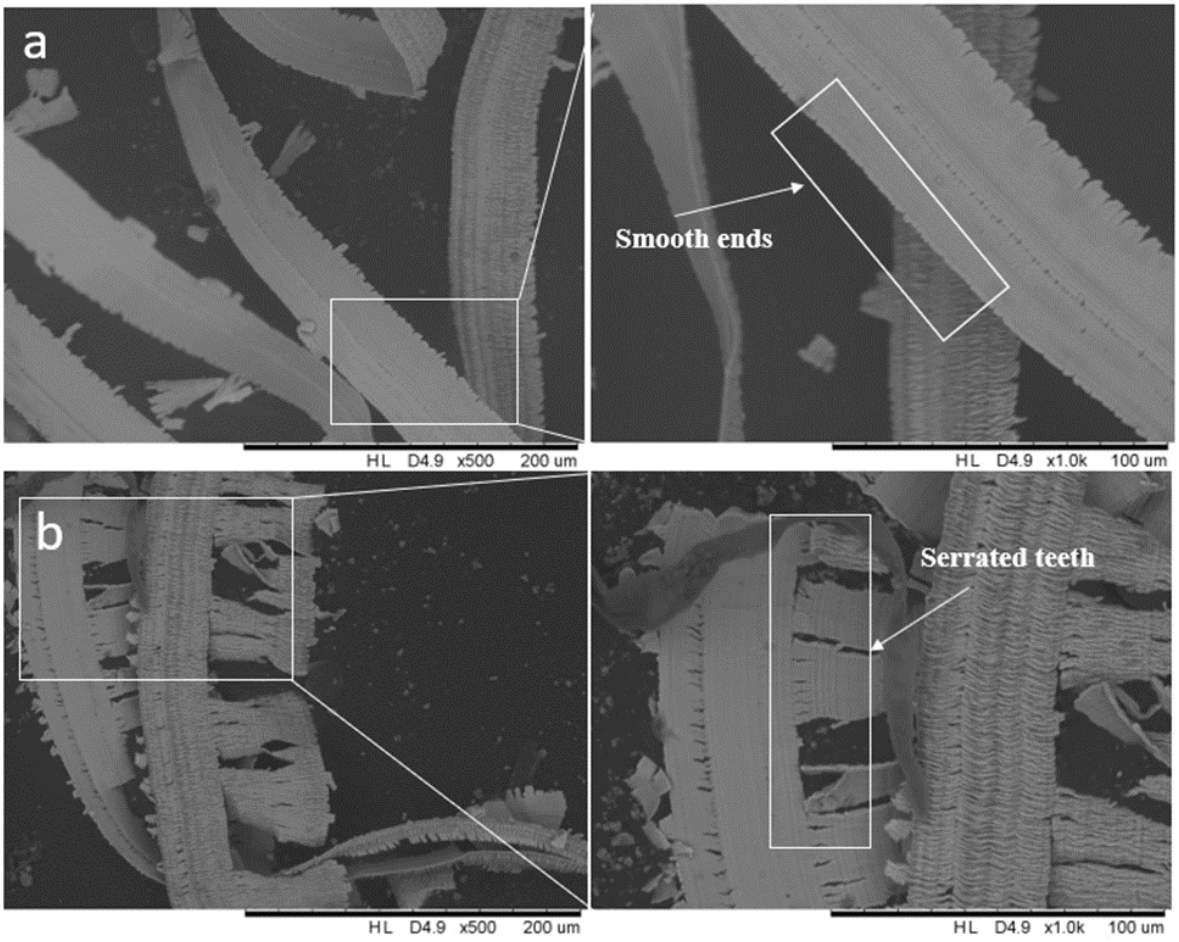

Figure 4.17 SEM images of chips formation in (a) MFDT, (b) CDT

4.6 Summary

In this chapter, the magnetic field effect is utilized in single-point diamond turning to modify the physical characteristics of titanium alloys, which are difficult to process. In this work, FEM was used to analyze the generated magnetic flux and to determine the magnet materials, shape, and dimensions to maximize the magnetic flux density and the covered cutting zone affected by the magnetic field. This can help attain the appropriate magnetic field strength during the UPM procedure. The influence of fracture energy on the cutting simulation of Ti-6Al-4V was also examined, revealing that chip formation varies with fracture energy values. In cutting experiments, the applied magnetic field system was adjusted, and the machining performances were evaluated based on the indicators of surface integrity, cutting tool

conditions, and chip formation. During the analysis phase, AFM, XRD, and optical profiler were utilized to examine the machined samples' surface morphology and composition.

For thermal analysis of magnetic field ultra-precision (MFUPM), finite element modeling FEM is built under the Johnson-Cook constitutive model and geometrical model, taking flow stress, strain, strain rate, and temperature into account, with the Johnson-Cook constitutive model serving as a link between material parameters, mechanical loading, effective stress, and heat at the tool/workpiece interface. The JC damage model was used, and the failure evolution-based fracture criteria were applied where the failure energy was considered. The geometric model includes tool settings, workpiece geometry, and machining conditions. An external magnetic field principle has been shown to improve Ti-6Al-4 V thermal conductivity during UPM. The experimental results in this study demonstrated that the magnetic field improves the UPM performance of the Ti-6Al-4V alloy, and the simulated and experimental results were consistent. These findings revealed improved surface integrity and increased diamond tool life. Also, in this study, the use of hazardous lubricants could be eliminated and replaced with a feasible machining method with the assistance of a magnetic field to reduce the cutting temperature.

Chapter 5: Conclusions and suggestions for future studies

5.1 Conclusions

Titanium alloys have unique properties compared to other alloys. Titanium alloys are utilized in a wide range of parts and fields. Their preference may be based on corrosion resistance or strength properties, with the additional biocompatibility features for applications involving biomedical implants (Koizumi et al., 2019). They are employed in power-generating systems, tanks, heat exchangers, reactor vessels, and other corrosion applications. High-strength titanium alloys, including Ti-6Al-4V, are used in applications for high-strength performance. Further, they are ideal for various industrial applications, including prosthetics, additive manufacturing, marine, and aviation. Due to their outstanding characteristics and high corrosion resistance, titanium alloys have become a vital structural material for many industrial items. They serve as promising bioengineering materials because they are biocompatible, have a density and flexibility like human bone, and have good corrosion resistance. Their use has addressed several key engineering and technical issues, accelerated scientific and technological progress, and provided substantial economic benefits.

Titanium alloys, however, have poor machinability and are difficult to cut. Their thermal conductivity is low, particularly at high temperatures, which has a negative impact on the materials' machining performance. Titanium alloys' poor thermal conductivity reduces the heat transmission rate out of the machining zone. As a result, the produced heat at the cutting area slowly dissipates. The presence of the confined heat at the cutting tool/workpiece contact area increases, leading to tool wear, which degrades machining performance and workpiece surface integrity, thereby reducing tool life. Many researchers have studied the challenges of machining titanium alloys to achieve adequate machining performance to overcome their low machinability.

Many methods have been investigated by researchers who have dealt with the machinability of titanium alloys that have relatively improved their machining performance. These investigations included optimizing cutting factors, coping with tool vibration during cutting, using advanced or coated cutting tools, various cooling methods, and applying physical approaches and treatment processes. In this thesis, UPM was utilized to enhance the titanium alloys' machinability with the assistance of the magnetic field effect. A magnetic field system was modeled and analyzed to affect the behavior of the workpiece material during operation. In this study, improving the cutting process performance of Ti-6Al-4V by utilizing the magnetic field was achieved. The main difficulty in cutting titanium is due to its inherited properties, mainly low thermal conduction, which primarily results in poor cutting performance due to accumulated heat at the cutting area that affects the condition of the cutting tool edges. When the cutting tool comes into contact with the workpiece, friction is created between them. The higher the movement speed, the greater the quantity of friction and heat generation, resulting in a rise in emerging temperatures and consequent cutting tool wear. Most studies usually apply lubrication and greasing; as a result, that can significantly reduce friction and heat. Lubrication is an additive used to reduce friction and wear caused by movement between cutting edges and workpiece surfaces. This means that lubricating the moving parts of various machine elements is a critical first step in ensuring that the machine elements perform correctly. In addition to the longer duration of the operation, the presence of lubrication eases of movement of machine parts, the speed of the process, and the quality of the production. However, lubricants are not recommended environmentally.

The heat is typically generated when the machining starts, especially if the work material is difficult to cut, like Ti-6Al-4V. Low machining performance leads to a severe deviation of surface accuracy due to friction and wear of the cutting edges, which is not desirable in metal cutting processes. So, the appropriate method is needed to overcome this

induced heat. Adequate heat dissipation must be ensured on an ongoing basis. Oily materials are basically a highly effective means of the cooling process; they can protect surfaces from wear. The oil absorbs the heat, increases the operation quality, prolongs the life span of the cutting tools, and maintains the operation smoothly. The cooling function was adjusted in this study by using a magnetic field. It's necessary to lower the temperature of the cutting tool due to friction caused by the cutting edge's penetration into the workpiece surface, allowing for longer operation times and higher quality. Proper transferring of the heat generated by the cutting process out of the cutting zone is needed. During the cutting process, the cutting tool edge of the turning machine is subjected to significant stress and friction due to its penetration into the workpiece to achieve the chipping process. This step induces a sharp temperature rise at the cutting area, especially with titanium alloys' poor thermal conductivity. A damaged cutting tool's edges and poor surface are produced without adequate heat transfer.

To summarize, the machining of titanium alloys causes a regular rise in cutting temperature, which substantially impacts the cutting tool and workpiece qualities. Heat should be reduced to prevent the cutting edges from rapidly consuming and to provide a well-machined surface. The magnetic field system was adopted as an alternative method for improving the machinability of Ti-6Al-4V. Applying the magnetic field added a machine tool life extension and produced high-quality machined parts. The assistance of the magnetic field in UPM of titanium alloys in this study is summarized as follows:

1) A magnetic field-assisted ultra-precision machining (MFUPM) system was developed utilizing a permanent magnet for creating the magnetic field with adjustable magnetic field strength. The permanent magnets were installed in fixture steel to generate a uniform magnetic field in accordance with Maxwell's magnetic field law. Based on preliminary experimental findings and a theoretical foundation, the ideal magnetic effect in UPM is produced by choosing the magnetic field intensity and the adjustable distance for

positioning magnets in the magnetic system. The crucial parameters for MFUPM are the magnetic field density and the distribution of magnetic flux in the cutting zone. The working principle is based on the force acting on an object surrounded by a magnetic field is determined by the properties of both fields and the target object. Applying the effective dipole moment method, where an equivalent point dipole replaces a magnetic object has a moment, the acting magnetic force on a magnetic microstructure can be modeled. As mentioned in chapter 3, the magnetic field sources' characteristics are changed by applying force to such a dipole. Additionally, it is affected by the separation distance between the source and the object. The existence of a magnetic field while operating the turning process has promoted chip passage and prevented the chips from clinging to the cutting tool edge, preventing the development of a built-up edge on the cutting tool. Additionally aids in chip transit, avoiding the cutting tool from developing a built-up edge and preventing chips from sticking to the tool edge. Furthermore, the produced chips could exit the cutting area quickly, and reduce heat accumulation in the cutting zone, which is crucial for efficient operation achievement. The finite element method FEM has demonstrated the impact of the permanent magnet device, and the simulation of the magnetic field system was presented; the finite element method FEM has shown the influence of the permanent magnets and the simulation of the magnetic field system. The model included the magnet's material and the fixation. The air region was included as well. The mesh study was controlled by selecting a proper element size. According to Maxwell's magnetic field law, magnetic flux was described.

2) Based on this study on the machinability of titanium alloys, the MFUPM was utilized to improve machinability and the quality surface of machined parts of titanium alloys. Several researchers have demonstrated the capability of using magnetic fields in metal cutting, which has been successfully employed to machine a variety of difficult-to-cut materials. It

was shown that the magnetic field could uplift the thermal conductivity of Ferro materials through the arrangement of the conducting atoms. Excessive heat causes the majority of machining challenges of titanium alloys because it accelerates tool wear and results in a degraded cutting edge; in this state, the workpiece material adheres to the cutting tool, resulting in a built-up edge. Therefore, in this part, the magnetic flux intensity firstly was tuned and experimentally confirmed in combination with the other machining parameters. Previous studies have shown that a magnetic field can enhance the physical characteristics of ferrometals, such as thermal conductivity. The movement of molecules has explained this and their alignments from their random states by the Law of Van der Waals to a regular and straight state when subjected to an applied magnetic field. As these molecules align, acting as expanded routes for heat transmission, the rate of heat transfer is increased. Many researchers reported on the effectiveness of the magnetic field in elevating the thermal conductivity for the same reason when the magnetic field applies, the random state of the particles becomes regular and aligned to facilitate the conveying of heat. It was reported that due to the effect of the Van der Waals forces, the particles attach randomly, as well as the impact of the dipole-dipole interaction; when a magnetic field is present, the alignment occurs, and a chain of magnet particles acts as a conductor for transferring the heat. Therefore, the thermophysical properties of materials can be changed based on the application of the magnetic field.

This study applies a magnetic field to the Ti-6Al-4V alloy during the machining process to increase the heat dissipation from the cutting zone. Consequently, the excessive heat in the cutting zone is reduced. The basic idea is that when a magnetic field is applied to a conductive workpiece, the magnetic particles align parallel to the direction of the provided magnetic field. As a result, the thermal conductivity of the machined area is improved, and the collected heat in the cutting zone is reduced. Turning the workpiece while providing a

magnetic field speeded up the heat transfer, reduced tool wear, and facilitated cutting temperature dissipation, all of which contributed to a successful machining operation.

Based on the experimental results, the machined surface of samples from the magnetic field has presented the lowest surface roughness, typically observed under smooth machining conditions caused by utilizing the magnetic field in this study as an assistive tool for increasing the heat dissipation from the cutting area. And the captured surface images of the samples at different magnifications have shown a significant difference between the surfaces obtained regarding the smoothness and integrity; the magnetic field samples presented fewer marks that can be hardly observed, and the surface is less wavy, indicating high surface integrity. And a highly mirrored was obtained that could increase the potential of titanium alloys' application in optical industries. The AFM results of the surface of the machined samples were captured and showed that tool marks are clearly visible and larger on the surface of the machined sample in the absence of the magnetic field. The XRD results for the Ti-6Al-4V alloy were used to determine the phases of the machined samples. The diffraction peaks of the α and β phases were observed, and both samples retained the same pattern after machining, indicating that the magnetic field had no detrimental effect on the compositions of the machined surface. As the cutting-edge status determines the profile accuracy, sharpness, and surface finish, many researchers consider the investigation of tool wear mechanism in UPM to be a crucial evaluation factor for a successful sustainable machining operation.

The magnetic field application reduced the trapped heat and friction, thereby protecting the cutting tool. SEM images of the cutting tool displayed that the cutting tool experienced adhesive wear caused by the cutting chips adhering to the cutting edge and the elevated cutting temperature with inadequate heat dissipation in the absence of the magnetic field. In comparison, severe adhesive wear was prevented when the magnetic field was applied

due to its ability to reduce the elevated heat. And the flank face exhibited abrasion wear. Flank wear accelerates when excess heat becomes trapped in the cutting zone. And under the influence of a magnetic field, the formed chips are smooth and continuous compared to the serrated chips, indicating a relatively lower machining performance and low-quality surface due to uncontrolled heat in the machining zone. In this study, the magnetic field effect is utilized in single-point diamond turning to modify the physical characteristics of titanium alloys, which are difficult to process. In cutting experiments, the applied magnetic field system was adjusted, and the machining performances were evaluated based on the indicators of surface integrity, cutting tool conditions, and chip formation. During the analysis phase, AFM, XRD, and an optical profiler were utilized to examine the machined samples' surface morphology and composition.

3) The effect of the material characteristics on Ti-6Al-4V machining performance was investigated using the finite element modeling method FEM. Researchers can explore the cutting behavior of various materials supported by the development of numerous models. Simulating the machining process can be a low-cost tool for analyzing cutting performance, such as studying the chipping mechanism or cutting temperature during the operation. The resulting data will be different if a specific model is employed. Many factors are intimately related to the simulation outcomes in any cutting simulation model. Modeling is a cost-effective approach that investigates the cutting mechanisms of various work materials. To further demonstrate the effects of the applied magnetic field on the cutting processes, the finite element method FEM was employed. The evolution of machining modeling enhanced operation performance, manufacturing capability, and productivity. Modeling also avoids the manufacturing cost and effort due to the expensive experiments and the involved difficulties. Applying numerical modelling in metal cutting processes can get difficult-to-obtain data such as stress distribution and cutting temperature from experiments. The

development of new models has enabled researchers to investigate the cutting behavior of various materials. Furthermore, the modelling approach of the machining processes can be utilized to examine the chip formation or the cutting temperature. In this study, orthogonal cutting was assumed and performed in a two-dimensional plane strain. The analysis step was set as Dynamic, Temp-disp, Explicit. And the Johnson-cook model has been proposed in this study. The chip formation step indicated by the workpiece's damage evolution was described using the Johnson-Cook fracture model. The energy-based fracture criterion is applied to the finite element model during the failure evolution step. A series of simulations were run with varying the failure energy to select the most proper value to investigate the effect of fracture energy on the cutting simulation of Ti-6Al-4V. It was clear that fracture energy influences the chip formation morphology. The thermal study was carried out based on changing the thermal conductivity coefficient values; as different values are used for thermal conduction property analysis; the effect of this change was monitored in the cutting process simulation of Ti-6Al-4V under different thermal conductivities. From the simulation results, It was discovered that there was a difference between the chip morphology in this study when the thermal conductivity changed. The temperature distribution over the titanium cutting simulation was shown as thermal conductivity increases, the adiabatic shear decreases and affects the chip formation slightly, and the heat generated from the cutting process decreases near the interface between the cutting tool and workpiece.

In this thesis, a magnetic field is used in UPM technology to offer a varied range of innovative applications. As a result, this method was linked to UPM technology to enhance cutting efficiency and product quality. When ferrometals are exposed to a magnetic field, their physical properties, such as thermal conductivity, can improve. During the turning operation, a magnetic field was applied to the Ti-6Al-4V alloy to enhance heat dissipation

released during cutting. As an outcome, high heat in the cutting zone is no longer a significant source of tool wear or a crucial point for surface quality. In this study, the assistance of the magnetic field was employed and introduced with UPM. The results of the experiments demonstrated that the magnetic field had improved the machining performance of Ti–6Al–4 V alloy. These findings showed that cutting tool life was prolonged and superior surface integrity was achieved.

5.2 Suggestions for the future work

This research intended to overcome the machining challenges always encountered in UPM of titanium alloys due to the machining variables and material properties. As a result, a hybrid machining approach was used. In this thesis, a magnetic field UPM system was first developed to address UPM's current machining challenges. The effects of the generated magnetic field distribution on the machining area were shown using the finite element method FEM to improve product precision, particularly for hard-to-cut materials like Ti-6Al-4V.

In light of the results of this study, it’s recommended that the following studies shall be carried out because of the usefulness of supporting the manufacturing processes with the physical approaches:

1) The presented machining technology does not limit the validity of machining materials to particular work materials. This research can be used on various materials to improve machinability by utilizing the magnetic field effect. Since the study has focused on improving the machinability of Ti-6Al-4V to benefit from their unique properties and the widespread application of titanium alloys, magnetic field-assisted machining is recommended as well for other special materials.

2) The necessity to adopt cleaner production technologies in ultra-precision machining research motivates to expand this research tool capacity and develop new manufacturing

methods to protect the environment. Intensifying the activity of research work for clean production technologies in the dissemination of the concept of cleaner production and developing techniques that guide the field of metal cutting on how to apply this concept, entitled "Application Guide for Cleaner production in the metal cutting operations." It should be noted that the application of cleaner production technologies in the industrial enterprise is no longer optional. Still, it has become necessary to review the traditional production patterns used in the manufacturing processes, which seek to create products for profit, even at the expense of the environment and human beings, rather than adopting a cleaner production strategy with different technologies to reduce damage to environmental resources.

3) A little research has concerned manufacturing unique materials and conducting machining operations. Manufacturing technologies are increasing to create materials with unique properties suitable for various advanced applications such as medical and aerospace. Medical applications are represented in the manufacture of prosthetic implants for the human body parts such as the knee, backbones, and joints. These materials are also used in aviation and energy applications. Complex elements of different shapes of these remarkable materials can be generated by other methods, such as additive manufacturing, and then operated under the effect of a magnetic field. Additive manufacturing can be seen as the latest gradual step in manufacturing technology development. Aerospace and aircraft industry researchers use additive manufacturing technology to make high-level product improvements. The technology is already using rapid construction of prototypes to help test and improve their designs and demonstrate their work's quality. Additive manufacturing is regarded as a fast-manufacturing technology that could be used to manufacture complicated parts with challenging capabilities using conventional design and manufacturing methods. It can also be used to optimize the designed features, create pieces in a single step that

would have needed numerous manufacturing processes, and combine multiple functions into a single component. One of the key benefits of this technology is considering the economic dimension. The proposed technique can save the raw material rather than the traditional manufacturing methods. And UPM, assisted by the magnetic field, can do the finishing machining operation. Another advantage is having new mechanical or physical properties of different materials combined in a single unique material capable of serving a wide range of fields.

Appendix A. Generation of the magnetic field

In the Magnesia region of central Asia, more than two thousand years ago, black natural rocks were discovered, these stones can attract some metals, such as small and nearby iron pieces, and they were called magnetic stones after the name of their discovery area (Beach et al., n.d.). These stones are known to have another characteristic when the stone is suspended from the center; it inclines when left free to move, and its ends indicate the directions of both the geographical north and south. If the direction of this suspended stone changes, it automatically turns back to its initial position (Katz, 2015). This way was used to determine the north and south magnetic directions and to manufacture the magnetic compass that has evolved into its current compass (Beach et al., n.d.). The characteristics of these stones can be transferred to other metal pieces of iron by rubbing both for some time in one direction; thus, some of the magnetic forces of the magnetic stone are transferred to the iron rod, turning it into a magnetic object.

In 1820, Dane Hans Christian Oersted discovered that electrical currents generate magnetic fields (Oersted, n.d.). This was achieved when he was conducting his electrical experiments; a free-moving magnetic needle was next to the wire through which an electrical current passed. He noticed when the electrical circuit was closed and the current passed through the wire, the needle deviated in a direction. When he changed the position of the wire so that it became below the needle, he noticed the deviation of the needle becomes in reverse to the first direction (Wormell and Urbanitzky, n.d.). This has been explained by the fact that the passage of the current into the wire causes a magnetic field to develop in the surrounding area (Dibner, 1961b). Thus, magnetic effects can arise from electrical effects. This was followed by a series of discoveries related to magnetism and its relationship to currents and electric fields, made by many scientists such as the American Joseph Henry and the Danish Michael Faraday, whose works showed that electricity could be generated by moving magnets (Ionescu-Pallas, 1972).

Appendix A. Generation of the magnetic field

When a magnetic rod is hung freely from the center, one end heads towards the north and the other towards the south. So, the first end of the magnet observing the north is named after this, the north pole of the magnet, and the second south-looking end by the magnet's south pole (Dunlop and Özdemir, 1997a). Scientific investigations have shown that the poles' magnet bars cannot be separated from each other. When a magnetic bar is broken and separated into parts, as in Figure 2.8, each part becomes a new integrated magnetic rod with a north and south pole (Oersted, n.d.). Continuing to break magnets into smaller parts will eventually conclude that the atom is a magnetic pole that is an infinitely small part of the original magnet (Heaviside, 1951).

The magnetic force between two magnetic poles is their mutual effect, whether by repulsion if the poles are similar or attraction if they are different (Garg, 2012). To show the level of that interaction effect experimentally, two magnetic bars that are equal in magnetic intensity and dimensions can be brought and then put the two magnets bars and get one close to the other, where two similar magnetic poles are close, they will have a certain distance (Silbert, 1974). Suppose the former magnets are replaced with another two magnets of higher magnetic intensity, considering that the two similar poles are close too. In that case, the distance will be increased, which means that the greater the magnetic strength, the longer the magnets in-between distance.

The strength of dissonance between similar poles is a tremendous force that can be used to lift heavy objects. Scientists have used this phenomenon in factories to make special magnetic corridors to transport and move heavy equipment easily instead of moving belts. Even scientists have utilized the magnetic field further, using this principle to make the fast trains swim in the air instead of touching the train rails and causing friction (Reis, 2013).

Appendix A. Generation of the magnetic field

It's known that electrical charges affect any close charge with electrical force, which means the electrical charge has an electric field (Kraus et al., 1984). By comparison, magnets also affect the magnetic materials nearby, and to illustrate this, let's bring a magnet that has been placed on an isolated surface such as wood and put a set of magnetic needles around it; it can be found that the magnet will affect and attract some of the close needles and leave others if they are far away, i.e., the strength of magnetic attraction is concentrated in its poles and decreases in other areas, as shown in Figure 2.9. From this, it turns out that there is an area surrounding the magnets from all sides and at all levels where the effect of magnetic force is shown, called the magnetic field, which is not visible, but its influence can be shown by iron pieces or a compass, as shown in Figure A. 1.

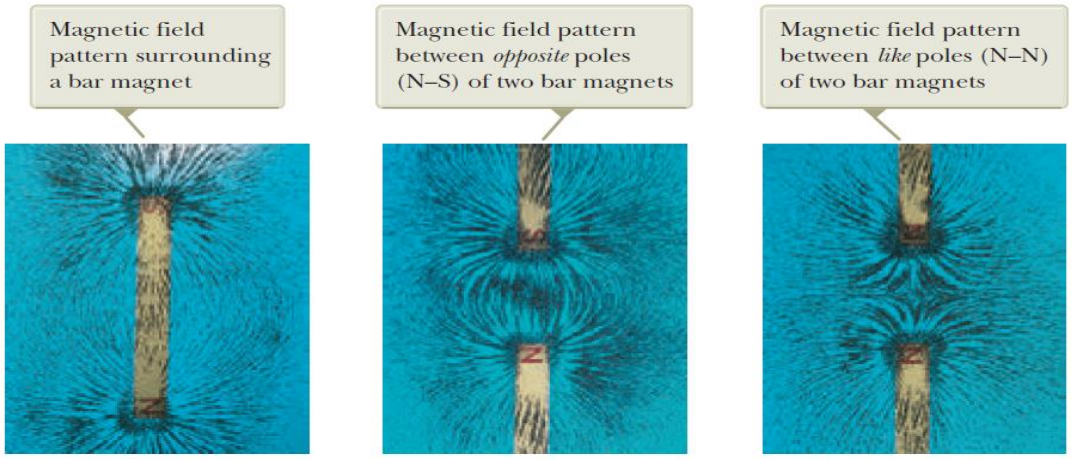

Figure A. 1 The arrangements of the iron chips forming the pattern of the magnetic field (Henry Leap and Jim Lehman).

The effect of a magnetic compass needle placed at some point within a magnetic field gives a way to draw the magnetic force lines next to a magnetic bar (Chow, 2005). The magnetic force lines are imaginary lines showing the path as a north pole in free movement in the magnetic field area of a magnetic bar. This indicates that magnetic force lines are closed because there can be no single magnetic pole, as we've shown before, unlike the electric field, where the electrical charge can exist alone (Aepinus and Wheaton, 1998). The magnetic force

line's direction at any point is the direction of the magnetic field from that point; if the force line is curved or straight, the tangent line at some point indicates the direction of the magnetic field, and its direction represents the direction of the magnetic field directly. Figure A. 2 shows the magnetic force lines of three magnets of different shapes.

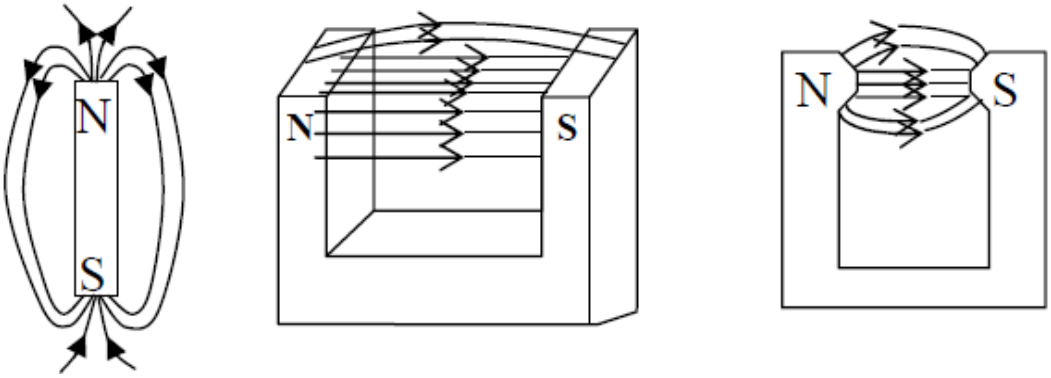

Figure A. 2 The magnetic field direction

It seems from these figures that magnetic force lines never intersect with each other, as do the electrical force lines because their intersection at any point in the magnetic field means that there is more than one direction of the magnetic field at that point, and this is practically unacceptable (Lyons, n.d.). Magnetic force lines are denser where the magnetic field is as intense as possible. The behavior of the magnetic force lines between two magnets can be different based on the polarity direction (Dunlop and Özdemir, 1997b) when the position of the opposing poles is different, as in Figure A. 3, there will be an attraction, and the magnetic force lines look as if they were a single magnetic pole. In a case where the two similar poles are close, a repulsion force will be generated, and the magnetic force lines show dissonance in the field next to the poles, as shown below.

Appendix A. Generation of the magnetic field

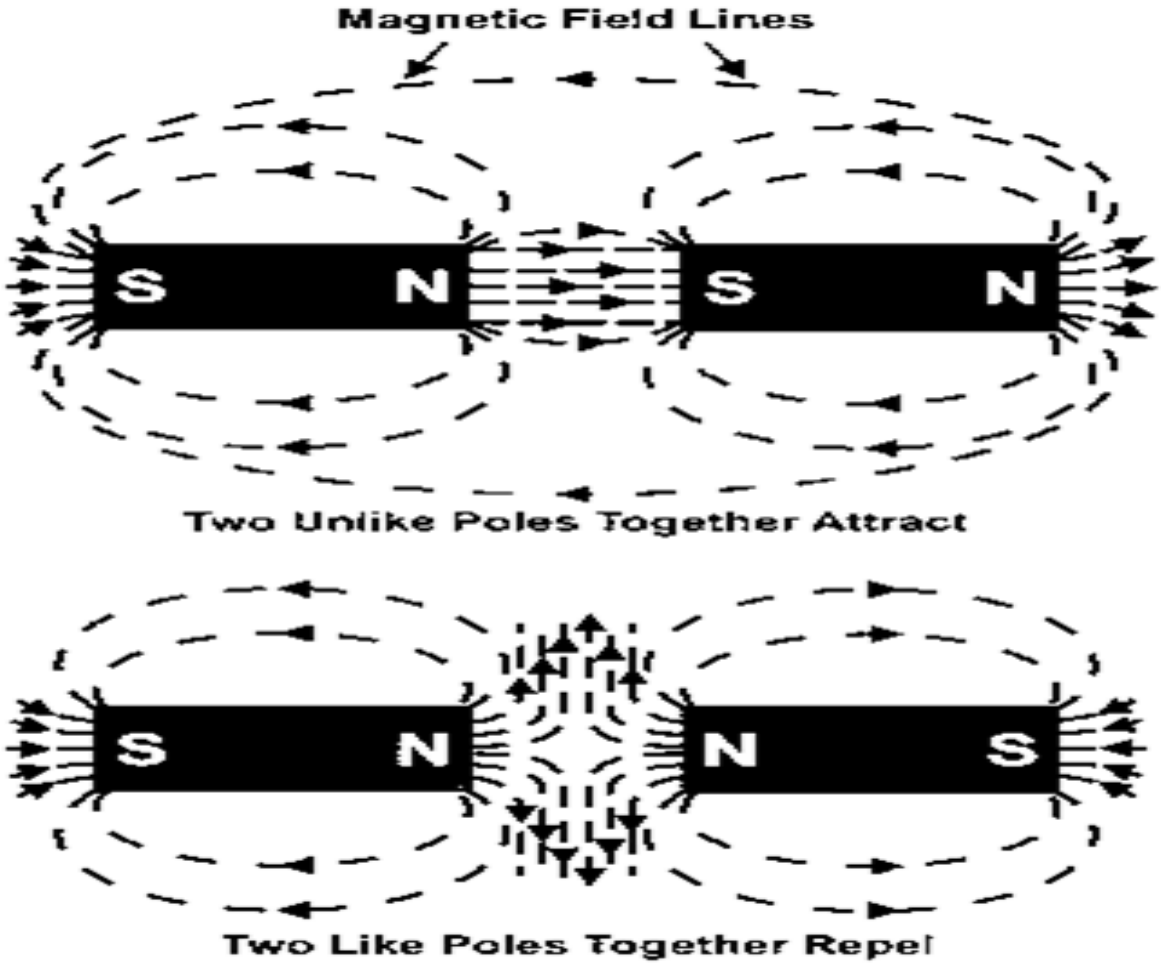

Figure A. 3 The behavior of the magnetic field lines based on the pole position.

The magnetic needle deviates when placed near a wire carrying an electrical current, and the current is the result of the movement of electrical charges. The deviation of the magnetic needle is due to its suffering from the strength of the magnetic field produced by these moving electrical charges. Thus, it has since been believed that all magnetic phenomena are generated by forces created by moving electrical charges. Any moving charge generates a magnetic field in the surrounding space and an electric field. The electric field generated by moving electrical charges or currents is often so small that the electric force that this electric field exerts on a moving charge can be neglected compared to the magnetic force affecting that charge (Owen, 1963; Benjamin, n.d.).

Appendix A. Generation of the magnetic field

Magnetic materials are influenced by the strength of the magnetic field when they are exposed to it. An indication of the magnetic force lines can define the intensity of the magnetic field at some point. The magnetic field intensity at a point can be defined as the number of magnetic force lines in the unit of area that traverse a vertical surface on a magnetic field close to that point (Planck, 1932). The total number of magnetic force lines that cross the surface is called the magnetic flux (ϕ). The magnetic flux penetrating the surface of area A can be expressed in equation (A-1).

$$\phi = BA\cos\theta \qquad \text{(A-1)}$$

When the area vector is perpendicular to the field vector B, i.e., when the angle θ is 90°, then the magnetic flux value is zero because there are no magnetic force lines that penetrate the surface area, and the magnetic flux becomes a maximum value when the angle θ is zero or 180°, and the flux is then positive or negative. The state in which the magnetic flux is positive indicates that magnetic force lines are in the direction of exiting the surface, but if the magnetic flux signal is negative, it indicates that the force lines are inside the surface, as shown in Figure 2.10. In both cases, the equation can be simplified as $\phi = \pm BA$.

In the international system (SI) of units, the magnetic flux is expressed by the Weber unit (Wb), which has been named after the German physicist, Weber, and it is clear from the equation that the weber is equivalent to Tesla. In square meters, thus, the intensity value of the magnetic field is measured by the unit of tesla and has another equivalent unit, the Webber per square meter (Wb/m^2) (Knoepfel, 2000). In the electromagnetic system, the magnetic flux is expressed as the Maxwell unit. The magnetic intensity of the magnetic field has another expression, the gauss, which is Maxwell per square centimeter (M/cm^2), sometimes the intensity of the magnetic field is called the intensity of magnetic flux or the intensity of the

magnetic flow as long as the intensity of the magnetic field at some point is equal to the magnetic flux in the unit of area (Heaviside, 1951).

Figure A. 4 represents the movement of a charged particle in a magnetic field B, and the particle has been projected with a velocity V in a perpendicular direction to field B. From the figure, it's found that the particle is affected by a force of qvB, which is always perpendicular to both B and V; this force only changes the direction of the speed of the affected particle without changing its value. Thus, the particle movement path is circular as long as the velocity of the particle aligned to the path is perpendicular to the magnetic field lines.

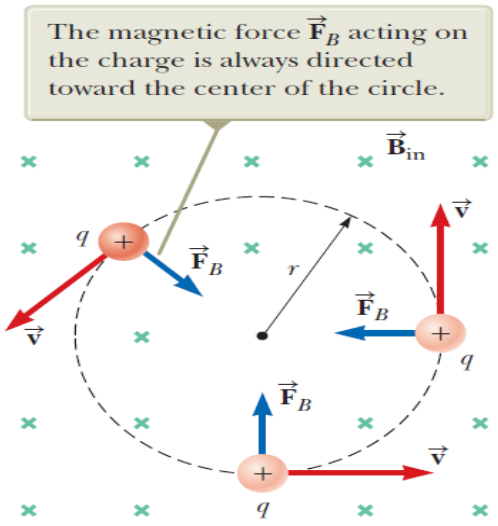

Figure A. 4 Charged particle in a circular motion at a region of a magnetic field (Chart, 1997).

It's noted that the negative particle rotates against the direction of the positive particle rotation, i.e., clockwise because the magnetic force affecting the negative particle is in the opposite direction of the force affecting the particle of the positive charge, as indicated by the method of selecting the direction of the force affecting the particle using the left-hand rule. Therefore, the sign of the particle charge can be determined whether negative or positive, as it

can be proved from the direction of curvature of the particle path, which is charged in the magnetic field (Abraham et al., 1932). The radius of the particle rotation r can be calculated as follow:

Let's consider the particle q that its mass, and velocity are m and v, respectively, and the magnetic force qvB is equal to the centripetal force $\frac{mv^2}{r}$ That is,

$$\frac{mv^2}{r} = qvB$$

Then,

$$r = \frac{mv}{qB} \qquad \text{(A-2)}$$

From equation (A-2), it's concluded that r depends on the velocity of the projectile particle in a magnetic field, assuming that the value of the magnetic field, the mass, and the charge of the particle are constant, and to calculate the angular velocity, the equation can be written as: $\omega = \frac{v}{r} = \frac{qB}{m}$

In 1819, the Danish physicist Oersted indicated that the magnetic field of a wire carrying an electric current affects a magnetic needle placed nearby. Faraday showed the opposite effect of this phenomenon. He reported that the magnetic field could affect the conductive wire with equal magnetic forces (Stauffer, 1957; Raychaudhuri, 2022). To show this, refer to the magnetic force affecting a charged particle moving freely in a magnetic field. Faraday carried out an experiment that has been able to achieve this concept, using an L-long straight wire and a cross-section area A within an electric circuit of battery and switch; he placed the wire vertically at a regular external magnetic field between two sides of a permanent magnet (Papachristou, 2017). The magnetic field does not affect the wire when the loop is open. But when the loop is closed, a current of negative charges in the wire runs, and the field

affects it with a magnetic force that pushes it down, and if the voltage is reversed, the current is reversed in the wire and pushed upwards by the force of the magnetic field. It can be concluded from the experiment that magnetic force does not affect the wire itself, but the moving charges within it and thus affects the wire (Beach et al., n.d.).

The definition of the magnetic field was presented, and its features and impact on a moving electrical charge in its field were discussed. The magnetic field direction can be identified by noticing the behavior of the magnetic compass. It's also reported that if a wire carrying an electric current is placed in a magnetic field, it will be exposed to magnetic force. Some phenomena that indicate the current is a source of the magnetic field that shows its effect on a magnetic compass close to it have been identified.

After Oersted discovered the magnetic effect of a wire-carrying current in 1819, Biot-Savart conducted several experiments with which the outcome was to build a mathematical relationship to calculate the intensity of the magnetic field at any point in the space around a conductive wire carrying an electric current (Mikerov, 2014; Dibner, 1961b). To show this, consider a wire of length S has an electric current and that the magnetic field of a small length element ds at a point in the space is always vertical at the plan that includes ds and displacement vector r as shown in Figure 2.11, Biot-Savart have found that the amount of dB is inversely proportional to the square of distance r and direct proportional with the amount of current passing in the wire. And they expressed these results in their law, known as Biot-Savart's law, as shown in Eq. (2-4), where the u_0 is the magnetic permeability (Wb/amp.m).

When considering making a circular ring that carries a current I where the circles representing magnetic flux lines appear to compete near the wire and diverge from it, as shown in Figure A. 5. It is noted that the intensity of the magnetic field of the current increases by approaching the wire and decreasing by moving away from it (Dunlop and Özdemir, 1997b;

Katz, 2015). If the radius of the ring is a, the intensity and value of the magnetic field at the center of the ring can be calculated from equation (A-3). The field intensity of N of identical rings can be expressed as in equation (A-4).

$$B = \frac{u_0 I}{2a} \tag{A-3}$$

$$B = \frac{N u_0 I}{2a} \tag{A-4}$$

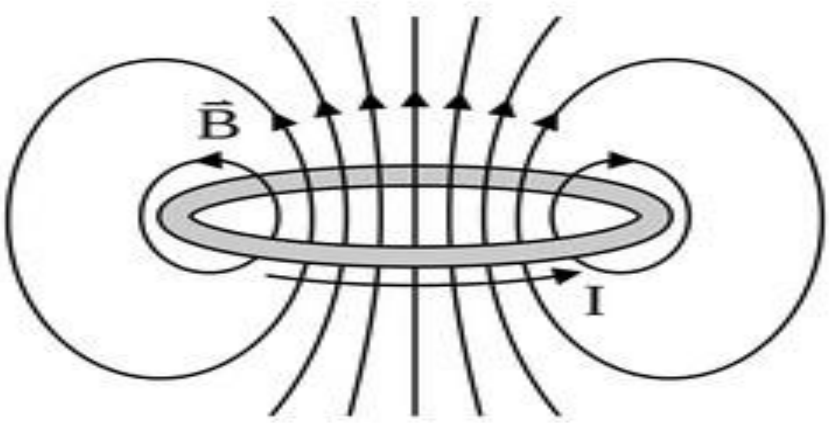

Figure A. 5 Magnetic field lines due to current through the circular loop.

Amber's law is another expression of the connection between the magnetic field and the current that arises from its integrative form (Assis and Chaib, 2015). It states that the linear integration of magnetic induction intensity is calculated at each closed curve, whatever its shape, and in any medium equal to the total current passing through the curved area, multiplied by the constant permeability of that medium. And it can be expressed in the following mathematical formula.

$$\int BdLcos\theta = u_0 I \tag{A-5}$$

$$\int BdL = u_0 I \tag{A-6}$$

Since B is constant, and the angle theta is zero for all points on the path, substituting the limits gives Amber's law as in equation (A-7).

$$B = \frac{u_0 I}{2\pi r} \tag{A-7}$$

Experiments have shown that Amber's law applies to all magnetic fields arising from different formations of fixed-value currents and any closed path surrounding those currents. One of the features of this law is that the calculation of linear integration is possible only in the area where the magnetic field has a symmetrical distribution, which is similar to Gauss's law, where its use was limited to electrical fields with symmetrical distribution (Dibner, 1961b). When considering a long straight wire carrying an electric current in the direction as shown in Figure A. 6, using the right-hand rule, it's found that the magnetic field lines are in concentric circles with the axis of the wire and are located at plans perpendicular to the wire.

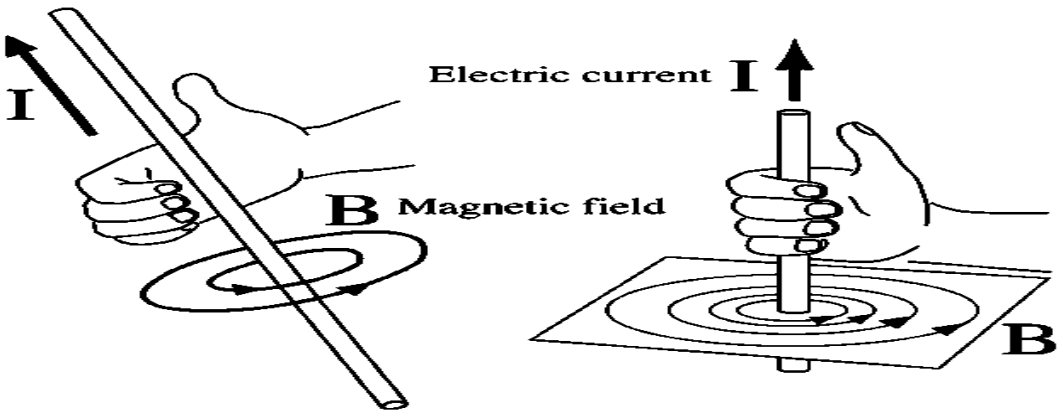

Figure A. 6 The magnetic field lines around a long wire carrying an electric current.

References

Abraham, M., Becker, R.L., b. Dougall, J., 1932. The classical theory of electricity and magnetism.

Abukhshim, N.A., Mativenga, P.T., Sheikh, M.A., 2006. Heat generation and temperature prediction in metal cutting: A review and implications for high speed machining. Int J Mach Tools Manuf 46, 782–800.

Aepinus, F.U.T., Wheaton, B.R., 1998. Essay on the Theory of Electricity and Magnetism. Am J Phys 48, 502.

Arrazola, P.J., Garay, A., Iriarte, L.M., Armendia, M., Marya, S., le Maître, F., 2009. Machinability of titanium alloys (Ti6Al4V and Ti555.3). J Mater Process Technol 209, 2223–2230. https://doi.org/10.1016/j.jmatprotec.2008.06.020

Assis, A.K.T., Chaib, J.P.M.C., 2015. Ampère's electrodynamics : analysis of the meaning and evolution of Ampère's force between current elements, together with a complete translation of his masterpiece: Theory of electrodynamic phenomena, uniquely deduced from experience.

Astakhov, V.P., 2004. The assessment of cutting tool wear. Int J Mach Tools Manuf 44, 637–647. https://doi.org/10.1016/j.ijmachtools.2003.11.006

Aydın, M., 2021. Numerical study of chip formation and cutting force in high-speed machining of Ti-6Al-4V bases on finite element modeling with ductile fracture criterion. International Journal of Material Forming 14, 1005–1018. https://doi.org/10.1007/s12289-021-01617-9

References

Ayyappan, S., Sivakumar, K., Kalaimathi, M., 2017. Electrochemical machining of 20MnCr5 alloy steel with magnetic flux assisted vibrating tool. Proc Inst Mech Eng C J Mech Eng Sci 231, 1956–1965. https://doi.org/10.1177/0954406215623310

Beach, R., Streubel, E.J., Ward, A.H.K., n.d. The story of electricity and magnetism : harnessing invisible energy for the service of mankind.

Benjamin, P., n.d. A History Of Electricity, The Intellectual Rise In Electricity, From Antiquity To The Days Of Benjamin Franklin.

Bermingham, M.J., Kirsch, J., Sun, S., Palanisamy, S., Dargusch, M.S., 2011. New observations on tool life, cutting forces and chip morphology in cryogenic machining Ti-6Al-4V. Int J Mach Tools Manuf 51, 500–511. https://doi.org/10.1016/j.ijmachtools.2011.02.009

Bermudo Gamboa, C., Andersson, T., Svensson, D., Trujillo Vilches, F.J., Martín-Béjar, S., Sevilla Hurtado, L., 2021. Modeling of the fracture energy on the finite element simulation in Ti6Al4V alloy machining. Sci Rep 11, 1–14. https://doi.org/10.1038/s41598-021-98041-5

Black, P.H., 1961. Theory of metal cutting.

Bordin, A., Bruschi, S., Ghiotti, A., Bariani, P.F., 2015. Analysis of tool wear in cryogenic machining of additive manufactured Ti6Al4V alloy. Wear 328–329, 89–99. https://doi.org/10.1016/j.wear.2015.01.030

Bowman, K.J., 2003. Mechanical Behavior of Materials.

Brinksmeier, E., Mutlugünes, Y., Klocke, F., Aurich, J.C., Shore, P., Ohmori, H., 2010. Ultra-precision grinding. CIRP Ann Manuf Technol 59, 652–671. https://doi.org/10.1016/j.cirp.2010.05.001

References

Budynas, R.G., Nisbett, J.K., 1983. Shigley's Mechanical Engineering Design.

Chart, P.C., 1997. C for scientists and engineers, Choice Reviews Online. https://doi.org/10.5860/choice.34-3910

Che-Haron, C.H., Jawaid, A., 2005. The effect of machining on surface integrity of titanium alloy Ti-6% Al-4% v. J Mater Process Technol 166, 188–192. https://doi.org/10.1016/j.jmatprotec.2004.08.012

Chen, X., Rowe, W.B., Cai, R., 2002. Precision grinding using CBN wheels. Int J Mach Tools Manuf 42, 585–593. https://doi.org/10.1016/S0890-6955(01)00152-3

Cheng, M.N., Cheung, C.F., Lee, W.B., To, S., Kong, L.B., 2008. Theoretical and experimental analysis of nano-surface generation in ultra-precision raster milling. Int J Mach Tools Manuf 48, 1090–1102. https://doi.org/10.1016/j.ijmachtools.2008.02.006

Chetan, Ghosh, S., Venkateswara Rao, P., 2015. Application of sustainable techniques in metal cutting for enhanced machinability: a review. J Clean Prod 100, 17–34. https://doi.org/https://doi.org/10.1016/j.jclepro.2015.03.039

Cheung, C.F., Ho, L.T., Charlton, P., Kong, L.B., To, S., Lee, W.B., 2010. Analysis of surface generation in the ultraprecision polishing of freeform surfaces. Proc Inst Mech Eng B J Eng Manuf 224, 59–73. https://doi.org/10.1243/09544054JEM1563

Cheung, C.F., Lee, W.B., 2000. Theoretical and experimental investigation of surface roughness formation in ultra-precision diamond turning. Int J Mach Tools Manuf 40, 979–1002. https://doi.org/10.1016/S0890-6955(99)00103-0

Cheung, W.M., Marsh, R., Griffin, P.W., Newnes, L.B., Mileham, A.R., Lanham, J.D., 2015. Towards cleaner production: a roadmap for predicting product end-of-life costs at early

design concept. J Clean Prod 87, 431–441. https://doi.org/https://doi.org/10.1016/j.jclepro.2014.10.033

Chow, T.L., 2005. Introduction To Electromagnetic Theory: A Modern Perspective.

CIRP, H.D.B.-A. of the, 1978, undefined, n.d. Effect of a magnetic field on the gap cleaning in EDM. ci.nii.ac.jp.

Clark, G.M., 1995. Introduction to Manufacturing Applications, in: WSC.

Çolak, O., 2014. Optimization of machining performance in high-pressure assisted turning of Ti6Al4V alloy. Strojniski Vestnik/Journal of Mechanical Engineering 60, 675–681. https://doi.org/10.5545/sv-jme.2013.1079

Creese, R.C., 1999. Introduction to manufacturing processes and materials.

da Silva, R.B., da Silva, M.B., Sales, W.F., Ezugwu, E.O., Machado, Á.R., 2016. Advances in the Turning of Titanium Alloys with Carbide and Superabrasive Cutting Tools. Adv Mat Res 1135, 234–254. https://doi.org/10.4028/www.scientific.net/amr.1135.234

da Silva, R.B., MacHado, Á.R., Ezugwu, E.O., Bonney, J., Sales, W.F., 2013. Tool life and wear mechanisms in high speed machining of Ti-6Al-4V alloy with PCD tools under various coolant pressures. J Mater Process Technol 213, 1459–1464. https://doi.org/10.1016/j.jmatprotec.2013.03.008

Dandekar, C.R., Shin, Y.C., Barnes, J., 2010. Machinability improvement of titanium alloy (Ti-6Al-4V) via LAM and hybrid machining. Int J Mach Tools Manuf 50, 174–182. https://doi.org/10.1016/j.ijmachtools.2009.10.013

Dearnley, P.A., Grearson, A.N., 1986. Evaluation of principal wear mechanisms of cemented carbides and ceramics used for machining titanium alloy IMI 318. Materials Science and Technology (United Kingdom) 2, 47–58. https://doi.org/10.1179/mst.1986.2.1.47

References

Denkena, B., Bergmann, B., Klemme, H., 2020. Cooling of motor spindles—a review. International Journal of Advanced Manufacturing Technology 110, 3273–3294. https://doi.org/10.1007/s00170-020-06069-0

Devillez, A., le Coz, G., Dominiak, S., Dudzinski, D., 2011. Dry machining of Inconel 718, workpiece surface integrity. J Mater Process Technol 211, 1590–1598. https://doi.org/10.1016/j.jmatprotec.2011.04.011

Dhar, N.R., Islam, S., Kamruzzaman, M., Paul, S., 2006a. Wear behavior of uncoated carbide inserts under dry, wet and cryogenic cooling conditions in turning C-60 steel. Journal of the Brazilian Society of Mechanical Sciences and Engineering 28, 146–152. https://doi.org/10.1590/S1678-58782006000200003

Dhar, N.R., Islam, S., Kamruzzaman, M., Paul, S., 2006b. Wear behavior of uncoated carbide inserts under dry, wet and cryogenic cooling conditions in turning C-60 steel. Journal of the Brazilian Society of Mechanical Sciences and Engineering 28, 146–152. https://doi.org/10.1590/S1678-58782006000200003

Dibner, B., 1961a. Oersted and the discovery of electromagnetism. Electrical Engineering 80, 321–325.

Dibner, B., 1961b. Part III: Oersted and the discovery of electromagnetism: Part III. Electrical Engineering 80, 582–586.

Doman, D.A., Warkentin, A., Bauer, R., 2009. Finite element modeling approaches in grinding. Int J Mach Tools Manuf 49, 109–116. https://doi.org/10.1016/j.ijmachtools.2008.10.002

Dormann, J.L., Fiorani, D., 1992. Magnetic properties of fine particles : proceedings of the International Workshop on Studies of Magnetic Properties of Fine Particles and their Relevance to Materials Science, Rome, Italy, November 4-8, 1991 430.

References

Dornfeld, D., 2011. Leveraging Manufacturing for a Sustainable Future, in: Hesselbach, J., Herrmann, C. (Eds.), Glocalized Solutions for Sustainability in Manufacturing. Springer Berlin Heidelberg, Berlin, Heidelberg, pp. 17–21.

Dowling, N.E., 1993. Mechanical Behavior of Materials: Engineering Methods for Deformation, Fracture, and Fatigue.

Dunlop, D.J., Özdemir, Ö., 1997a. Rock Magnetism: Fundamentals and Frontiers.

Dunlop, D.J., Özdemir, Ö., 1997b. Rock Magnetism: Fundamentals of magnetism.

el Mansori, M., Pierron, F., Paulmier, D., 2003. Reduction of tool wear in metal cutting using external electromotive sources. Surf Coat Technol 163–164, 472–477. https://doi.org/10.1016/S0257-8972(02)00644-8

Eren Sarici, D., Ozdemir, E., 2018. Utilization of granite waste as alternative abrasive material in marble grinding processes. J Clean Prod 201, 516–525. https://doi.org/10.1016/j.jclepro.2018.08.050

Ezugwu, E.O., 2005. Key improvements in the machining of difficult-to-cut aerospace superalloys. Int J Mach Tools Manuf 45, 1353–1367. https://doi.org/10.1016/j.ijmachtools.2005.02.003

Fan, Z., Tian, Y., Liu, Z., Shi, C., Zhao, Y., 2019. Investigation of a novel finishing tool in magnetic field assisted finishing for titanium alloy Ti-6Al-4V. J Manuf Process 43, 74–82. https://doi.org/10.1016/j.jmapro.2019.05.007

Fan ZJ, Zhang LX, T.L., 2008. No Title. Chin J Mech 21, 11–4.

Garg, A., 2012. Classical Electromagnetism in a Nutshell.

References

Gavili, A., Zabihi, F., Isfahani, T.D., Sabbaghzadeh, J., 2012. The thermal conductivity of water base ferrofluids under magnetic field. Exp Therm Fluid Sci 41, 94–98. https://doi.org/10.1016/j.expthermflusci.2012.03.016

Goel, S., Luo, X., Reuben, R.L., 2012. Molecular dynamics simulation model for the quantitative assessment of tool wear during single point diamond turning of cubic silicon carbide. Comput Mater Sci 51, 402–408. https://doi.org/10.1016/j.commatsci.2011.07.052

González, J.E.G., Mirza-Rosca, J.C., 1999. Study of the corrosion behavior of titanium and some of its alloys for biomedical and dental implant applications. Journal of Electroanalytical Chemistry 471, 109–115.

Groover, M.P., 210AD. FUNDAMENTALS OF MODERN MANUFACTURING Materials,Processes,andSystems. Wiley 98–132.

Guo, J., Tan, Z.E., Au, K.H., Liu, K., 2017. Experimental investigation into the effect of abrasive and force conditions in magnetic field-assisted finishing. International Journal of Advanced Manufacturing Technology 90, 1881–1888. https://doi.org/10.1007/s00170-016-9491-6

Guo, Z., Jin, T., Xie, G., Lu, A., Qu, M., 2019. Approaches enhancing the process accuracy of fluid jet polishing for making ultra-precision optical components. Precis Eng 56, 20–37. https://doi.org/10.1016/j.precisioneng.2018.08.021

Gupta, H.N., (Firm), P., 2009. Manufacturing Process. New Age International Limited.

Hadad, M., Sadeghi, B., 2013. Minimum quantity lubrication-MQL turning of AISI 4140 steel alloy. J Clean Prod 54, 332–343. https://doi.org/10.1016/j.jclepro.2013.05.011

References

Hadad, M., Sadeghi, B., 2012. Thermal analysis of minimum quantity lubrication-MQL grinding process. Int J Mach Tools Manuf 63, 1–15. https://doi.org/10.1016/j.ijmachtools.2012.07.003

Hamdan, A., Sarhan, A.A.D., Hamdi, M., 2012. An optimization method of the machining parameters in high-speed machining of stainless steel using coated carbide tool for best surface finish. The International Journal of Advanced Manufacturing Technology 58, 81–91.

Harzallah, M., Pottier, T., Senatore, J., Mousseigne, M., Germain, G., Landon, Y., 2017. Numerical and experimental investigations of Ti-6Al-4V chip generation and thermo-mechanical couplings in orthogonal cutting. Int J Mech Sci 134, 189–202. https://doi.org/10.1016/j.ijmecsci.2017.10.017

Heaviside, O., 1951. Electromagnetic theory : the complete and unabridged edition of vol.1,2 \& 3.

Hong, S.Y., Ding, Y., 2001. Cooling approaches and cutting temperatures in cryogenic machining of Ti-6Al-4V. Int J Mach Tools Manuf 41, 1417–1437. https://doi.org/10.1016/S0890-6955(01)00026-8

Hou, G., Li, A., Song, X., Sun, H., Zhao, J., 2018. Effect of cutting parameters on surface quality in multi-step turning of Ti-6Al-4V titanium alloy. International Journal of Advanced Manufacturing Technology 98, 1355–1365. https://doi.org/10.1007/s00170-018-2317-y

Huang, Y., Fan, B., Wan, Y., Li, S., 2018. Improving the performance of single point diamond turning surface with ion beam figuring. Optik (Stuttg) 172, 540–544. https://doi.org/10.1016/j.ijleo.2018.07.039

References

Ichida, Y., 2008. Mechanical properties and grinding performance of ultrafine-crystalline cBN abrasive grains. Diam Relat Mater 17, 1791–1795. https://doi.org/10.1016/j.diamond.2008.01.076

Ionescu-Pallas, N., 1972. symmetrical theory of electricity and magnetism.

Jayswal, S.C., Jain, V.K., Dixit, P.M., 2005. Modeling and simulation of magnetic abrasive finishing process. International Journal of Advanced Manufacturing Technology 26, 477–490. https://doi.org/10.1007/s00170-004-2180-x

Jiang, Z., Feng, J., Deng, X., 2012. FEA simulation of the influence of cutting parameters on serrated chip formation in machining titanium alloy Ti-6Al-4V. Adv Mat Res 500, 152–156. https://doi.org/10.4028/www.scientific.net/AMR.500.152

Johnson, G.R., Cook, W.H., 1983. A Computational Constitutive Model and Data for Metals Subjected to Large Strain, High Strain Rates and High Pressures. the Seventh International Symposium on Ballistics 541–547.

Jozić, S., Vrsalović, L., Bajić, D., Gudić, S., 2022. Investigation of different cutting conditions in the machining of steel — Towards cleaner production. J Clean Prod 356, 131881. https://doi.org/10.1016/j.jclepro.2022.131881

Kalpakjian, S.R.S., 1984. Manufacturing Processes for Engineering Materials.

Kara, F., Aslantaş, K., Çiçek, A., 2016. Prediction of cutting temperature in orthogonal machining of AISI 316L using artificial neural network. Appl Soft Comput 38, 64–74. https://doi.org/https://doi.org/10.1016/j.asoc.2015.09.034

Katz, D.M., 2015. Physics for Scientists and Engineers: Foundations and Connections, Advance Edition, Volume 1.

References

Kaufman, J.G., Rooy, E.L., 2021. Stress-Strain Curves. Aluminum Alloy Castings 193–209. https://doi.org/10.31399/asm.tb.aacppa.t51140193

Kaur, M., Singh, K., 2019. Review on titanium and titanium based alloys as biomaterials for orthopaedic applications. Materials Science and Engineering C 102, 844–862. https://doi.org/10.1016/j.msec.2019.04.064

Khalil, A.K., Yip, W.S., To, S., 2022. Theoretical and experimental investigations of magnetic field assisted ultra-precision machining of titanium alloys. J Mater Process Technol 300, 117429. https://doi.org/10.1016/J.JMATPROTEC.2021.117429

Khalili, N.R., Duecker, S., Ashton, W., Chavez, F., 2015. From cleaner production to sustainable development: the role of academia. J Clean Prod 96, 30–43. https://doi.org/https://doi.org/10.1016/j.jclepro.2014.01.099

Kim, J. Du, Jin, D.X., Choi, M.S., 1997. Study on the effect of a magnetic field on an electrolytic finishing process. Int J Mach Tools Manuf 37, 401–408. https://doi.org/10.1016/S0890-6955(96)00071-5

Knoepfel, H.E., 2000. Magnetic fields : a comprehensive theoretical treatise for practical use. Am J Phys 69, 525.

Koizumi, H., Takeuchi, Y., Imai, H., Kawai, T., Yoneyama, T., 2019. Application of titanium and titanium alloys to fixed dental prostheses. J Prosthodont Res 63, 266–270. https://doi.org/10.1016/j.jpor.2019.04.011

Komanduri, R., Chandrasekaran, N., Raff, L.M., 2000. M.D. Simulation of nanometric cutting of single crystal aluminum–effect of crystal orientation and direction of cutting. Wear 242, 60–88. https://doi.org/https://doi.org/10.1016/S0043-1648(00)00389-6

References

Komanduri, R., von Turkovich, B.F., 1981. New observations on the mechanism of chip formation when machining titanium alloys. Wear 69, 179–188. https://doi.org/10.1016/0043-1648(81)90242-8

Kong, L.B., Cheung, C.F., To, S., Lee, W.B., 2009. An investigation into surface generation in ultra-precision raster milling. J Mater Process Technol 209, 4178–4185. https://doi.org/10.1016/j.jmatprotec.2008.11.002

Kraus, J.D., Fleisch, D.A., Russ, S.H., 1984. Electromagnetics with Applications.

Lajvardi, M., Moghimi-Rad, J., Hadi, I., Gavili, A., Dallali Isfahani, T., Zabihi, F., Sabbaghzadeh, J., 2010. Experimental investigation for enhanced ferrofluid heat transfer under magnetic field effect. J Magn Magn Mater 322, 3508–3513. https://doi.org/10.1016/j.jmmm.2010.06.054

Lawal, S.A., Choudhury, I.A., Nukman, Y., 2013. A critical assessment of lubrication techniques in machining processes: a case for minimum quantity lubrication using vegetable oil-based lubricant. J Clean Prod 41, 210–221. https://doi.org/https://doi.org/10.1016/j.jclepro.2012.10.016

Lee, W.B., Cheung, C.F., Chiu, W.M., Leung, T.P., 2000. Investigation of residual form error compensation in the ultra-precision machining of aspheric surfaces. J Mater Process Technol 99, 129–134. https://doi.org/10.1016/S0924-0136(99)00403-3

Liang, X., Liu, Z., 2017. Experimental investigations on effects of tool flank wear on surface integrity during orthogonal dry cutting of Ti-6Al-4V. International Journal of Advanced Manufacturing Technology 93, 1617–1626. https://doi.org/10.1007/s00170-017-0654-x

References

Lin, Y.C., Chen, Y.F., Wang, D.A., Lee, H.S., 2009. Optimization of machining parameters in magnetic force assisted EDM based on Taguchi method. J Mater Process Technol 209, 3374–3383. https://doi.org/10.1016/j.jmatprotec.2008.07.052

Lin, Y.C., Lee, H.S., 2008. Machining characteristics of magnetic force-assisted EDM. Int J Mach Tools Manuf 48, 1179–1186. https://doi.org/10.1016/j.ijmachtools.2008.04.004

Lou, Y., Wu, H., 2017. Improving machinability of titanium alloy by electro-pulsing treatment in ultra-precision machining. International Journal of Advanced Manufacturing Technology 93, 2299–2304. https://doi.org/10.1007/s00170-017-0674-6

Lu, J., Chen, J., Fang, Q., Liu, B., Liu, Y., Jin, T., 2016. Finite element simulation for Ti-6Al-4V alloy deformation near the exit of orthogonal cutting. International Journal of Advanced Manufacturing Technology 85, 2377–2388. https://doi.org/10.1007/s00170-015-8077-z

Lyons, T.A., n.d. A Treatise on Electromagnetic Phenomena and on the Compass and its Deviations aboard Ship Mathematical, Theoretical and Practical. Nature 64, 125.

Maurotto, A., Muhammad, R., Roy, A., Silberschmidt, V. v., 2013. Enhanced ultrasonically assisted turning of a β-titanium alloy. Ultrasonics 53, 1242–1250. https://doi.org/10.1016/j.ultras.2013.03.006

Meyers, M.A., Chawla, K.K., 1998. Mechanical Behavior of Materials.

Mia, M., Gupta, M.K., Singh, G., Królczyk, G., Pimenov, D.Y., 2018. An approach to cleaner production for machining hardened steel using different cooling-lubrication conditions. J Clean Prod 187, 1069–1081. https://doi.org/https://doi.org/10.1016/j.jclepro.2018.03.279

References

Mikerov, A.G., 2014. From history of Electrical Engineering III: Electromagnetism discovery and its fundamental laws in the first half of 19-th century. Proceedings of the 2014 IEEE NW Russia Young Researchers in Electrical and Electronic Engineering Conference 1–7.

Mikulčić, H., Baleta, J., Klemeš, J.J., 2022. Cleaner technologies for sustainable development. Clean Eng Technol 7, 100445. https://doi.org/https://doi.org/10.1016/j.clet.2022.100445

Ming, W., Xie, Z., Ma, J., Du, J., Zhang, G., Cao, C., Zhang, Y., 2021. Critical review on sustainable techniques in electrical discharge machining. J Manuf Process 72, 375–399. https://doi.org/https://doi.org/10.1016/j.jmapro.2021.10.035

Ming, W., Zhang, Z., Wang, S., Zhang, Y., Shen, F., Zhang, G., 2019. Comparative study of energy efficiency and environmental impact in magnetic field assisted and conventional electrical discharge machining. J Clean Prod 214, 12–28. https://doi.org/10.1016/j.jclepro.2018.12.231

Mir, A., Luo, X., Sun, J., 2016. The investigation of influence of tool wear on ductile to brittle transition in single point diamond turning of silicon. Wear 364–365, 233–243. https://doi.org/10.1016/j.wear.2016.08.003

Molinari, A., Soldani, X., Miguélez, M.H., 2013. Adiabatic shear banding and scaling laws in chip formation with application to cutting of Ti-6Al-4V. J Mech Phys Solids 61, 2331–2359. https://doi.org/10.1016/j.jmps.2013.05.006

Mouritz, A.P. (Ed.), 2012. 1 - Introduction to aerospace materials, in: Introduction to Aerospace Materials. Woodhead Publishing, pp. 1–14. https://doi.org/https://doi.org/10.1533/9780857095152.1

References

Mu, X., Zhou, M., Zhang, J., Lu, N., Ye, Q., 2022. Intelligent electrical discharge machining (EDM) molybdenum-titanium-zirconium alloy by an extended adaptive control system. J Manuf Process 77, 207–218. https://doi.org/https://doi.org/10.1016/j.jmapro.2022.03.003

Munsamy, M., Telukdarie, A., Zhang, W., 2014. Cleaner technology systems for surface finishing: evaporative coolers for close circuiting low temperature plating process. J Clean Prod 66, 664–671. https://doi.org/https://doi.org/10.1016/j.jclepro.2013.11.038

Nandy, A.K., Gowrishankar, M.C., Paul, S., 2009. Some studies on high-pressure cooling in turning of Ti-6Al-4V. Int J Mach Tools Manuf 49, 182–198. https://doi.org/10.1016/j.ijmachtools.2008.08.008

Naumov, A., Vereschaka, Alexey, Batako, A., Vereschaka, Anatoly, 2016. System of High-performance Cutting with Enhanced Combined Effect of Cooling and Lubrication Medium Based on Ranque-hilsch Effect. Procedia CIRP 57, 457–460. https://doi.org/10.1016/j.procir.2016.11.079

Naveen Anthuvan, R., Krishnaraj, V., Parthiban, M., 2021. Magnetic field-assisted electrical discharge machining of micro-holes on Ti-6Al-4V. Mater Today Proc 39, 1688–1694. https://doi.org/https://doi.org/10.1016/j.matpr.2020.06.153

Niinomi, M., 2018. 4.1 - Titanium spinal-fixation implants, in: Froes, F.H., Qian, M. (Eds.), Titanium in Medical and Dental Applications, Woodhead Publishing Series in Biomaterials. Woodhead Publishing, pp. 347–369. https://doi.org/https://doi.org/10.1016/B978-0-12-812456-7.00016-0

Niinomi, M., 2003a. Recent research and development in titanium alloys for biomedical applications and healthcare goods. Sci Technol Adv Mater 4, 445–454. https://doi.org/https://doi.org/10.1016/j.stam.2003.09.002

References

Niinomi, M., 2003b. Recent research and development in titanium alloys for biomedical applications and healthcare goods. Sci Technol Adv Mater. https://doi.org/10.1016/j.stam.2003.09.002

Oersted, H.C., n.d. OERSTED, Hans Christian. Experiments on the Effect of a Current of Electricity on the Magnetic Needle. Annals of Philosophy 1820, vol. 16, p. 273-277.

Oersted, H.C., n.d. Experiments on the Effect of a Current of Electricity on the Magnetic Needle, 1820.

O'Handley, R.C., 1999. Modern Magnetic Materials. Physics Bulletin 13, 768.

Olortegui-Yume, J.A., Kwon, P.Y., 2007. Tool wear mechanisms in machining. International Journal of Machining and Machinability of Materials 2, 316–334. https://doi.org/10.1504/ijmmm.2007.015469

Owen, G.E., 1963. Introduction to electromagnetic theory.

Papachristou, C.J., 2017. Introduction to Electromagnetic Theory and the Physics of Conducting Solids. arXiv: Materials Science.

Park, C.H., Lee, E.S., Lee, H., 1999. Review on research in ultra precision engineering at KIMM. Int J Mach Tools Manuf 39, 1793–1805. https://doi.org/10.1016/S0890-6955(99)00032-2

Pearson Education, Inc., 2012. Prentice Hall Writing Coach. Pearson Prentice Hall.

Pervaiz, S., Kannan, S., Kishawy, H.A., 2018. An extensive review of the water consumption and cutting fluid based sustainability concerns in the metal cutting sector. J Clean Prod 197, 134–153. https://doi.org/10.1016/j.jclepro.2018.06.190

References

Peters, M., Kumpfert, J., Ward, C.H., Leyens, C., 2003. Titanium alloys for aerospace applications. Adv Eng Mater 5, 419–427. https://doi.org/10.1002/adem.200310095

Phys. Rev. E 73, 061919 (2006) - Analytical model of magnetic nanoparticle transport and capture in the microvasculature [WWW Document], n.d. URL https://journals.aps.org/pre/abstract/10.1103/PhysRevE.73.061919 (accessed 12.30.20).

Planck, M., 1932. Theory of electricity and magnetism.

Pramanik, A., Littlefair, G., 2015. Machining of titanium alloy (Ti-6Al-4V)-theory to application. Machining Science and Technology 19, 1–49. https://doi.org/10.1080/10910344.2014.991031

Qian, X., Duan, X., 2019. Constitutive model and cutting simulation of titanium alloy Ti6Al4V after heat treatment. Materials 12, 1–13. https://doi.org/10.3390/ma1224145

QIN, X., GUI, L., LI, H., RONG, B., WANG, D., ZHANG, H., ZUO, G., 2012. Feasibility Study on the Minimum Quantity Lubrication in High-Speed Helical Milling of Ti-6Al-4V. Journal of Advanced Mechanical Design, Systems, and Manufacturing 6, 1222–1233. https://doi.org/10.1299/jamdsm.6.1222

Quinn, J., McFadden, R., Chan, C.-W., Carson, L., 2020. Titanium for Orthopedic Applications: An Overview of Surface Modification to Improve Biocompatibility and Prevent Bacterial Biofilm Formation. iScience 23, 101745. https://doi.org/https://doi.org/10.1016/j.isci.2020.101745

Rahim, E.A., Sasahara, H., 2011. A study of the effect of palm oil as MQL lubricant on high speed drilling of titanium alloys. Tribol Int 44, 309–317. https://doi.org/10.1016/j.triboint.2010.10.032

References

Raychaudhuri, A., 2022. Classical Theory of Electricity and Magnetism. Texts and Readings in Physical Sciences.

Recht, R.F., 1964. Catastrophic Thermoplastic Shear. J Appl Mech 31, 189–193. https://doi.org/10.1115/1.3629585

Reddy, T.Y., 1986. Engineering design. A materials and processing approach: by G. Dieter, McGraw Hill International Book Co., Tokyo, 1983, ISBN 0-07-066265-7, xiv + 592 pages, Illustrated, flexi-cover, £9.50. Journal of Mechanical Working Technology 13, 108–109.

Reddy, T.Y., 1985. Mechanical engineering design: 4th edition, by joseph e. shigley and larry d. mitchell, mcgraw-hill book co., new york, 1983. isbn 0-07-956888-x, xix + 869 pages, hard cover, £30.25. Journal of Mechanical Working Technology 11, 378–379.

Reis, M.S., 2013. Fundamentals of Magnetism.

Ren, L., Zhang, G., Zhang, L., Zhang, Z., Huang, Y., 2019. Modelling and investigation of material removal profile for computer controlled ultra-precision polishing. Precis Eng 55, 144–153. https://doi.org/10.1016/j.precisioneng.2018.08.020

Richtmyer, R.D., 1964. Introduction to electromagnetic theory.

Rothbart, H.A., Wahl, A.M., 1964. Mechanical Design and Systems Handbook.

Ruibin, X., Wu, H., 2016. Study on cutting mechanism of Ti6Al4V in ultra-precision machining. International Journal of Advanced Manufacturing Technology 86, 1311–1317. https://doi.org/10.1007/s00170-015-8304-7

Sacchelli, S., Bernetti, I., de Meo, I., Fiori, L., Paletto, A., Zambelli, P., Ciolli, M., 2014. Matching socio-economic and environmental efficiency of wood-residues energy chain:

a partial equilibrium model for a case study in Alpine area. J Clean Prod 66, 431–442. https://doi.org/https://doi.org/10.1016/j.jclepro.2013.11.059

Saxena, K.K., Bellotti, M., Qian, J., Reynaerts, D., Lauwers, B., Luo, X., 2018. Overview of Hybrid Machining Processes, Hybrid Machining. Elsevier Ltd. https://doi.org/10.1016/b978-0-12-813059-9.00002-6

Setti, D., Sinha, M.K., Ghosh, S., Venkateswara Rao, P., 2015. Performance evaluation of Ti-6Al-4V grinding using chip formation and coefficient of friction under the influence of nanofluids. Int J Mach Tools Manuf 88, 237–248. https://doi.org/10.1016/j.ijmachtools.2014.10.005

Severo, E.A., de Guimarães, J.C.F., Dorion, E.C.H., Nodari, C.H., 2015. Cleaner production, environmental sustainability and organizational performance: an empirical study in the Brazilian Metal-Mechanic industry. J Clean Prod 96, 118–125. https://doi.org/https://doi.org/10.1016/j.jclepro.2014.06.027

Shigley, J.E., 1972. Mechanical engineering design.

Shokoohi, Y., Khosrojerdi, E., Rassolian Shiadhi, B. h., 2015. Machining and ecological effects of a new developed cutting fluid in combination with different cooling techniques on turning operation. J Clean Prod 94, 330–339. https://doi.org/https://doi.org/10.1016/j.jclepro.2015.01.055

Shokrani, A., Dhokia, V., Newman, S.T., 2012. Environmentally conscious machining of difficult-to-machine materials with regard to cutting fluids. Int J Mach Tools Manuf 57, 83–101. https://doi.org/10.1016/j.ijmachtools.2012.02.002

Silbert, M., 1974. An Introduction to Electromagnetic Theory.

References

Smith, A.J., Dieppe, P., Vernon, K., Porter, M., Blom, A.W., 2012. Failure rates of stemmed metal-on-metal hip replacements: analysis of data from the National Joint Registry of England and Wales. The Lancet 379, 1199–1204. https://doi.org/https://doi.org/10.1016/S0140-6736(12)60353-5

Soliman, H.A., Shash, A.Y., el Hossainy, T.M., Abd-Rabou, M., 2020. Investigation of process parameters in orthogonal cutting using finite element approaches. Heliyon 6, e05498. https://doi.org/10.1016/j.heliyon.2020.e05498

Stauffer, R.C., 1957. Speculation and Experiment in the Background of Oersted's Discovery of Electromagnetism. Isis 48, 33–50.

Stephenson, D.A., Agapiou, J.S., 2016. Metal Cutting Theory and Practice, Third Edition.

Stephenson, D.A., Agapiou, J.S., 1996. Metal Cutting Theory and Practice.

Suzuki, H., Moriwaki, T., Okino, T., Ando, Y., 2006. Development of ultrasonic vibration assisted polishing machine for micro aspheric die and mold. CIRP Ann Manuf Technol 55, 385–388. https://doi.org/10.1016/S0007-8506(07)60441-7

Suzuki, H., Okada, M., Lin, W., Morita, S., Yamagata, Y., Hanada, H., Araki, H., Kashima, S., 2014. Fine finishing of ground DOE lens of synthetic silica by magnetic field-assisted polishing. CIRP Ann Manuf Technol 63, 313–316. https://doi.org/10.1016/j.cirp.2014.03.027

Tan, R., Zhao, X., Guo, S., Zou, X., He, Y., Geng, Y., Hu, Z., Sun, T., 2020. Sustainable production of dry-ultra-precision machining of Ti–6Al–4V alloy using PCD tool under ultrasonic elliptical vibration-assisted cutting. J Clean Prod 248, 119254. https://doi.org/10.1016/j.jclepro.2019.119254

References

Taniguchi, N., 1983. Current Status in, and Future Trends of, Ultraprecision Machining and Ultrafine Materials Processing. CIRP Ann Manuf Technol 32, 573–582. https://doi.org/10.1016/S0007-8506(07)60185-1

Tawakoli, T., Hadad, M.J., Sadeghi, M.H., Daneshi, A., Stöckert, S., Rasifard, A., 2009. An experimental investigation of the effects of workpiece and grinding parameters on minimum quantity lubrication-MQL grinding. Int J Mach Tools Manuf 49, 924–932. https://doi.org/10.1016/j.ijmachtools.2009.06.015

Teimouri, R., Baseri, H., 2014. Optimization of magnetic field assisted EDM using the continuous ACO algorithm. Applied Soft Computing Journal 14, 381–389. https://doi.org/10.1016/j.asoc.2013.10.006

Tlusty, J., 2000. Manufacturing processes and equipment / Jiri Tlusty., Manufacturing processes and equipment. Prentice-Hall, Upper Saddle River, NJ.

To, S., Lee, W.B., Zhu, Y.H., 2002. Ultra-precision machining induced surface structural changes of Zn-Al alloy. Materials Science and Engineering A 325, 497–502. https://doi.org/10.1016/S0921-5093(01)01753-1

To, S., Zhu, Y.H., Lee, W.B., Liu, X.M., 2010. Dynamic Electropulsing Induced Phase Transformations in a Furnace Cooled Zn-Al Based Alloy (ZA22). Mater Trans 51, 1997–2004. https://doi.org/10.2320/matertrans.m2010130

V. P. astakhov, 2014. هامvip Machining of Hard Materials.pdf, Surface and Coatings Technology.

Veiga, C., Davim, J.P., 2013. Review on Machinability of Titanium Alloys : the Process Perspective 34, 148–164.

References

Veiga, C., Davim, J.P., Loureiro, A.J.R., 2013. Review on machinability of titanium alloys: The process perspective. Reviews on Advanced Materials Science 34, 148–164.

Wang, C., Cheung, C.F., Ho, L.T., Yung, K.L., Kong, L., 2020. A novel magnetic field-assisted mass polishing of freeform surfaces. J Mater Process Technol 279, 116552. https://doi.org/10.1016/j.jmatprotec.2019.116552

Wang, D., Shinmura, T., Yamaguchi, H., 2004. Study of magnetic field assisted mechanochemical polishing process for inner surface of Si3N4 ceramic components finishing characteristics under wet finishing using distilled water. Int J Mach Tools Manuf 44, 1547–1553. https://doi.org/10.1016/j.ijmachtools.2004.04.024

Wang, H., To, S., Chan, C.Y., 2013. Investigation on the influence of tool-tip vibration on surface roughness and its representative measurement in ultra-precision diamond turning. Int J Mach Tools Manuf 69, 20–29. https://doi.org/10.1016/j.ijmachtools.2013.02.006

Wang, Y., Wu, Y., Guo, H., Fujimoto, M., Nomura, M., Shimada, K., 2015. A new magnetic compound fluid slurry and its performance in magnetic field-assisted polishing of oxygen-free copper. J Appl Phys. https://doi.org/10.1063/1.4914058

Williams, D.F., 1981. Implants in dental and maxillofacial surgery. Biomaterials 2, 133–146. https://doi.org/https://doi.org/10.1016/0142-9612(81)90039-9

Wormell, R., Urbanitzky, A., n.d. Electricity in the service of man : a popular and practical treatise on the applications of electricity in modern life : from the German of Dr. Alfred Ritter von Arbanitzky.

Wu, H.Y., Lee, W.B., Cheung, C.F., To, S., Chen, Y.P., 2005. Computer simulation of single-point diamond turning using finite element method. J Mater Process Technol 167, 549–554. https://doi.org/10.1016/j.jmatprotec.2005.06.015

References

Wu, J., Zou, Y., Sugiyama, H., 2016. Study on finishing characteristics of magnetic abrasive finishing process using low-frequency alternating magnetic field. International Journal of Advanced Manufacturing Technology 85, 585–594. https://doi.org/10.1007/s00170-015-7962-9

Wu, J., Zou, Y., Sugiyama, H., 2015. Study on ultra-precision magnetic abrasive finishing process using low frequency alternating magnetic field. J Magn Magn Mater 386, 50–59. https://doi.org/10.1016/j.jmmm.2015.03.041

Xia, Z., Fang, F., Ahearne, E., Tao, M., 2020. Advances in polishing of optical freeform surfaces: A review. J Mater Process Technol 286, 116828. https://doi.org/10.1016/j.jmatprotec.2020.116828

Xu, X., Outeiro, J., Zhang, J., Xu, B., Zhao, W., Astakhov, V., 2021. Machining simulation of Ti6Al4V using coupled Eulerian-Lagrangian approach and a constitutive model considering the state of stress. Simul Model Pract Theory 110. https://doi.org/10.1016/j.simpat.2021.102312

Yaich, M., Ayed, Y., Bouaziz, Z., Germain, G., 2017. Numerical analysis of constitutive coefficients effects on FE simulation of the 2D orthogonal cutting process: application to the Ti6Al4V. International Journal of Advanced Manufacturing Technology 93, 283–303. https://doi.org/10.1007/s00170-016-8934-4

Yamaguchi, H., Shinmura, T., 2004. Internal finishing process for alumina ceramic components by a magnetic field assisted finishing process. Precis Eng 28, 135–142. https://doi.org/10.1016/j.precisioneng.2003.07.001

Yang, Z., Chu, Y., Xu, X., Huang, H., Zhu, D., Yan, S., Ding, H., 2021. Prediction and analysis of material removal characteristics for robotic belt grinding based on single spherical

abrasive grain model. Int J Mech Sci 190, 106005. https://doi.org/10.1016/j.ijmecsci.2020.106005

Yip, W.S., To, S., 2019. Reduction of Minimum Cutting Thickness of Titanium Alloys in Micro Cutting by a Magnetic Field Assistance. IEEE Access 7, 152034–152041. https://doi.org/10.1109/ACCESS.2019.2945526

Yip, W.S., To, S., 2017a. An application of eddy current damping effect on single point diamond turning of titanium alloys. J Phys D Appl Phys 50. https://doi.org/10.1088/1361-6463/aa86fc

Yip, W.S., To, S., 2017b. Reduction of material swelling and recovery of titanium alloys in diamond cutting by magnetic field assistance. J Alloys Compd 722, 525–531. https://doi.org/10.1016/j.jallcom.2017.06.167

Yip, W.S., To, S., 2017c. Tool life enhancement in dry diamond turning of titanium alloys using an eddy current damping and a magnetic field for sustainable manufacturing. J Clean Prod 168, 929–939. https://doi.org/10.1016/j.jclepro.2017.09.100

Yip, W.S., To, S., Zhou, H.T., 2020. Social network analysis for optimal machining conditions in ultra-precision manufacturing. J Manuf Syst 56, 93–103. https://doi.org/10.1016/j.jmsy.2020.03.011

Yoshiaki, S., Tatsuhiko, S., Hiroki, S., 2015. Multi-objective optimization for creating a low-carbon logistics system through community-based action. Journal of Advanced Mechanical Design, Systems, and Manufacturing 9, 1–12. https://doi.org/10.1299/jamdsm.2015jamdsm00

References

Zareena, A.R., Veldhuis, S.C., 2012a. Tool wear mechanisms and tool life enhancement in ultra-precision machining of titanium. J Mater Process Technol 212, 560–570. https://doi.org/10.1016/j.jmatprotec.2011.10.014

Zareena, A.R., Veldhuis, S.C., 2012b. Tool wear mechanisms and tool life enhancement in ultra-precision machining of titanium. J Mater Process Technol 212, 560–570. https://doi.org/10.1016/j.jmatprotec.2011.10.014

Zhang, G., To, S., 2015. A novel surface quality evaluation method in ultra-precision raster milling using cutting chips. J Mater Process Technol 219, 328–338. https://doi.org/10.1016/j.jmatprotec.2014.10.010

Zhang, G., To, S., Xiao, G., 2014a. Novel tool wear monitoring method in ultra-precision raster milling using cutting chips. Precis Eng 38, 555–560. https://doi.org/10.1016/j.precisioneng.2014.02.004

Zhang, G., To, S., Xiao, G., 2014b. The relation between chip morphology and tool wear in ultra-precision raster milling. Int J Mach Tools Manuf 80–81, 11–17. https://doi.org/10.1016/j.ijmachtools.2014.02.005

Zhang, S., Li, J.F., Wang, Y.W., 2012. Tool life and cutting forces in end milling Inconel 718 under dry and minimum quantity cooling lubrication cutting conditions. J Clean Prod 32, 81–87. https://doi.org/10.1016/j.jclepro.2012.03.014

Zhang, S.J., To, S., 2013a. A theoretical and experimental study of surface generation under spindle vibration in ultra-precision raster milling. Int J Mach Tools Manuf 75, 36–45. https://doi.org/10.1016/j.ijmachtools.2013.08.003

References

Zhang, S.J., To, S., 2013b. The effects of spindle vibration on surface generation in ultra-precision raster milling. Int J Mach Tools Manuf 71, 52–56. https://doi.org/10.1016/j.ijmachtools.2013.04.005

Zhang, S.J., To, S., Zhang, G.Q., 2017a. Diamond tool wear in ultra-precision machining. International Journal of Advanced Manufacturing Technology 88, 613–641. https://doi.org/10.1007/s00170-016-8751-9

Zhang, S.J., To, S., Zhang, G.Q., 2017b. Diamond tool wear in ultra-precision machining. International Journal of Advanced Manufacturing Technology 88, 613–641. https://doi.org/10.1007/s00170-016-8751-9

Zhang, Y., Zhang, Z., Zhang, G., Li, W., 2020. Reduction of Energy Consumption and Thermal Deformation in WEDM by Magnetic Field Assisted Technology. International Journal of Precision Engineering and Manufacturing - Green Technology 7, 391–404. https://doi.org/10.1007/s40684-019-00086-5

Zhang, Z., Huang, H., Ming, W., Xu, Z., Huang, Y., Zhang, G., 2016. Study on machining characteristics of WEDM with ultrasonic vibration and magnetic field assisted techniques. J Mater Process Technol 234, 342–352. https://doi.org/https://doi.org/10.1016/j.jmatprotec.2016.04.007

Zhang, Z., Zhang, Yi, Ming, W., Zhang, Yanming, Cao, C., Zhang, G., 2021a. A review on magnetic field assisted electrical discharge machining. J Manuf Process 64, 694–722. https://doi.org/https://doi.org/10.1016/j.jmapro.2021.01.054

Zhang, Z., Zhang, Yi, Ming, W., Zhang, Yanming, Cao, C., Zhang, G., 2021b. A review on magnetic field assisted electrical discharge machining. J Manuf Process 64, 694–722. https://doi.org/10.1016/j.jmapro.2021.01.054

References

Zhong, Z., 2002. Surface finish of precision machined advanced materials. J Mater Process Technol 122, 173–178. https://doi.org/10.1016/S0924-0136(02)00076-6

Zhu, Y.H., To, S., Lee, W.B., Liu, X.M., Jiang, Y.B., Tang, G.Y., 2009. Effects of dynamic electropulsing on microstructure and elongation of a Zn-Al alloy. Materials Science and Engineering A 501, 125–132. https://doi.org/10.1016/j.msea.2008.09.080

Zhu, Y.H., To, S., Lee, W.B., Zhang, S.J., Cheung, C.F., 2010. Ultra-precision raster milling-induced phase decomposition and plastic deformation at the surface of a Zn-Al-based alloy. Scr Mater 62, 101–104. https://doi.org/10.1016/j.scriptamat.2009.09.021

Zlatin, N., Field, M., 1973. R. I. Jaffee et al. (eds.), 489–504.

Zorev, N., 1963. Interrelationship Between Shear Processes Occurring Along Tool Face and on Shear Plane in Metal Cutting. Proceedings of the International Production Engineering Research Conference, Pittsburgh 42–49.

哲夫松尾, 1984. The Machining of Metals, E.J.A.Armarego \& R.H.Brown, Prentice-Hall, Inc., 1969. Journal of The Japan Society for Precision Engineering 50, 43.